Aluminum Stress on Suberin Biosynthesis in Barley (*Hordeum vulgare*) Roots

Dissertation
zur
Erlangung des Doktorgrades (Dr. rer. nat.)
der
Mathematisch-Naturwissenschaftlichen Fakultät
der
Rheinischen Friedrich-Wilhelms-Universität Bonn

vorgelegt von

Hongjun Meng

aus

Jilin, China

Bonn, August 2023

Angefertigt mit Genehmigung der Mathematisch-Naturwissenschaftlichen Fakultät
der Rheinischen Friedrich-Wilhelms-Universität Bonn

Gutachter and Betreuer: Prof. Dr. Lukas Schreiber
Gutachter: PD Dr. Frantisek Baluska

Tag der Promotion: 15.08.2023
Erscheinungsjahr: 2023

Declaration on Oath

I hereby declare that the enclosed Ph.D. dissertation has been developed and written without help and by myself. To the best of my knowledge, no sources or means were used in this thesis without declaration in the text. All methods or thoughts from others are clearly cited.

This Ph.D. thesis was not used in the same or similar version to achieve any other academic grading.

Bonn, _____ _____

Abstract

Aluminum (Al) toxicity is a major factor inhibiting plant growth in acidic soils worldwide, and the root barrier formed by suberized cells is an important mechanism for plants to resist environmental stress. The aim of this study was to investigate the effect of Al stress on the synthesis of suberin in barley (*Hordeum vulgare*) roots and the role of suberin in resisting Al stress.

This study investigated the effect of different pH conditions on root development and suberin biosynthesis in barley seedlings, with a particular focus on the impact of Al stress and silicon supplementation. The results indicated that the length and dry weight of seminal roots in barley were not significantly affected by pH, but Al stress led to a noticeable reduction in root growth. However, the addition of Si to the solution medium containing 50 μM Al mitigated the adverse effects of Al stress on root growth. The results also showed that 4 days of Al stress could significantly increase the distribution and content of suberin in barley roots through FY staining observation and GC chemical analysis. The analysis of the aliphatic suberin monomer composition in various zones of barley roots grown under distinct pH conditions also showed no significant differences. However, the amount of suberin increased under Al stress, with Si supplementation leading to a reduction in suberin deposition. Analysis of RNA-seq data and qPCR analysis showed that Al stress could induce the expression of a series of genes related to suberin synthesis, among which the key gene for suberin synthesis, CYP86B1, was crucial in the Al stress response. Under Al stress, Al-induced suberization in the barley cyp86b1 mutants was significantly lower than in wild-type barley. In parallel, a series of ABA-related genes involved in ABA biosynthesis, degradation, and signalling were upregulated under Al stress, indicating that Al treatment could induce ABA synthesis and possibly regulate Al-induced suberization by modulating the ABA pathway. Furthermore, in the presence of the ABA synthesis inhibitor fluridone, Al stress could no longer induce changes in suberin. Morin staining showed that the presence or absence of suberin lamellae had a significant effect on the transport of Al in roots. In the absence of suberin,

more Al entered the xylem of the root. However, after 4 days of Al treatment, the presence or absence of suberin did not affect the growth status of the barley aboveground part.

Content

1. Introduction

1.1 Aluminum toxicity in plants

Aluminum (Al) toxicity is a widespread issue in acidic soils, which are prevalent in various regions worldwide (Kochian, 1995). Acidic soils cover around 30% to 40% of arable land and half of the world's potential arable land (Figure 1.1) (Von Uexküll and Mutert, 1995). Normally, when the soil pH is above 5.5, aluminum remains in an insoluble and non-toxic state; however, when soil pH drops below 5.5, some of the mineral-bound aluminum dissociates, releasing Al^{3+} which is highly toxic, leading to aluminum toxicity (Kochian, 1995). The high concentration of Al^{3+} in the soil inhibits root growth and function, leading to reduced uptake of essential nutrients and water, and decreased plant growth and yield.

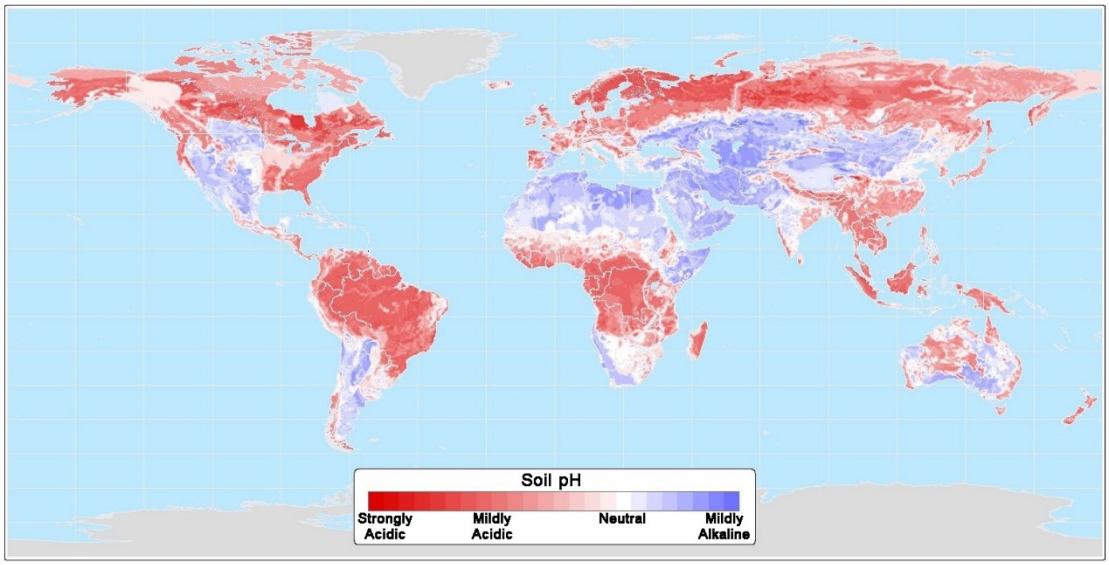

Figure 1.1 World soil pH. Data taken from: IGBP Global Soils Data Task, France, 1998.

Advancements in modern molecular biology have enabled researchers to discover genetic differences in a plant's ability to resist aluminum, leading to the selection of strongly resistant crops through genetic improvement methods. This approach is more efficient than soil improvement methods (such as applying calcium, magnesium, phosphorus fertilizer, limestone, or organic matter) and is also sustainable. Researchers worldwide have since focused on studying the genetic response of plants to aluminum stress.

The tolerance to aluminum toxicity or acidic soils varies significantly among cereal species, and barley (*Hordeum vulgare L.*), which ranks fourth in importance among cereal crops, is typically considered one of the most vulnerable cereal species to aluminum stress (Ishikawa et al., 2000; Wang et al., 2006a). The deleterious effects of aluminum on barley roots manifest in diminished root growth and altered root anatomy, including reduced root elongation and diminished root hair density. These alterations lead to a decrease in the root surface area available for the absorption of water and nutrients, resulting in decreased plant growth and productivity. Research indicates that barley cultivars display varying degrees of tolerance to aluminum stress (Furukawa et al., 2007; Zhao et al., 2003), with some cultivars demonstrating enhanced tolerance through genetic variation in root morphology and anatomy, or in the mechanism of aluminum uptake and detoxification.

Aluminum stress presents an ongoing challenge to barley production, particularly in regions with acidic soils. To increase food security and support sustainable agriculture, additional investigation is required to develop effective strategies for mitigating the adverse impacts of aluminum stress on barley growth and yield.

1.1.1 Symptoms of plants Al toxicity

The symptoms of Al toxicity in plants are characterized by the inhibition of root growth, which is typically the earliest and most prominent symptom. After several decades of research, it has been determined that Al toxicity affects various aspects of plant growth. It is generally believed that the major inhibition caused by Al is the growth of root cells (Llugany et al., 1995). Nevertheless, prolonged Al toxicity can also suppress the division of root tip cells, resulting in decreased volume and necrosis of root tip epidermal cells, damage to cortex and epidermal cells, reduced root hairs, and loss of root cap (Nezames et al., 2012). Furthermore, Al can disrupt Ca^{2+} intracellular transport across the membrane, interfering with Ca^{2+}-mediated signal transduction processes (Delhaize and Ryan, 1995). Al can also bind to the phosphate group of DNA, causing chromatin destruction and

disrupting cell division (Kochian, 1995). Moreover, Al can alter the arrangement of microtubule proteins and depolymerize microtubules and microfilaments in the cell skeleton (Sasaki et al., 2012), induce programmed death of root tip cells (Pan et al., 2001), bind to phospholipids in the cell membrane, altering its permeability (MacKinnon et al., 2006), and compete with magnesium for ATPase binding sites, thereby impeding normal ATPase activity and affecting the plant's normal growth and development (Ma, 2007).

1.1.2 Action sites of Al toxicity in plants

Research has found that the structure of the root cap cells in maize (*Zea mays*) undergoes significant changes under Al treatment, indicating that the root cap may be the site of Al recognition (Bennet and Breen, 1991). Furthermore, researchers discovered differences in the Al content between Al-sensitive and Al-tolerant wheat varieties, with the greatest variation observed in the root tip regions of 0-2 mm and 0-5 mm, suggesting that this meristem tissue may be crucial to the mechanism of Al tolerance (Rincón and Gonzales, 1992). Subsequent research found that the inhibition of root growth in maize was due to the initial Al toxicity occurring at the region of 2-3 mm in the root tip, which is commonly referred to as the Distal Part of the Transition Zone (DTZ), a region that is critical to the preparation stage of rapid growth (Ryan et al., 1993). Lastly, quantitative measurement of Al accumulation in various regions of maize root tips revealed that the distal tip region (1-2 mm) is the area of Al toxicity (Sivaguru and Horst, 1998).

The complex nature of Al toxicity entails differences arising from various factors such as species, duration, and concentration of Al treatment. According to a review of research in this field (Zheng and Yang, 2005), it was concluded that the meristematic region of the root apices, DTZ, or elongation zone may all be the site of Al toxicity in plants.

1.2 Al resistance mechanisms of plants

The long-term evolutionary adaptation of plants to Al toxicity has resulted in a diverse range of physiological strategies. These strategies are categorized into external exclusion

and internal tolerance mechanisms based on their detoxifying parts (Horst et al., 2010; Kochian, 1995; Li et al., 2017). External exclusion mechanisms involve the removal of Al from the root system to prevent its entry into plant cells. This is achieved through the secretion of organic acids (Ma et al., 2001), cell wall fixation (Zheng and Yang, 2005), and other Al exclusion mechanisms (Degenhardt et al., 1998). Internal tolerance mechanisms, on the other hand, aim to reduce the binding of Al to active metabolic sites within cells. This can be achieved through complexation between Al and organic ligands like small organic acids and phenolic substances (Nagata et al., 1992), vacuole compartmentalization (Shen et al., 2002), and synthesis of Al-induced proteins and Al-tolerant enzymes. Plant species adopt different mechanisms to adapt to Al stress (Zhang et al., 2018), and recent studies have shown that plants can coordinate both external exclusion and internal tolerance mechanisms to alleviate Al toxicity (Wang et al., 2017). In addition, barley germplasm from East Asia and Europe have developed independent yet equivalent gene insertion and demethylation strategies to resist Al toxicity (Kashino-Fujii et al., 2018).

1.2.1 Al exclusion mechanisms

1.2.1.1 Secretion of organic acids

The underlying principle of secretion of organic acids can be summarized as the organic acids secreted by the root system transforming ionic aluminum into mineral aluminum. Currently, three organic acids have been identified as being induced by aluminum secretion: malate, citrate, and oxalate. Researchers generally believe that when these organic acids combine with aluminum to achieve a specific molar ratio, they can even detoxify aluminum to plants (Ma et al., 2001; Zheng et al., 1998). A comprehensive review of numerous studies reveals that the organic acids secreted by different plant species under aluminum stress are different; the stronger the aluminum tolerance of the plant, the more organic acids secreted by the root tip and the less root tip aluminum accumulation. Oxalic acid secretion is rapid and does not require re-synthesis in the plant

body, and its secretion patterns and regulatory mechanisms vary by species (Ma et al., 1997a; Yang et al., 2011; Zheng et al., 1998; Zhu et al., 2011). Citric acid and malic acid are the main metabolic products of the tricarboxylic acid cycle, while oxalic acid is the final product of secondary metabolism, its accumulation is harmful to cell function and must be strictly controlled. However, to date, the gene encoding the transport protein inducing oxalic acid secretion has not been found, and this is also the research direction of scholars who are concerned with the topic of aluminum-induced oxalic acid secretion.

Based on the time difference between the onset of aluminum stress and corresponding organic acid secretion, plants can be classified into two major patterns: Pattern I plants, which respond quickly to aluminum stress within a few tens of minutes, such as wheat and buckwheat (*Fagopyrum esculentum Moench*); and Pattern II plants, in which organic acid secretion is delayed by several hours, such as cassia and maize (Ma et al., 2001). Recent research has shown that Al-induced citric acid secretion in rice bean (*Vigna umbellata*) includes two stages: an early stage with only a small amount of citric acid secretion, and a second stage with a large amount of citric acid secretion, induced by Al for a long time. Further research has found that two different citric acid transporters belonging to the same transporter family are involved in these two different stages (Liu et al., 2009).

As research on organic acid secretion progressed to the molecular level, the first gene that can directly regulate Al resistance was cloned. This gene encodes an aluminum-induced malate transporter protein (*Aluminum-induced Malate Transporter, ALMT1*), which is located on the plasma membrane (Sasaki et al., 2004). Its expressed protein increases the Al tolerance of barley and wheat (Delhaize et al., 2004; Yamaguchi et al., 2005). Homologous genes to wheat *TaALMT1* have also been cloned in different plants, such as Arabidopsis (Hoekenga et al., 2006), rapeseed (*Brassica napus L.*) (Ligaba et al., 2006), and maize (Pineros et al., 2008).

Subsequently, the membrane-bound Al-induced citrate transporter proteins HvAACT1 and SbMATE were cloned from barley and sorghum (*Sorghum bicolor (L.) Moench*) root tips. Sequence alignment analysis revealed that both belong to the Multi-drug and Toxic Compounds Extrusion (MATE) family (Furukawa et al., 2007; Magalhaes et al., 2007). *HvAACT1* showed good correlation with citrate secretion and Al tolerance (Furukawa et al., 2007), indicating it is a major gene in barley associated with Al tolerance. Researchers have obtained MATE genes from different plants using homologous cloning, such as Arabidopsis (Liu et al., 2009), maize (Maron et al., 2010), poplar (Li et al., 2017), and soybean (Zhou et al., 2019). Additionally, proton pumps play a role in Al-induced organic acid secretion. Low levels of Mg in the environment can enhance plasma membrane H^+-ATPase activity and citrate secretion to alleviate Al toxicity. Under Al stress, the synergistic action of vacuolar H^+-ATPase and plasma membrane H+-ATPase determines the distribution of organic acids in the vacuole or extracellular space, and thus determines the plant's tolerance to Al (Rengel et al., 2015; Zhang et al., 2019; Zhang et al., 2020).

1.2.1.2 The fixation of the cell wall

The cell wall plays an important role in plant tolerance to aluminum. Al mainly inhibits cell elongation and hinders normal root growth (Kochian, 1995). Cell elongation means that the cell volume continually increases under turgor pressure, making the normal elasticity and extensibility of the cell wall particularly important. The plant cell wall not only regulates normal growth and development, but also serves as the first physical barrier for sensing Al toxicity and is the main site of Al binding (Zhu et al., 2014). The cell wall is a dynamic structure that determines cell shape and size, provides structural support, protects cells from pathogen invasion, and acts as a communication node between the cytoplasm and extracellular matrix (Polko and Kieber, 2019). It can be divided into primary and secondary cell walls based on structure. The primary cell wall contains polysaccharides (cellulose, pectins, and hemicelluloses), various enzymes, and structural proteins (Figure 1.2); the secondary cell wall also includes lignin.

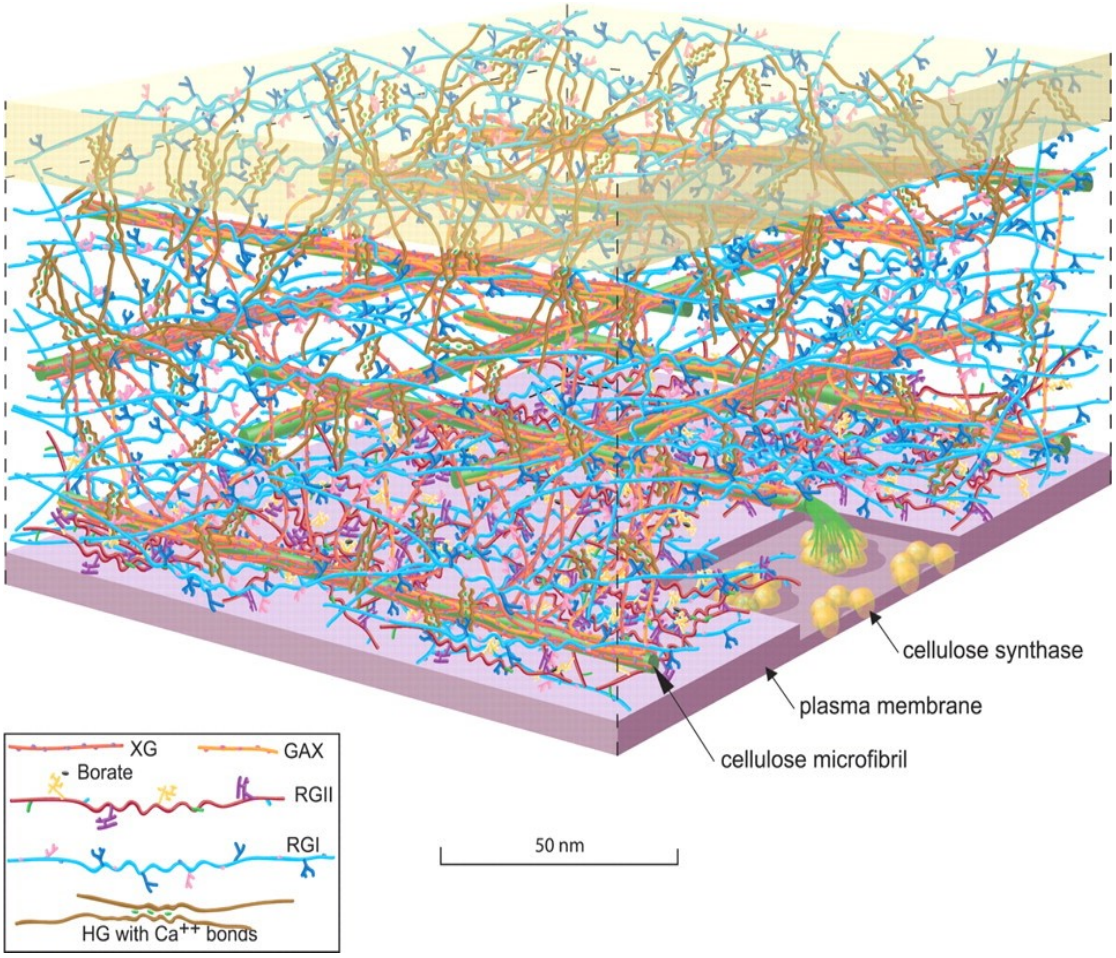

Figure 1.2 Scale model of cell walls. The hemicellulose cross-links [shown in dark orange (xyloglucan, XG) or light orange (glucoronoarabinoxylan, GAX)] are abnormally extended. Cited from (Somerville et al., 2004).

The main load-bearing component of plant cell walls is cellulose, which accounts for approximately one quarter of the dry weight of the primary wall. Plant cellulose is assembled in the Golgi apparatus through the action of cellulose synthase complexes and transferred to the plasma membrane for synthesis (Polko and Kieber, 2019). The structure of cellulose is a semi-crystalline structure formed by inter- and intra-chain hydrogen bonds and van der Waals forces (Nishiyama, 2009). This supports the structural integrity of the entire cell wall and regulates the direction of cell development. Due to the simple composition and structure of cellulose, as well as its chemically inert nature as a large macromolecule, it is generally believed that cellulose is not a potential binding site for Al.

In dicotyledonous plants, pectin is found in the cell walls in amounts of about 30% of the dry weight. It is present in smaller amounts, 5-10% of dry weight, in grasses and is abundant in gymnosperms. Pectin helps regulate cell wall porosity, intercellular adhesion, cell expansion, and pathogen defense (Mohnen, 2008). Pectin can be divided into four types based on its main chain structure and side chain composition, with homogalacturonan pectin being the most common (Willats et al., 2001). Researchers have long believed that pectin is the main site of Al binding in cell walls because of its carboxyl group's high affinity for metal ions (Chang et al., 1999). It has also been established that pectin content is related to Al binding and fixation in plants (Li et al., 2009; Yang et al., 2011; Zhou et al., 2012). It was found that changes in pectin structure under Al stress in two maize varieties with different Al resistance were related to changes in the distribution of pectin in the cell walls, and these changes were related to the degree of root growth inhibition. This suggests that the stability of pectin structure may be necessary for normal root growth.

The structure of hemicelluloses is complex, including multiple hexoses or pentoses, such as xyloglucan, arabinoxylan, xylan and β-(1-3,1-4)-D-glucuronoxylan (Cosgrove, 2005). Its most important function is to strengthen the cell wall by bonding with cellulose microfibrils through hydrogen bonds and forming a high-level structure (Roland et al., 1989). The composition and structure of hemicelluloses are related to the species, cell type, or growth stage of the plant (Zhu et al., 2012). The main components of hemicelluloses are different in monocotyledonous and dicotyledonous plants and in monocotyledonous plants and non-monocotyledonous single-leaf plants and dicotyledonous plants (e.g. *Arabidopsis thaliana*). The former is arabinogalactan and β-(1-3,1-4)-D-glucuronoxylan, with a low content of xyloglucan (Hazen et al., 2002); the latter is mainly xyloglucan.

Traditionally, researchers were convinced that pectin was the sole component responsible for binding and immobilizing aluminum (Schmohl and Horst, 2000). However, subsequent reports have increasingly challenged this notion. It has been discovered that there are covalent connections between pectin and hemicellulose (Thompson and Fry, 2000), and that pectin masks the antigenic determinant clusters of xyloglucan, thus seemingly protecting some of the aluminum binding sites in hemicellulose (Marcus et al., 2008). Additionally, it has been demonstrated through tests on the adsorption of Al by various components of the cell wall that the contribution of the hemicellulose component in adsorbing Al is the greatest, far surpassing that of pectin. Therefore, it is imperative to understand the structure and modification of the main components of hemicellulose (Yang et al., 2011). The main component of hemicellulose in Arabidopsis thaliana is xyloglucan. Its main chain is composed of straight chains of β-(1-4)-D-glucose residues, and the side chain (xylose residues) first bonds to O-6 positions of glucose residues. Some xylose residues may then bind to galactose or fucose (Cosgrove, 2005). By adding xyloglucan to the culture solution containing aluminum, it was found that the accumulation of aluminum in the roots was significantly reduced, thus removing the toxic effects of aluminum. Al-NMR confirmed that xyloglucan can clearly bind to aluminum (Zhu et al., 2012). This challenges the traditional view that pectin is the primary site of aluminum binding.

1.2.1.3 Other Al exclusion mechanisms

Phenolic compounds refer to a large group of plant organic compounds that contain one or more hydroxylated aromatic rings, similar to alkaloids and flavonoids. They can form stable compounds with Al^{3+} under neutral conditions. Research has found a correlation between flavonoids such as catechins and the Al tolerance of maize (Kidd et al., 2001). Additionally, the phenolic hydroxyl groups of tannins and oenothein B in *Eucalyptus camaldulensis* can bind with Al (Tahara et al., 2014).

The activity of individual Al^{3+} largely depends on the pH value of the root system. Therefore, maintaining a high pH value around the root zone can reduce the dominance of Al^{3+} in the medium, thereby alleviating its toxicity to plants (Zhang et al., 2020). Wheat can maintain a relatively high pH value in the rhizosphere to enhance its Al resistance (Wang et al., 2006b). Moreover, most plants can produce a mucilage layer or root border cells, forming a thick barrier that prevents Al from entering the cells.

1.2.2 Al tolerance mechanisms

1.2.2.1 Compartmentalization of Vacuoles

Vacuoles are relatively independent organelles with functions that include regulating cell osmotic pressure, accumulating metabolic substances within cells, facilitating movement and storage, and participating in the biochemical cycling of substances within cells. Compartmentalization of vacuoles is particularly important for plants to respond to non-biological stress.

In 1991, the ability of vacuoles and chloroplasts to accumulate Al was first discovered (Cuenca et al., 1991). Subsequently, the phenomenon of Al compartmentalization in the vacuoles of Al-tolerant buckwheat leaf blades was identified (Shen et al., 2002). Transporters involved in the intracellular redistribution of Al have since been identified, such as *Aluminum Sensitive Factor 3* (*ALS3*), which is located in the cortex and encodes an Al-induced ABC transporter that moves Al from sensitive to insensitive regions of the plant's metabolism (Larsen et al., 2005). Subsequently, half-type ABC transporter ALS1, located in the vacuolar membrane, was thought to be the transporter that moves Al from the cytoplasm to the vacuole (Larsen et al., 2007). In Arabidopsis, *AtALS1* is primarily expressed in the vascular system and root tips and is not induced by Al, whereas *ALS3* is primarily located in the phloem and leaf hydathodes, the cortex, and the root epidermis and it is induced by Al. Later, the vacuolar membrane-localized *OsALS1* was cloned from rice (Oryza sativa), and its encoded Al transporter was found to compartmentalize Al into

vacuoles to relieve Al toxicity (Huang et al., 2012). In buckwheat, proteomic analysis identified two half-type ABC transporters, FeASL1.1 and FeALS1.2, which participate in the internal detoxification of roots and leaves by compartmentalizing Al into vacuoles (Lei et al., 2017). Recent reports suggest that ALS3 interacts with the Al-resistant gene-encoded protein STAR1, forming an ATP-binding cassette-type transporter complex on the vacuolar membrane, and plays a role in root growth inhibition caused by phosphate deficiency (Godon et al., 2019; Wang et al., 2019), indicating that these transporters may have additional functions beyond responding to Al toxicity.

1.2.2.2 Complexation of small molecule organic acids and phenolic compounds

The plant itself is capable of chelating Al to cellular proteins, nucleic acids, or phospholipids, thereby allowing Al to exist in a non-toxic or less toxic form. Additionally, small organic acids and phenolic compounds present in the plant play a crucial role in compartmentalization in the vacuole and internal detoxification of the plant in the above-ground tissues. *Camellia sinensis*, buckwheat, and *Hoya carnosa* are typical plants following these strategies: in buckwheat, Al in the leaves under Al stress is mainly present as Al^{3+}-oxalate (1:3 molar ratio) in the cellular sap, with minimal impact on Al toxicity to the plant; *Hoya carnosa* is a typical plant with high Al resistance, Al in the leaves under Al stress is mainly present as Al^{3+}-citrate (1:1 molar ratio) and approximately 75% of Al is located in the cellular sap, which detoxifies Al (Ma et al., 1997b). In *Eucalyptus*, the phytochelatin B can bind to Al in a chelate, thereby reducing Al's toxicity to the plant (Tahara et al., 2014).

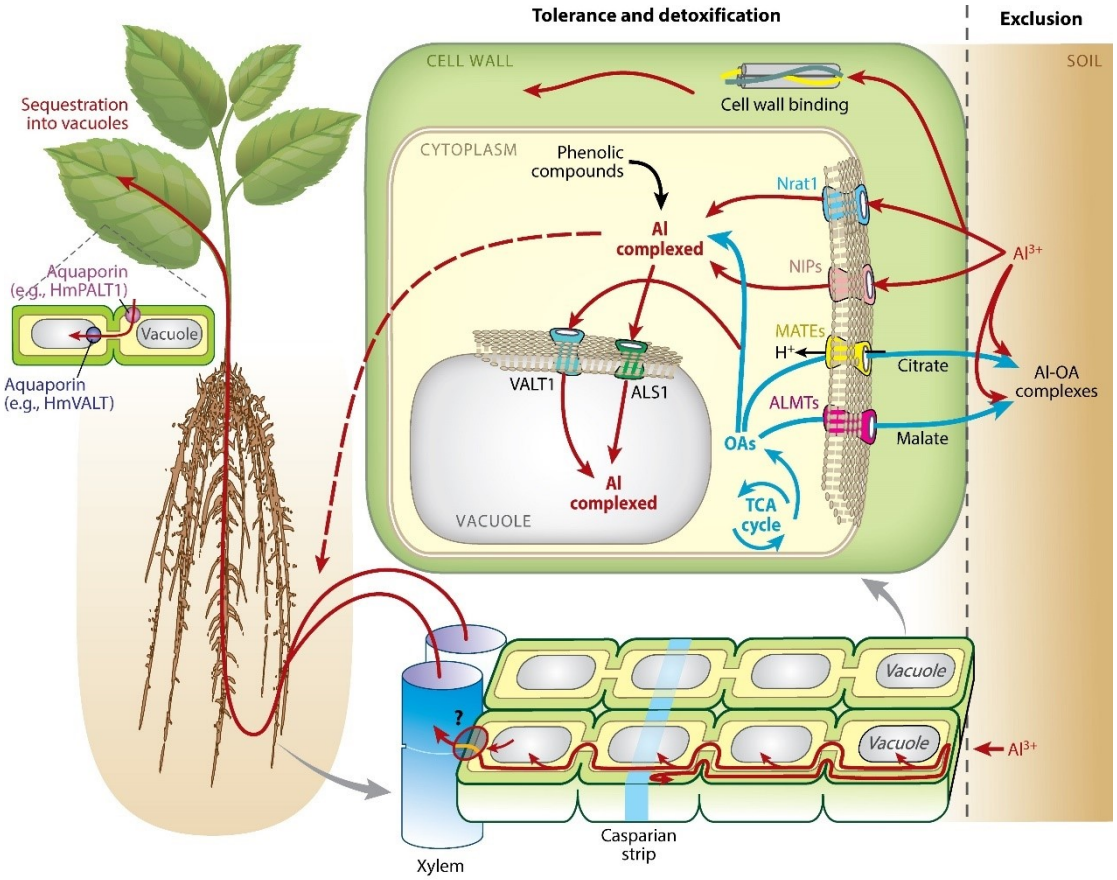

Figure 1.3 General model illustrating mechanisms of Al resistance. Cited from (Kochian et al., 2015). The red arrows denote Al fluxes into and within the cell, and the blue arrows denote fluxes of OA anions. Abbreviations: ABC, ATP-binding cassette; Al, aluminum; ALMT, Al-activated malate transporter; ALS1, Al-sensitive 1; MATE, multidrug and toxic compound extrusion; NIP, nodulin 26–like intrinsic protein; Nramp, natural resistance-associated macrophage protein; Nrat1, Nramp Al transporter 1; OA, organic acid; PALT1, plasma membrane Al transporter 1; TCA, tricarboxylic acid; VALT, vacuolar Al transporter.

1.3 Apoplastic barriers in plants

1.3.1 Plasticity of endodermal differentiation

Plants possess a unique defense system based on phenolic and aliphatic polymers, which protect them from various environmental stresses, such as drought and pathogen infection. The formation of cell wall modifications, such as cutin and suberin, is particularly important in this defense mechanism. The root endodermis that bears the Casparian strip

forms a barrier for apoplastic (intercellular) transport, which separates two distinct spaces within the root: the central stele that transports nutrients with the vascular tissue, and the outer cortex that is connected to the soil through intercellular (apoplastic) space. Mineral nutrients are transported radially from the root periphery to its center through three pathways: symplastic, apoplastic, or coupled trans-cellular pathway (Andersen et al., 2015; Barberon and Geldner, 2014; Geldner, 2013; Robbins et al., 2014). The root endodermis bears two distinct stages of differentiation, namely the actively absorbing epithelium (State I) and a predominantly protective state (State II). The defining feature of the State II endodermis is the formation of hydrophobic suberin polymer around its surface (Layers, 2013). The protective function of the State II endodermis is evident in many plant species (Layers, 2013)

Suberin can control the efflux of water and solutes and plays a crucial role in plant resistance to stresses such as drought, salt, and pathogen infection (Franke and Schreiber, 2007; Schreiber, 2010). Suberin deposition is tissue-specific, such as in the periderm of secondary shoots and roots, and in the endodermis of roots (Harman-Ware et al., 2021; Kumar et al., 2016). As the outermost protective layer of plants, these boundary tissues regulate the movement of water, minerals, and major gases, defending against microbial attack and preventing the infiltration of toxic compounds. Furthermore, suberin is also widely present in tissues that have been damaged by abiotic and biotic stresses, such as injuries caused by non-biological stress and microbial invasion (Enstone et al., 2003; Kolattukudy, 2001).

Suberin deposition occurs as a layer between the plasma membrane and the primary cell wall, finally covering the entire surface of the root endodermis (Haas and Carothers, 1975; Robards et al., 1973). Endodermal suberization occurs in a "switch-like" manner, where individual endodermal cells rapidly and randomly suberize, leading to a "patchy" area that eventually develops into a continuous suberization zone. This process is highly

plastic and can respond to various nutritional stress conditions through the ethylene and abscisic acid (ABA) hormonal pathways, which regulate the formation of suberin through the activation of peroxidases (Barberon et al., 2016).

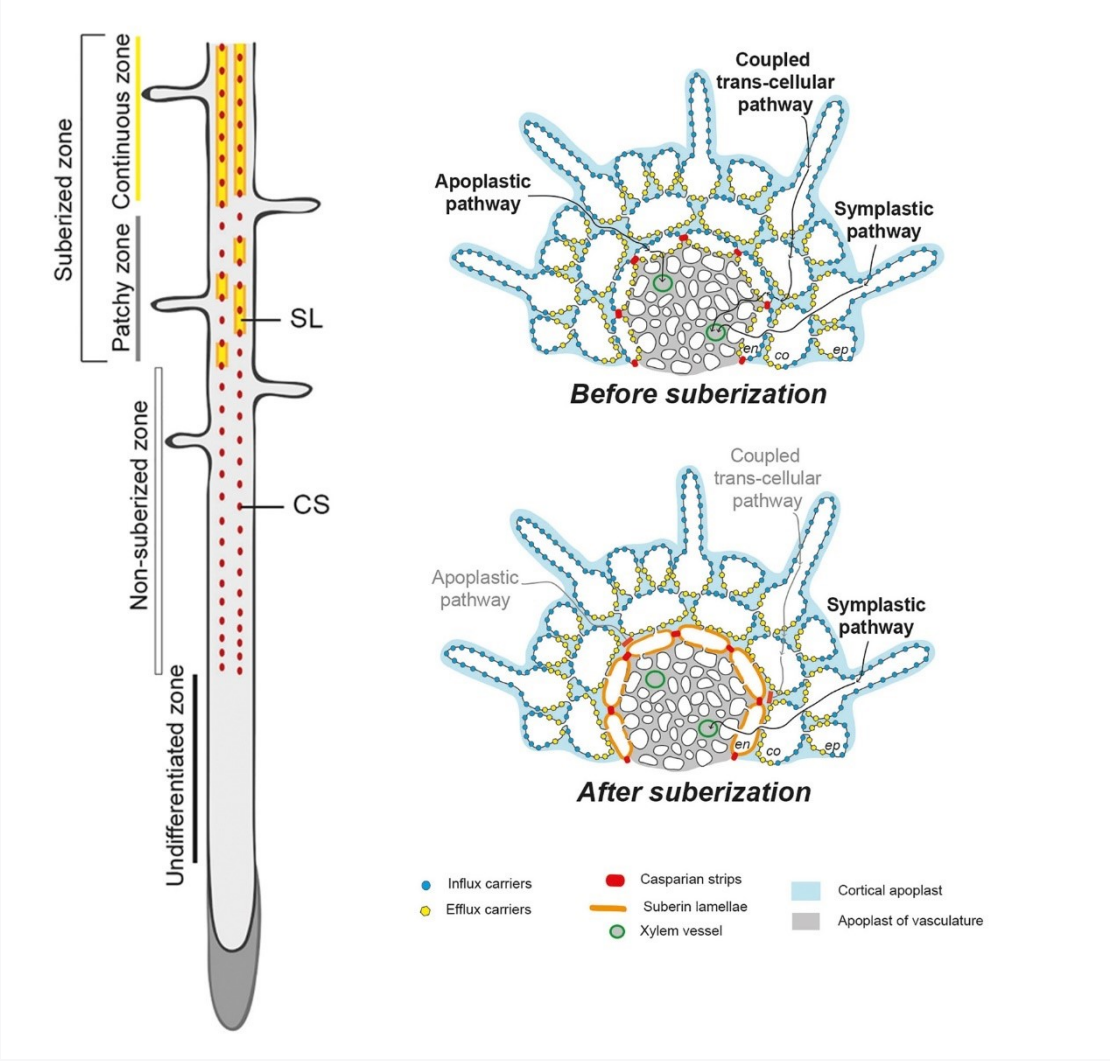

Figure 1.4 General model of root endodermal suberization. Cited from (Barberon et al., 2016).

1.3.2 Suberin biosynthesis

Suberin is a complex polymer composed of glycerol and a variety of chemical compounds, including polyaromatics, fatty substances, and partial waxes that are associated with the cell wall (Franke and Schreiber, 2007; Pollard et al., 2008). The fatty substances in suberin include saturated or unsaturated long- and ultra-long-chain hydroxydicarboxylic acids, which are either epoxidized or substituted by diol groups in the middle of the chain.

Additionally, medium-chain oxidized fatty acids and fatty alcohols are also present, which are typically esterified with acyl-CoA to connect with the phenolic regions (Graça and Pereira, 1997; Kolattukudy, 2001; Pollard et al., 2008). Glycerol in suberin is esterified into ω-hydroxyglycerides and α, ω-dicarboxylic glycerides (Graça and Pereira, 2000). The suberin monomers comprising are similar to those of cutin monomers, but in suberin, the fatty acid chains are longer, and the proportion of α, ω-dicarboxylic acids is higher. The suberin monomers in Arabidopsis include aliphatic substances such as ω-hydroxy acids with chain lengths of C16-C24, α, ω-dicarboxylic acids, unoxidized long-chain fatty acids (>C18), fatty alcohols with chain lengths of C18-C22, and phenolic compounds such as ferulic acid (Franke et al., 2005; Molina et al., 2006). Although studies on the monomeric composition of suberin in various plants have been conducted for several decades, many aspects of suberin biosynthesis, such as the sequence of biosynthetic reactions, the transport mechanism of monomers, and polymerization, still remain partially unclear.

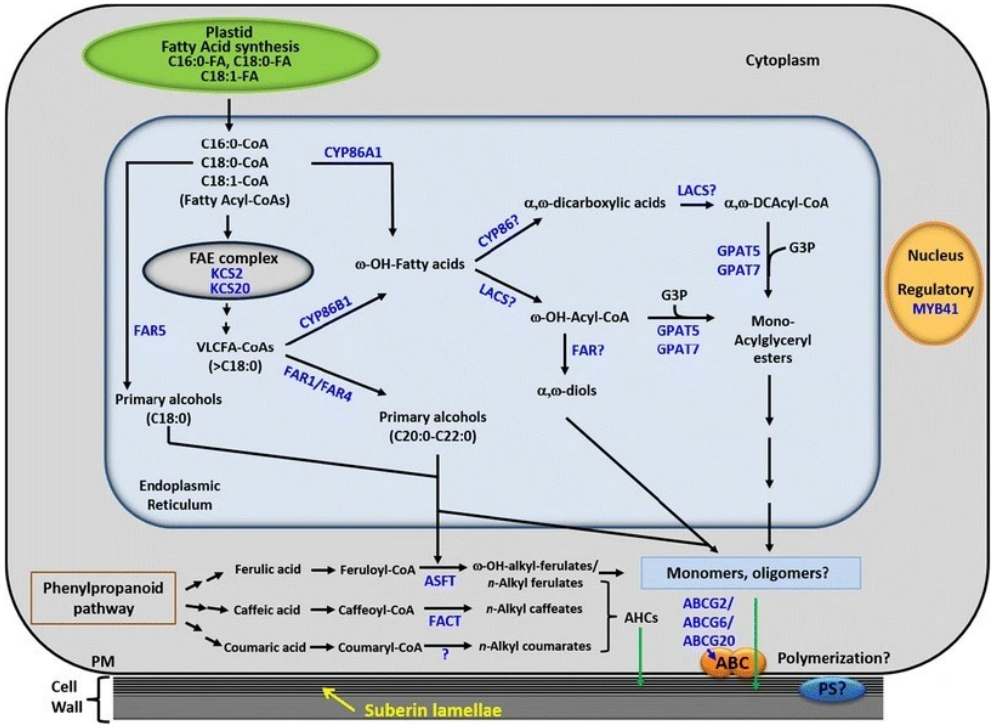

Figure 1.5 Overview of the suberin biosynthetic pathway with subsequent export to the cell wall. Cited from (Vishwanath et al., 2015)

Enzymes that participate in suberin biosynthesis include cytochrome P450 monooxygenases, glycerol-3-phosphate acyltransferases, fatty acid elongases, and peroxidases. They are involved in the hydroxylation of fatty acids, dicarboxylic acid formation, fatty acid elongation, and polymeric aromatic compound polymerization, and their activities have been detected in the polyester formation processes of various plant tissues (Razem and Bernards, 2003; Schreiber et al., 2005).

CYP86 subfamily cytochrome P450 monooxygenases catalyze the ω-hydroxylation of fatty acids, which is an essential step in the formation of suberin monomers (Pinot, 2011). Similar to *CYP* genes, *Glycerol-3-phosphate acyltransferase 5* (*GPAT5*) is one of the first genes identified to be involved in suberization and is mainly expressed in the endodermal layer tissue of roots (Beisson et al., 2007). *GPAT5* is involved in the formation of C22 and C24 very-long-chain acyl monomers in suberin in roots and seed coat. The chemical composition of cutin and suberin differs in the composition of their fatty polyesters. Cutin is mainly composed of C16 and C18 fatty polyesters, whereas suberin contains very-long-chain fatty monomers and their polyesters (Franke et al., 2005; Pollard et al., 2008). Therefore, another molecular target for suberin synthesis is fatty acid elongase (FAE). The β-ketoacyl-CoA synthase (KCS) encoded by the *KCS* gene is a component of the FAE complex and a key enzyme in fatty acid elongation (Joubès et al., 2008). Saturated long-chain (C18, C20, and C22) alcohols are common components of suberin (Franke et al., 2005). Studies on the enzymes involved in suberin synthesis in jojoba (*Simmondsia chinensis*) seeds have shown that the reaction process that generates alcohols from very-long-chain fatty acids is catalyzed by fatty acyl reductase (FAR) (Kolattukudy, 1977; Metz, 2000; Vioque and Kolattukudy, 1997). After fatty acid synthesis, it is generally converted to acyl-CoA esters by long-chain acyl-CoA synthetases (LACSs). Recent studies have shown that at least three LACS isozymes are involved in Arabidopsis wax synthesis and catalyze the activation of free fatty acids to form fatty acyl-CoA thioesters (Jessen et al., 2011; Lu et al., 2009; Weng and Chapple, 2010).

1.4 Objectives

Aluminum toxicity is a major plant growth inhibitor in acid soils worldwide, and barley as an important cereal crop is particularly sensitive to the Al toxicity. However, the primary cause of Al toxicity in plants still lacks clarity, and most studies on Al toxicity have predominantly focused on seedling stages and short-term exposure to Al. In such brief experimental durations, the root cell walls are unlikely to have undergone secondary biochemical modifications, such as suberization. Nonetheless, it is well-known that the apoplastic barrier formed by suberin deposition in root cell walls plays an important role not only in controlling water and nutrient element transport and limiting pathogen invasion, but also in resistance to environmental stress. The aim of this study was to investigate the effects of Al stress on suberin synthesis in barley and the role of suberin in the defense against Al toxicity. Specifically, the study explored the relationship between Al toxicity and root suberization, and whether suberin acts as a barrier to Al. The study involved measuring various physiological indicators and root suberin under different growth conditions, analyzing the expression patterns of suberin-related genes, and measuring Al levels in barley roots. Measurements were conducted in barley (*Hordeum vulgare* L. spp. *vulgare* cv Scarlett) treated with Al for 4 days, and compared with barley *cyp86b1* mutants obtained in *Hordeum vulgare* L. spp. *vulgare* cv Golden promise.

2. Materials and Methods

2.1 Plant material and treatments

2.1.1 Plant material and growth conditions

In this study, barley seeds of the cultivars "Scarlett" and "Golden Promise" were germinated by incubating them in moistened paper towels for three days in darkness at a temperature of 25 °C. The three-day-old seedlings were then grown hydroponically in 3.5-liter pots containing a modified Magnavaca nutrient solution (Famoso et al., 2010) while being supplied with a continuous stream of air. The growth environment was maintained with a photoperiod of 16 hours of light and 8 hours of darkness, with day/night temperatures of 23 °C and 20 °C, respectively. After 6 days of growth (3 days of germination and 3 days of hydroponic growth), the plants were transferred to treatment solutions for further 4 days (as shown in Figure 2.1).

Modified Magnavaca nutrient solution

Compound	Concentration
KCl	1 mM
NH_4NO_3	1.5 mM
CaCl	1 mM
KH_2PO_4	45 µM
$MgSO_4$	200 µM
$Mg(NO_3)_2$	500 µM
$MgCl_2$	155 µM
$MnCl_2 \cdot 4H_2O$	11.8 µM
H_3BO_3	33 µM
$ZnSO_4 \cdot 7H_2O$	3.06 µM
$CuSO_4 \cdot 5H_2O$	0.8 µM
$Na_2MoO_4 \cdot H_2O$	1.07 µM
Fe-HEDTA	77 µM

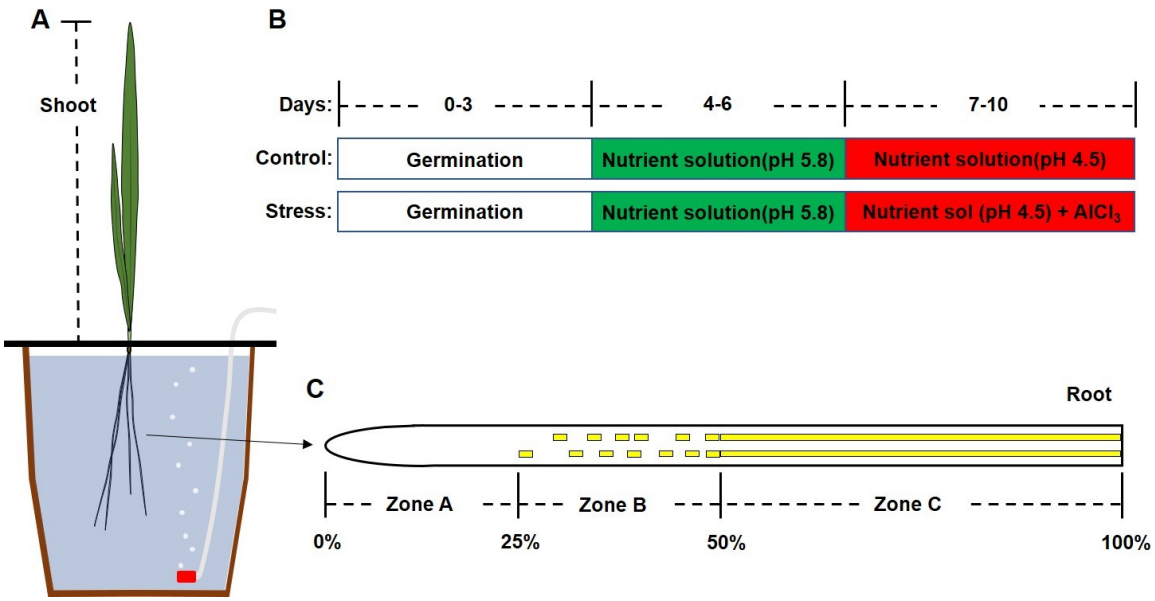

Figure 2.1 Experimental setup of Al stress. (A) Schematic diagram of barley grown in hydroponic pots with a continuous stream of air. (B) Schematic diagram of growth conditions. After 3 d of germination, seedlings were transferred to hydroponic nutrient solution. For Al stress treatment, the nutrient solution was exchanged with nutrient solution with 50 or 100 μM $AlCl_3$ at day 6. When the plants were 10-d-old, they were harvested for experiments. (C) Schematic diagram showing the different root zones which were harvested. The seminal roots of barley grown in nutrient solution at pH 5.8 were divided into three zones based on the development of suberin lamellae (Kreszies et al., 2019).

2.1.2 Stress application

2.1.2.1 Aluminum stress

Six-day-old plants were subjected to aluminum stress by transferring them to the Al treatment solution. The treatment solution contained 50 μM or 100 μM $AlCl_3$, added after pH adjustment to 7.8 with KOH to prevent Al precipitation, and the final pH was adjusted to 4.5 with HCl. A control group of plants was maintained in the same nutrient solution at a pH of 4.5, but without the addition of aluminum.

2.1.2.2 Silicon condition

The modified Magnavaca nutrient solution contained 50 µM or 100 µM $AlCl_3$ supplemented with 1 mM Si ($NaSiO_3$). Solution pH was adjusted to 4.5 with HCl before $NaSiO_3$ added and adjusted to 4.5 again.

2.1.2.3 Fluridone treatment

Fluridone cannot be dissolved in water. To obtain a 100 mM fluridone stock solutions, it was first dissolved in 3 ml DMSO. After the addition of 3 ml TWEEN 20, this solution was filled to 50 ml with water. In this way, fluridone could be completely dissolved in water. Six-day-old plants were transferred to a modified Magnavaca nutrient solution in the presence of 10 µM fluridone. Fluridone was added after adjusting pH to 4.5.

2.2 Harvest and zone segregation of roots

After 10 days of growth, the seedlings were harvested and the lengths of their roots and shoots were recorded. Shoot refers to all the above ground plant material including leaves. The seminal roots of the barley were then segmented into three distinct zones based on relative suberin deposition and cut with fresh razor blades, (Figure 2.1C), as previously described by Kreszies et al. (2019). The harvested roots were then subjected to histochemical analysis, analytical procedures, real-time quantitative PCR (RT-qPCR), and elemental variation analysis.

2.3 Histochemical analysis

Histochemical analysis was performed on the barley roots along their length to detect the presence of suberin lamellae. Seminal roots were cut into pieces of 1 cm length, which contained the region of interest and immersed in fixation solution (4% paraformaldehyde in 1XPBS), and immediately vacuum infiltrate samples for 1h then overnight at 4 °C. After fixation, samples were washed three times in 1XPBS. Fixed samples were incubated in ClearSee solution by gently shaking at room temperature for 5 days. Exchange the ClearSee solution regularly, until solution remains clear.

The visualization of suberin lamellae was accomplished through the utilization of Fluorol Yellow 088 (FY) staining. This particular dye is known to specifically stain lipid structures in a bright yellow hue, thereby imparting contrast to suberin lamellae (Brundrett et al., 1991). FY stock solution was prepared by dissolving 1% FY in DMSO. the FY stock solution was diluted to a 0.01% FY working solution using ethanol and stored at 4°C in darkness. For suberin staining, fixed and cleared tissue was rinsed once in ddH_2O and immersed in 0.01% FY solution for 30 min at room temperature, stained samples were washed three times in ddH_2O and the green fluorescence signal was observed using a confocal laser scanning microscope (FV1000, Olympus, Japan). For cross-sectioning, stained root fragments were embedded in 5% agarose and sectioned by hand or by a vibratome. Cross-sections were observed under UV light with an epifluorescence microscope (Zeiss AxioPlan, Carl Zeiss, Germany). Images were captured using a Canon EOS 600D SLR camera (Canon Inc., Tokyo, Japan)

ClearSee solution

Compound	Concentration, w/v
Xylitol Powder	10%
Sodium Deoxycholate	15%
Urea	25%

1XPBS (pH=7.4)

Compound	Concentration
NaCl	137 mM
KCl	2.7 mM
Na_2HPO4	10 mM
KH_2PO4	1.8 mM

For Al staining, roots were stained in 0.01% morin for 30 min, then excised and embedded in 5% (w/v) agarose. Root tips were transversely sectioned from the apex, and the green fluorescence signal was observed using a confocal microscope (FV1000, Olympus).

2.4 Chemical analytics of suberin in roots

Seminal roots of barley were segregated as elaborated in section 2.2. The chemical composition of suberin in seminal roots of barley was determined by relating the suberin amounts (µg) to the endodermal surface area (cm^2). The endodermal area of each root zone was calculated using the formula, $A = 2\pi rL$ (where r represents the endodermis radius and L represents the length of the individual root zone), endodermis radius of cross-sections of roots were determined by using ImageJ software. In each replicate, about 10 segments were pooled for each zone per treatment and three biological replicates were utilized for each experiment. The seminal root segments underwent enzymatic digestion prior to being analyzed by gas chromatography.

2.4.1 Sample preparation and suberin extraction

Enzymatic cell wall isolation

The cellular components of a typical plant cell wall, such as proteins, aromatic components, cellulose, pectin, lignin, and hemicelluloses, were targeted in the process of wall component separation. The harvested root samples were subjected to an aqueous solution of pH 3 containing cellulase and pectinase along with 1 mM NaN_3 to prevent microbial growth. This process led to the separation of endodermal and hypodermal cell walls. The root samples were vacuum infiltrated and continuously shaken in the enzyme solution, which was changed every 3-5 days for a period of three weeks.

To remove soluble phenolic compounds, borax buffer (0.01 M sodium tetraborate) of pH 9 was added, and after two days, the isolated cell walls were suspended in a chloroform/methanol solution (1:1) to remove soluble lipids. The solution was changed every two or three days for a week. Finally, the root samples were dried on PTFE in a

desiccator. The glass vials used for analysis were cleaned with chloroform by placing them horizontally on a rolling bench apparatus for more than 20 min at 100 rpm. The chloroform was then dispensed and the vials were completely dried. The dry weights of the samples were determined with high accuracy using the Sartorius MC 21S weighing balance with a maximum error of ±1 µg. A maximum of 5 mg of the samples was used for analysis.

Enzyme solution

Compound	Concentration
Citric acid	10 mM
Cellulase	0.5%, w/v
Pectinase	0.5%, w/v
Sodium azide	1 mM

Transesterification with BF_3/MeOH

The process of transesterification was conducted on root samples to release suberin monomers. The addition of BF_3/MeOH led to the formation of aromatic monomers and esterified long-chain fatty acid derivatives, including ω-hydroxy acids and α,ω-dicarboxylic acids, which are constituents of the typical suberin polymer (Zeier and Schreiber, 1997). The transesterification reaction involves the initial protonation of the ester, followed by replacement with an alcohol.

The samples were transesterified in a vial containing 4-9 ml of the BF_3/MeOH solution for a duration of 16 hours at a temperature of 70 °C in a heat block. After this period, the vials were removed from the heat block and allowed to cool down to room temperature. 50 µl of internal standard dotriacontane was added to each transesterified solution, followed by vortexing. The transesterification reaction was subsequently terminated by

transferring the samples to a vial containing 2 ml of saturated $NaHCO_3/H_2O$ solution, which was added slowly to prevent the formation of gas bubbles.

Extraction with chloroform

To extract the polar suberin monomer, 1-2 ml of chloroform was added to the vials containing the samples, and the mixture was vortexed to facilitate phase separation. The lower phase was then transferred to clean glass vials and the process was repeated twice. The polar suberin monomer, glycerol, was not extracted with the chloroform and thus remained in the aqueous phase. The extracts were then washed with 1-2 ml of HPLC water, and the upper phase was discarded. The extracts were dried with anhydrous sodium sulphate and transferred to reaction vials. Finally, the extracts were concentrated by evaporating under a nitrogen stream at 60 °C.

Derivatisation of the extracts

The monomers obtained after transesterification and chloroform extraction were modified by N, O-Bis(trimethylsilyl)-trifluoroacetamide (BSTFA) derivatization in order to transform free hydroxyl and carboxyl groups into their trimethylsilyl derivatives. This derivatization process, catalyzed by pyridine, confers thermal stability and volatility to the sample, making it suitable for gas chromatography analysis. 20 µl of pyridine and BSTFA were added to the reaction vials, followed by incubation at 70 °C for 40 min in a heating block, to perform the derivatization of the samples.

2.4.2 Gas chromatography analysis (GC-MS/FID)

Gas Chromatography was utilized to perform quantitative and qualitative analysis of suberin. The analysis was carried out using a combination of GC-Mass Spectrometry (GC-MS, Agilent technologies, 7890B/5977A Series Gas Chromatograph/Mass Selective Detector) and GC-Flame Ionization Detector (GC-FID, Agilent technologies, 6890N Network Gas Chromatography) techniques.

GC-MS was employed to identify the characteristic compounds of suberin utilizing a quadruple mass analyzer that identifies compounds based on mass to charge ratio. The peaks in the chromatograms were identified by comparing the data with a database established in the laboratory of Professor Schreiber at the Department of Ecophysiology, Institute of Cellular and Molecular Botany in Bonn, Germany. Further analysis was aided by the Agilent software, GC/MSD Mass Hunter Acquisition and Mass Hunter and Classic Chem Station Data Analysis.

Temperature profiles of GC-MS for the analysis of suberin

Final temperature °C	Temperature rise °C/min	Temperature hold min
50		2
200	45	1
300	3	15

On the other hand, GC-FID was used to quantify the concentration of suberin monomers from the peak area in the chromatograms. The instrument utilized hydrogen flame as a carrier gas and had a 30 m long and 0.32 mm diameter column coated with 0.1 µm poly (dimethylsiloxane). The derivatized sample of approximately 200 µl volume was transferred to autosampler vials and upon injection of 1 µl of sample, the compounds within the sample disintegrated into free ions and the electric signals were detected at the outlet.

The quality of the column was evaluated by analyzing an acid standard solution containing alkane (C24) and three carboxylic acids (C29, C30, C31) in chloroform. The solution was derivatized and an appropriate temperature profile (Table 7) was adapted for the analysis. The ratio of the area concentration of alkane to that of C31 was calculated and a ratio of ≤ 1.3 was considered indicative of sufficient column quality for future analysis.

2.5 RNA isolation and RT–qPCR analysis

Total RNA was extracted using the NucleoSpin RNA Plant Mini Kit (MACHEREY-NAGEL, Germany). The barley seminal roots under different treatments were cut using newly prepared acetone-treated blades and washed with diethylpyrocarbonate (DEPC)-treated water. Each zone was then cut and collected into a 2 ml RNase free centrifuge tube, and quickly frozen in liquid nitrogen, followed by storage at -80 °C. Add alcohol to a clean mortar and ignite to sterilize it. Then pre-chill the mortar with liquid nitrogen and grind the root samples in liquid nitrogen. Proceed with the protocol provided in the kit. The quality of RNA was assessed using Nanodrop (Thermo Fischer Scientific, USA) and agarose gel electrophoresis. Dilute all RNA samples to the same concentration and employ the RevertAid First Strand cDNA Synthesis Kit (Thermo Fischer Scientific, USA) to perform reverse transcription and synthesize cDNA. Add the following reagents into a sterile, nuclease-free tube on ice and incubate at 65 °C for 5 min by a PCR instrument.

Compound	Concentration
Total RNA	3 μl (1 μg)
Oligo $(dT)_{18}$ primer	1 μl
RNase free water	8 μl

Then put the tube on ice, spin down and put the vial back on ice. Add the following components, incubate at 45 °C for 60 min and terminate the reaction by heating at 70 °C for 5 min. The obtained 20 μl cDNA should be diluted to 60 μl with nuclease-free water. The diluted cDNA can be used directly for qPCR or stored long-term at -20 °C.

Compound	Concentration
Above reaction solution	12 μl
5X Reaction Buffer	4 μl
RiboLock RNase Inhibitor	1 μl
10 mM dNTP Mix	2 μl
RevertAid M-MuLV RT	1 μl

RT–qPCR was performed in a QuantStudio™ 3 Real Time PCR System (Applied Biosystems, Penzberg, Germany) using the my-Budget 5X EvaGreen® QPCR-Mix II kit (Bio-Budget Technologies GmbH, Krefeld, Germany). Add the following reagents into the nuclease-free PCR tube on ice.

Compound	Concentration
5X EvaGreen® QPCR-Mix	4 µl
cDNA	1 µl
Primers	1 µl
nuclease-free water	14 µl

The PCR reaction was conducted under the following conditions: pre-denaturation at 95 °C for 15 minutes; followed by 40 cycles of denaturation at 95 °C for 10 seconds, annealing at 60 °C for 10 seconds, and extension at 72 °C for 10 seconds.

At least three biological replicates of each sample and three technical replicates of each biological replicate were performed to ensure the accuracy of the results. Biological replicates were defined as distinct RNA samples extracted from individual plants, while technical replicates referred to the performance of three qPCR reactions for each sample. Relative expression levels were normalized to zone A of control, which was set as 1. All data were presented as $2^{-\Delta\Delta Ct}$. The reference gene *GADPH* or *Actin* was utilized as an internal control for the analysis. The primer sequences used for RT-qPCR were detailed in the table S1.

2.6 Barley mutants identification

Wild-type barley and barley mutants were germinated under the same conditions for three days, then fresh barley shoots were collected for DNA extraction. DNA was extracted using the NucleoSpin Plant II Mini kit (MACHEREY-NAGEL, Germany) according to the manufacturer's protocol.

Gene-specific primers (table S1) were used to PCR-amplify the *CYP86B1* gene in both wild-type and mutants barley DNA using Q5 High-Fidelity DNA polymerase (New England Biolabs). The PCR reagents used were as follows.

Compound	Concentration
Q5® High-Fidelity 2X Master Mix	12.5 µl
Template DNA	2.5 µl
10 µM Primers (F and R)	2.5 µl
ddH_2O	7.5 µl

The PCR reaction was conducted under the following conditions: pre-denaturation at 98 °C for 30 seconds; followed by 32 cycles of denaturation at 98 °C for 10 seconds, annealing at 66 °C for 15 seconds, and extension at 72 °C for 20 seconds.

The PCR products were analyzed by 1% agarose gel electrophoresis, and correctly sized bands were extracted using the NucleoSpin Gel and PCR Clean-up Mini kit (MACHEREY-NAGEL, Germany). The extracted PCR products were then subjected to Sanger sequencing (Microsynth AG, Switzerland). Resulting FASTA files were proceeded with SnapGene software.

2.7 Leaf pigments and physiological parameters

Leaf pigments (chlorophyll content, flavonoid index, anthocyanin index, and nitrogen balance index) were non-destructively measured using a handheld Dualex® Scientific instrument (Force A DX16641, Paris, France). The quantum efficiencies of photosynthetic electron transport through photosystem II (PhiPS2) were measured using a portable handheld LI-600 porometer system integrated with a fluorometer (LI-COR Biosciences, Lincoln, USA). After transferring barley to the treatment solution, day 0 was set as the starting point. The measurements were conducted every day from 11:30 am to 12:00 pm. Each measurement included 9 or more biological replicates, and the same leaf position of the same leaf was used for each measurement every day.

2.8 Statistical analysis

For multiple comparisons between different treatment, one-way ANOVA was performed followed by Tukey's test for multiple comparison procedures. Binary comparisons were performed using Student t-test. In cases where the data did not meet the linear model assumption, Kruskal-Wallis and non-parametric Tukey's tests were performed for multiple comparisons, and the Wilcoxon-Mann-Whitney test was used for binary comparisons.

3. Results

3.1 Effect of Al stress on root development in barley seedlings

First, the effect of different pH on root development in barley seedlings was investigated. Specifically, the length and dry weight of the seminal roots of 10-day-old barley seedlings were examined under two different pH conditions: pH 4.5 (control) and pH 5.8. The results revealed that there was no significant difference in the length and dry weight of the seminal roots of barley under the two pH conditions (Figure 3.1). However, when the concentration of Al was increased, a noticeable reduction was observed in root length and dry weight as compared to the control group. The length of the seminal roots in the control group was found to be 16.47 ± 5.6 cm, whereas the root lengths in the 50 µM and 100 µM Al treatments were 11.02 ± 4.4 cm and 10.89 ± 4.0 cm, respectively (Figure 3.1A). Similarly, a decrease in root dry weight was also observed, with the control group having a dry weight of 13.68 ± 3.6 mg, while the reductions in the 50 µM and 100 µM Al treatments were to 8.43 ± 2.6 mg and 7.68 ± 1.5 mg, respectively (Figure 3.1B).

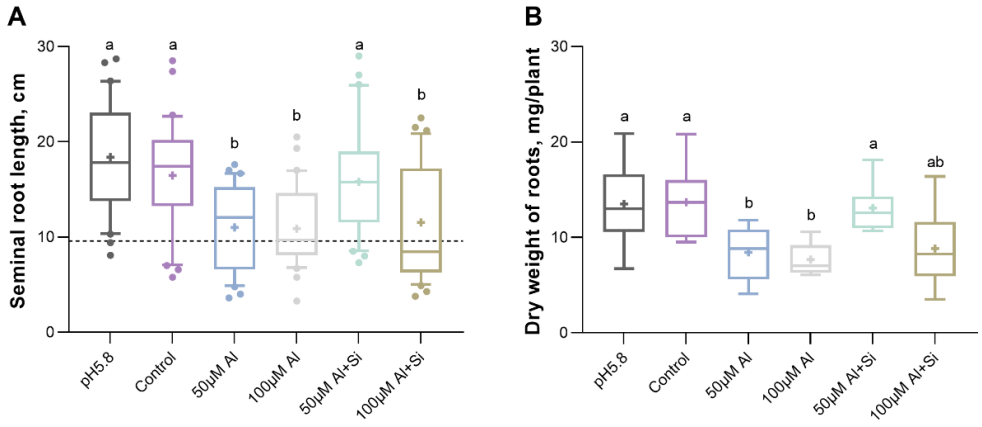

Figure 3.1 Effect of Al and Si on root elongation and dry weight. Seminal root lengths (A) and roots dry weight (B) of 10-d-old barley plants grown under different conditions. The boxes range from the 10 to 90 percentiles. The "+" in the box represents the mean value. The whiskers range to the outliers. The dotted line represents the average root length before processing Error bars represent SD, different letters indicate significant differences ($p < 0.05$).

Upon conducting further analysis, it was discovered that the addition of silicon to the solution medium containing 50 µM Al resulted in a seminal root length and dry weight of barley seedlings that were comparable to those observed in the control group. However, it was observed that the growth inhibition caused by 100 µM Al was not significantly improved with the addition of 1 mM Si. These results indicate that the growth of barley seminal roots is highly sensitive to Al stress and that Si supplementation can mitigate the adverse effects of Al stress to some extent.

3.2 Effect of Al stress on barley endodermal suberization

3.2.1 Suberization of barley roots under different conditions

The staining technique, Fluorol Yellow 088, was employed to highlight the suberin lamellae, which were identified as bright yellow deposits across endodermal cells (Figure 3.2 and 3.3). Upon examining barley roots grown in a nutrient solution at pH 5.8, it was observed that there was no suberin deposition in the younger root zone up to 25% of the relative root length (Zone A). Zone B (25-50%) exhibited patchy suberization, with only some cells displaying suberin deposits. Zone C (50-100%) was identified as the mature part of the root near the root base, where all endodermal cells were characterized by suberin deposits (Figure 3.2). In contrast, the control group plants that were grown at pH 4.5 exhibited reduced suberization, with a delayed and mainly discontinuous suberization pattern (Figure 3.2 and 3.3).

Compared to the control group, it was observed that plants grown under 50 µM Al and 100 µM Al stress conditions exhibited earlier and more rapid development of suberin lamellae, which led to a stage of continuous suberization at just 20% of the root length. In contrast, when roots were grown under 50 µM or 100 µM Al stress with the additional application of Si, the number of suberized cells in the endodermis was significantly lower in comparison to the 50 µM Al stress conditions without the additional application of Si (Figure 3.2 and 3.3).

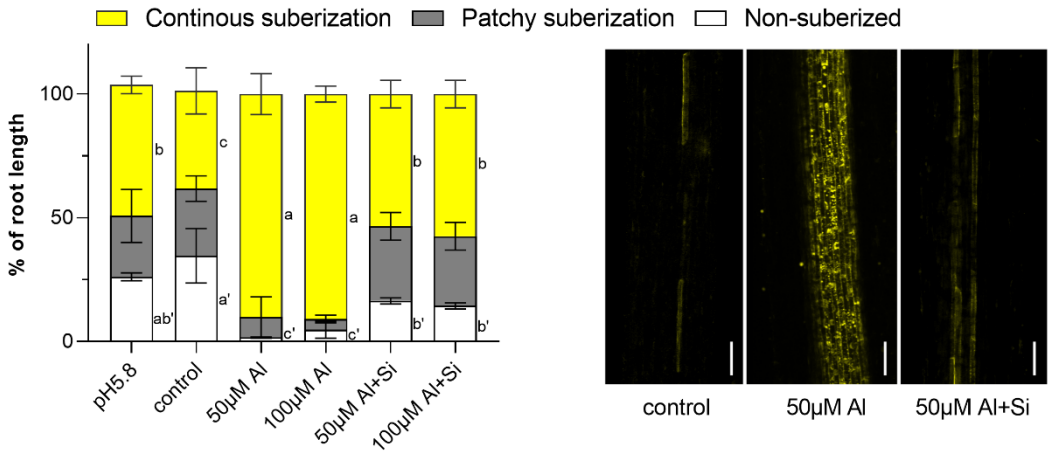

Figure 3.2 FY staining and suberization of barley roots under different conditions. Pictures taken in similar parts of the roots. The scale bar represents 100 µm. Suberin deposition was quantified along the root axis, using three different zones: non-suberized, patchy, and continuous. Data are presented as percentage of root length. Error bars represent SD, different letter indicate significant differences ($p< 0.05$).

3.2.2 Chemical analysis of suberin in response to Al stress

The chemical analysis of suberin content in roots involved dividing the roots into three zones (A, B, and C), based on microscopic staining observations. Zone A corresponded to 0-25% of the total root length, while Zone B and Zone C corresponded to 25-50% and 50-100%, respectively. Ten root fragments were combined from each zone to form a replicate, and three biological replicates were conducted for each zone per treatment.

At first the impact of different pH conditions on suberin biosynthesis was examined. The results indicate that there is no significant difference in the total amounts of aliphatic and aromatic suberin in barley seminal roots grown in nutrient solution at pH 4.5 or 5.8 (as depicted in Figure 3.4). Therefore, it can be concluded that pH does not significantly affect the production of suberin in barley roots.

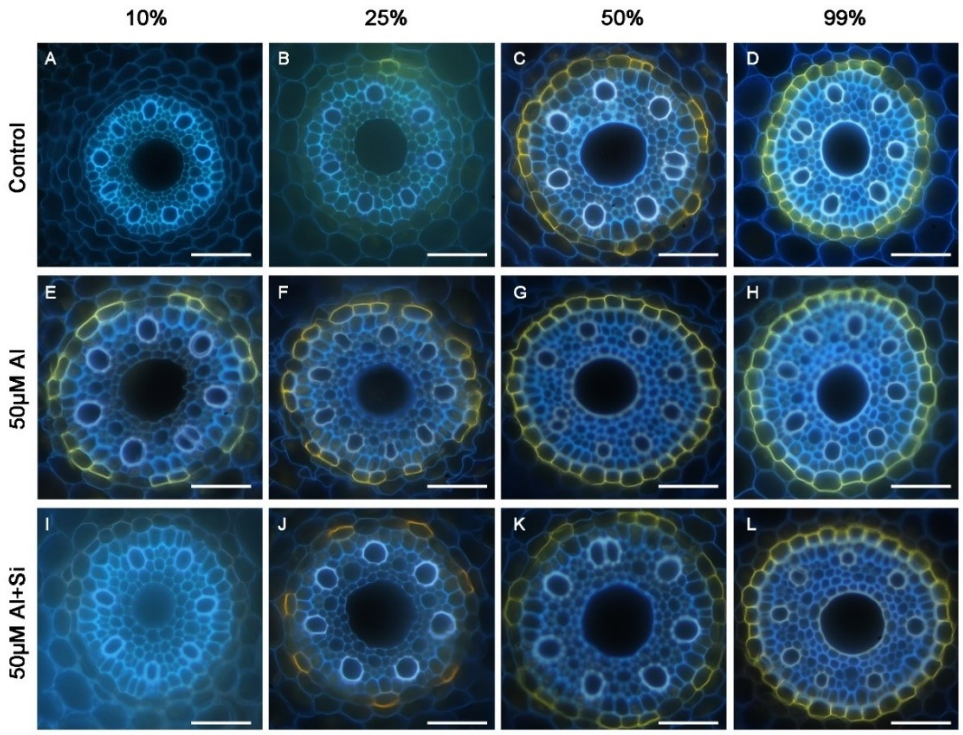

Figure 3.3 Development of suberin lamellae in the endodermis of barley seminal roots. Suberin lamellae in roots grown under different conditions were stained with FY088. The presence of suberin lamellae is indicated by a bright yellow fluorescence. At 12.5% of relative root length (A, E, I), at 25% of relative root length (B, F, J), at 50% of relative root length (C, G, K), and the end of the root (D, H, L). The scale bar represents 50 µm.

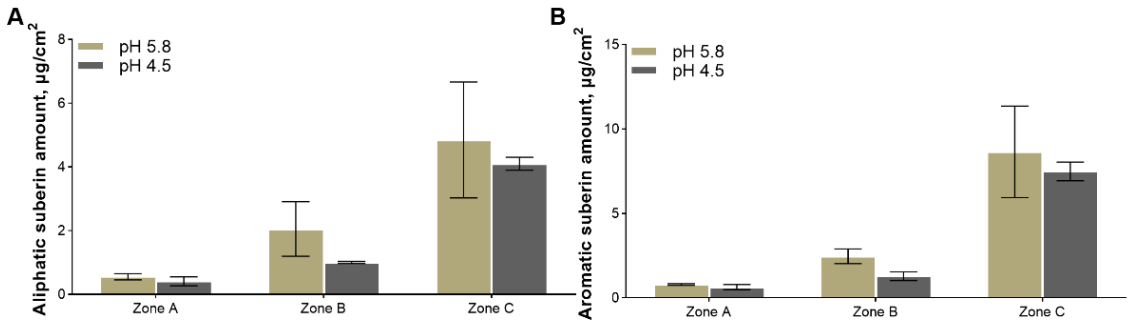

Figure 3.4 Total amounts of suberin in barley roots grown under different pH conditions. Total amounts of (A) aliphatic and (B) aromatic suberin in barley seminal roots grown in nutrient solution at pH 4.5 or 5.8. Results are shown as mean expression ±SD of three biological replicates. No significant difference was detected.

An analysis of the aliphatic suberin monomer composition in various zones of barley roots grown under distinct pH conditions was also conducted (Figure 3.5). The aliphatic suberin monomers consist of diverse classes, including alcohols, diacids, fatty acids, and ω-hydroxy acids. The results indicate no significant differences in the levels of primary alcohols, fatty acids, α–ω dicarboxylic acids, and ω-hydroxy acids in different zones of barley roots grown at pH 4.5 or 5.8. As illustrated in Figure 3.6, there was no significant variation in the substance classes of aliphatic suberin in barley seminal roots grown under different pH conditions. Therefore, these findings suggest that pH does not exert a considerable influence on the monomer composition of aliphatic suberin in barley roots.

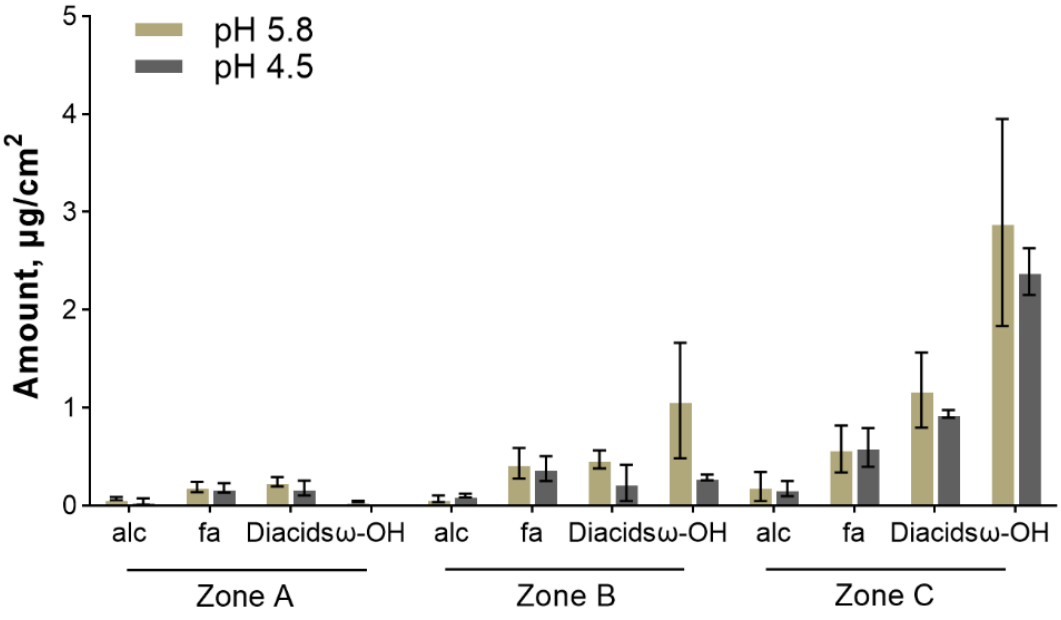

Figure 3.5 Amounts of substance classes of aliphatic suberin in barley seminal roots grown under different pH conditions. Results are shown as mean expression ±SD of three biological replicates. No significant difference was detected. alc, primary alcohols; fa, fatty acids; diacids, α–ω dicarboxylic acids; ω-OH acids, ω-hydroxy acids.

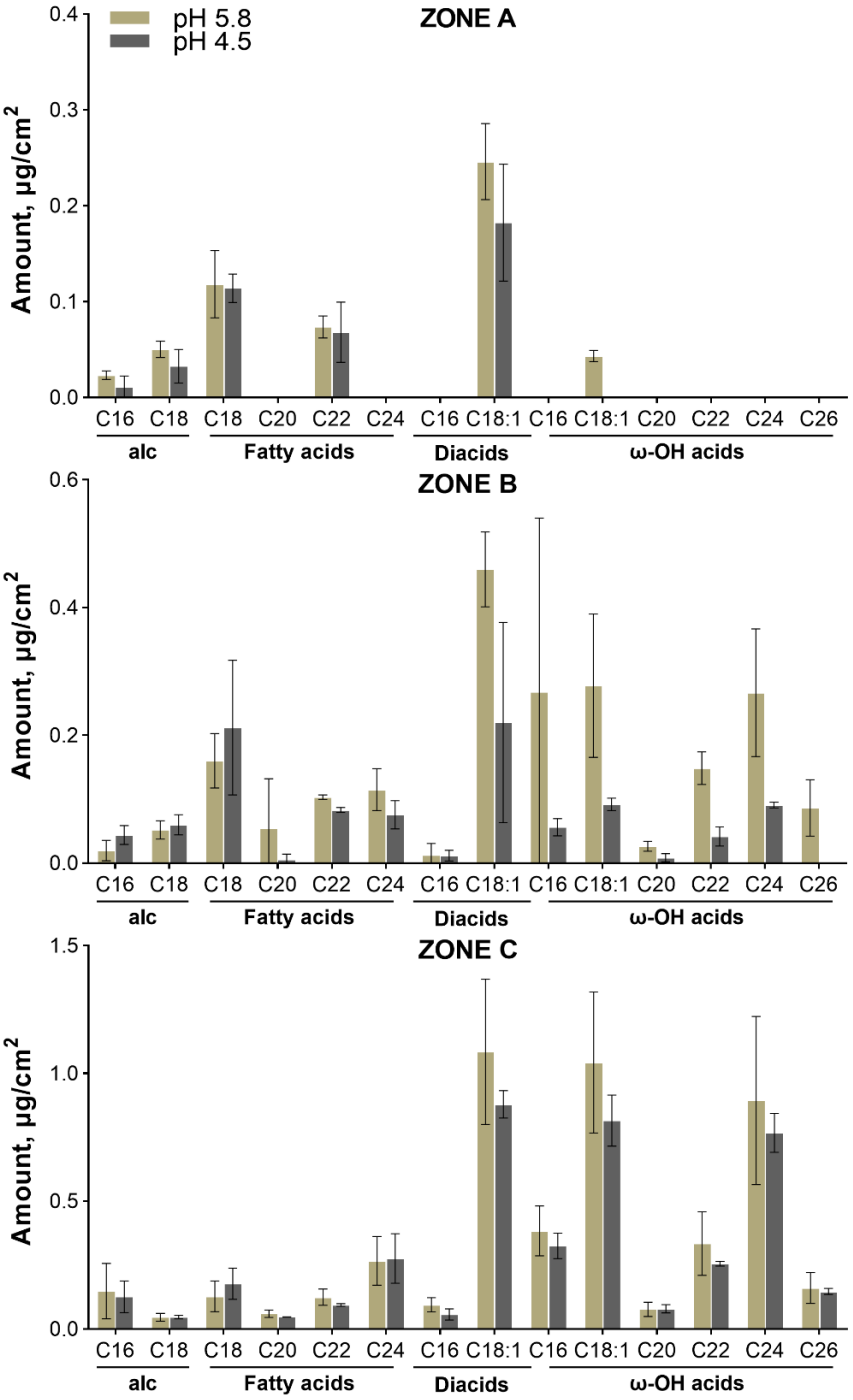

Figure 3.6 Amounts of monomers of aliphatic suberin in different zones of barley roots grown under different pH conditions. Results are shown as mean expression ±SD of three biological replicates. No significant difference was detected. alc, primary alcohols; diacids, α–ω dicarboxylic acids; ω-OH acids, ω-hydroxy acids.

To compare suberin biosynthesis under Al treatments, the amounts of aliphatic and aromatic suberin in barley roots were analyzed (Figure 3.7). The analysis was conducted on barley plants grown under 50 µM or 100 µM Al treatment, with or without Si conditions, and compared to barley plants grown in nutrient solution at pH 4.5, which served as the control. The results indicate that both the total amounts of aliphatic and aromatic suberin in barley seminal roots are significantly affected by Al treatment conditions. In response to Al stress, the seminal roots of barley exhibited a significant increase in aliphatic content along their length (Figure 3.7A). The Al-stressed roots exposed to 50 µM Al displayed a total aliphatic suberin content of 3.47 ± 0.41 µg cm-2 in Zone A, exhibiting an 8.5-fold increase relative to control roots. In Zone B, the total amount was characterized by significant variability, with levels of 4.59 ± 1.27 µg cm^{-2} in 50 µM Al-stressed roots and 5.01 ± 1.69 µg cm^{-2} in 100 µM Al-treated roots, presenting a positive fold change of 4.5 and 5.0, respectively. The concentration of aliphatic content in Zone C varied between 10.22 ± 0.55 and 8.66 ± 0.74 µg cm^{-2} in roots treated with 50 µM Al and 100 µM Al, respectively. However, the total aliphatic suberin content in barley roots grown under conditions that included both Al and Si did not show a significant difference compared to the control group. Specifically, the amounts of aliphatic suberin were higher under the 100 µM Al treatment with Si condition compared to the 50 µM Al treatment without Si condition.

Similarly, the total aromatic suberin content in the Al and Si stressed seminal roots of barley showed an increase compared to the control (Figure 3.7B). In Zone A, the total aromatic suberin content increased 10.9 times and 7.9 times in roots exposed to 50 µM Al and 100 µM Al, respectively, with amounts of 7.13 ± 2.0 and 5.16 ± 1.3 µg cm^{-2}, respectively. There was also a significant increase in both Zone B and C in the total aromatic suberin content of roots treated with either 50 µM or 100 µM Al compared to the control. However, the total aromatic suberin content did not significantly differ in barley roots grown under both Al and Si conditions and the control group. These findings

suggest that the production of both aliphatic and aromatic suberin in barley seminal roots is affected by Al stress and that Si has the potential to alleviate the impact of Al stress on suberin production.

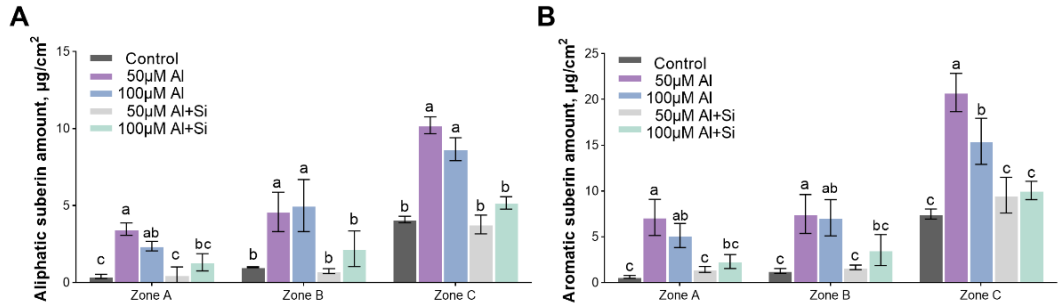

Figure 3.7 Total amounts of suberin in barley roots grown under different treatment conditions. Total amounts of (A) aliphatic and (B) aromatic suberin in barley seminal roots grown under 50 µM or 100 µM Al treatment with or without Si conditions. Barley plants grown in nutrient solution at pH 4.5 presented as control. Results are shown as mean expression ±SD of three biological replicates, different letters indicate significant differences ($p < 0.05$).

The quantities of aliphatic suberin monomers in various regions of barley roots grown under different conditions were analyzed (as presented in Figures 3.8 and 3.9). The aliphatic component of the seminal roots of barley demonstrated a distinct increase in concentration along the root length and in reaction to Al stress. The amounts of α–ω dicarboxylic acids and ω-hydroxy acids considerably increased in all three zones when 50 µM and 100 µM Al were added in comparison to the control group. The highest concentration of ω-hydroxy acids in the control group was observed in Zone C, with a maximum of 2.40 ± 0.24 µg cm^{-2}. The application of Al stress resulted in a significant increase in ω-hydroxy acids in Zone C, with values of 6.44 ± 0.53 µg cm^{-2} and 5.37 ± 0.66 µg cm^{-2} for the 50 µM Al and 100 µM Al treatments, respectively. Likewise, α–ω dicarboxylic acids showed a significant increase in Zone C under Al stress, with values of 2.28 ± 0.11 µg cm^{-2} and 1.86 ± 0.19 µg cm^{-2} for 50 µM Al and 100 µM Al treatments,

respectively. However, no significant change was observed in primary alcohols and fatty acids in response to Al treatment.

Remarkably, the addition of Si in conjunction with 50 µM and 100 µM Al resulted in a decrease in the amounts of all four substance classes of aliphatic suberin in zone A, B, and C compared to the groups exposed to Al stress alone.

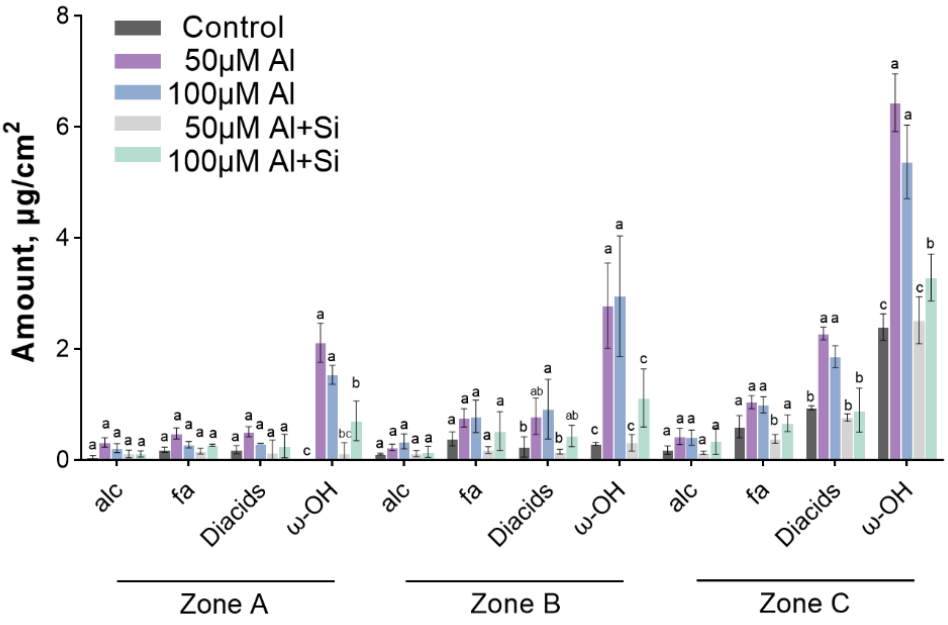

Figure 3.8 Amounts of substance classes of aliphatic suberin in barley seminal roots grown under different conditions. Results are shown as mean expression ±SD of three biological replicates, different letters indicate significant differences ($p < 0.05$). alc, primary alcohols; fa, fatty acids; diacids, α–ω dicarboxylic acids; ω-OH acids, ω-hydroxy acids.

The individual monomeric units with the entire aliphatic composition have been shown in Figure 3.9. C18 α–ω dicarboxylic acids and C18 ω-hydroxy acids were found to be the most abundant components in roots grown under Al stress in all three zones. Of all the components, C18 ω-OH showed the highest upregulation under Al treatment, with fold changes of 12.84 and 7.26 in response to 50 µM and 100 µM Al treatments, respectively. The second highest upregulated component was C16 ω-OH, with fold changes of 11.02 and 6.74 under 50 µM and 100 µM Al treatments, respectively. The vast majority of the

ω-hydroxy acids were significantly increased. These results suggest that the suberin monomer components are differentially regulated in response to Al stress, with a particular sensitivity of ω-hydroxy acids to Al exposure.

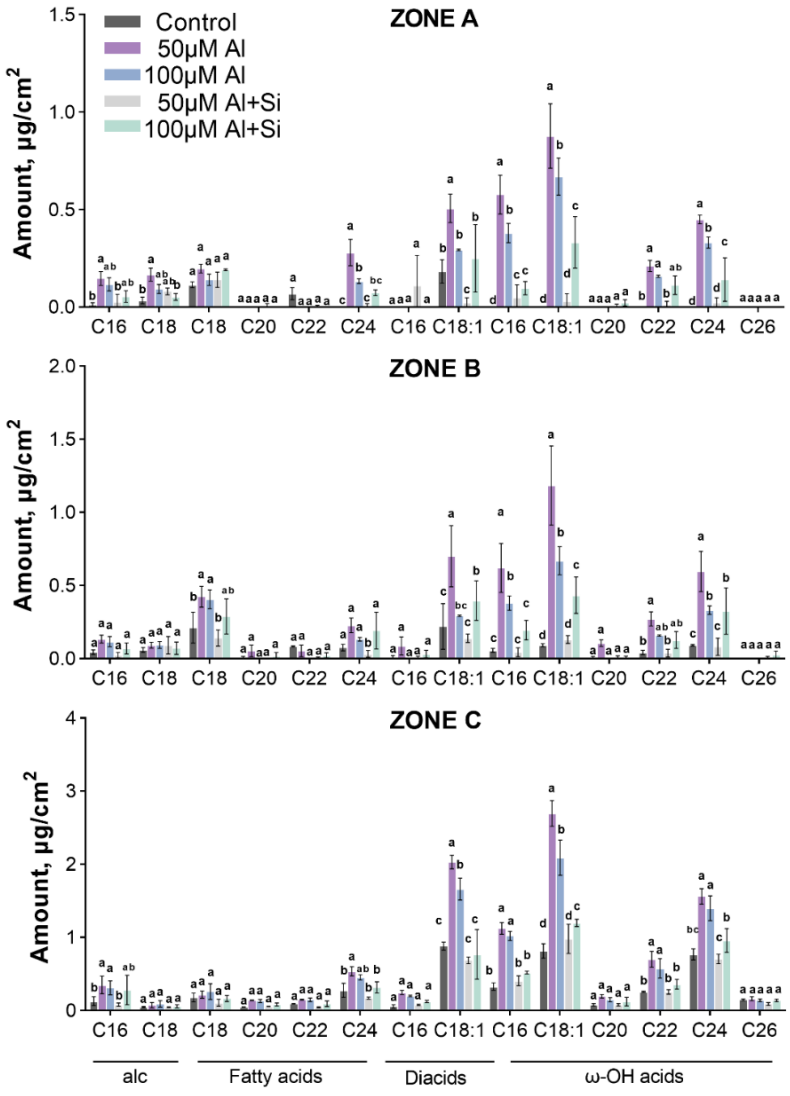

Figure 3.9 Amounts of monomers of aliphatic suberin in different zones of barley roots grown under different treatment conditions. Barley plants grown under 50 μM or 100 μM Al treatment with or without Si conditions (at pH 4.5). Barley plants grown in nutrient solution at pH 4.5 presented as control. Results are shown as mean expression ±SD of three biological replicates, different letters indicate significant differences ($p < 0.05$). alc, primary alcohols; diacids, α–ω dicarboxylic acids; ω-OH acids, ω-hydroxy acids.

3.3 Al enhanced suberin development is related to ABA

3.3.1 Expression of suberin and ABA related genes in response to Al stress

A search of online data obtained from RNA-sequencing analysis by Szurman-Zubrzycka et al., 2021 was conducted to establish the signalling pathways involved in Al-induced suberization. The results show the expression levels of selected suberin-biosynthesis genes in barley plants under different treatment conditions, as presented in Figure 3.10. The expression profile for each gene is presented as the log-ratio of signal intensity (log2 treat/control). The treatments included long-term exposure to 10 µM Al^{3+} at pH 4.0 (Al long-term), short-term exposure to 10 µM Al^{3+} at pH 4.0 (Al short-term), long-term exposure to low pH (pH 4.0) for 7 days (low pH long-term), short-term exposure to low pH (pH 4.0) for 24 h (low pH short-term), and control at pH 6.0. The selected genes include *KCS* (*β-Ketoacyl-CoA Synthase*), *CYP* (*Cytochrome P450*), *GPAT* (*Glycerol-3-phosphate Acyltransferase*), *ABCG* (*ATP-binding Cassette Transporter G*), and *FAR* (*Fatty acyl-coA Reductase*).

According to the results of the RNA-sequencing analysis, certain suberin-biosynthesis genes in barley roots were found to be up-regulated under long-term Al treatment. Specifically, *CYP86B1* showed a log-ratio of 3.64, while *KCS1* and *GPAT4* had log-ratios of 2.07 and 3.18, respectively. *GDSL*, a gene that encodes a lipid hydrolysis enzyme involved in suberization, driving root suberin plasticity., exhibited the highest up-regulation with a log-ratio of 6.63 under Al long-term treatment. On the other hand, there were no significant changes observed in gene expression under low pH short-term treatment or Al short-term treatment. These results suggest that suberin-biosynthesis genes in barley roots are differentially regulated in response to Al treatment.

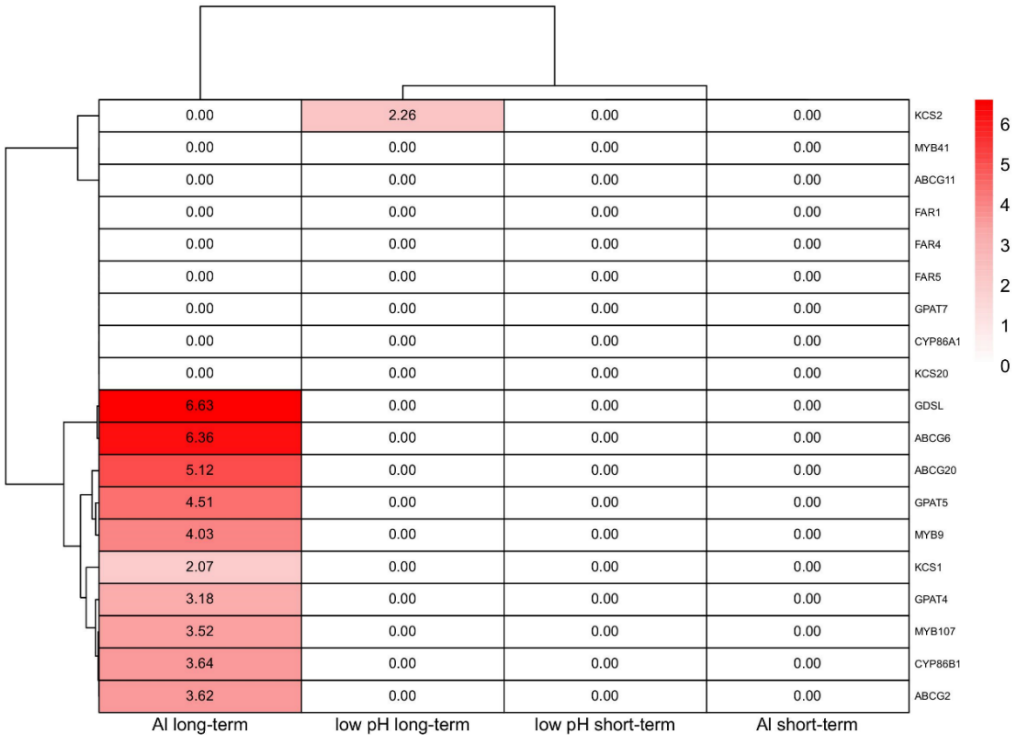

Figure 3.10 Expressions of selected suberin-biosynthesis genes of barley under different conditions. Expression data were obtained from (Szurman-Zubrzycka et al., 2021). The expression profile for each gene is shown as the log-ratio of signal intensity (log2 treat/control). Al long-term, 10 µM Al^{3+} for 7 days at pH 4.0; Al short-term, 10 µM Al^{3+} for 24 h at pH 4.0; low pH long-term, 7 days at pH 4.0; low pH short-term, 24 h at pH 4.0; control at pH 6.0. Gene annotation: *KCS*, *β-Ketoacyl-CoA Synthase*; *CYP*, *Cytochrome P450*; *GPAT*, *Glycerol-3-phosphate Acyltransferase*; *ABCG*, *ATP-binding Cassette Transporter G*; *FAR*, *Fatty acyl-coA Reductase*.

The expression of ABA-related genes in barley under different conditions was also investigated (Figure 3.11). The expression of ABA-related genes in barley was investigated under different conditions. *AHG1* (*ABA-hypersensitive germination 1*), a putative protein phosphatase 2C; *ABF2* (*Abscisic Acid Responsive Element-binding Factor 2*), a transcription factor that interacts with ABA-responsive element sequences; and *RBOHD* (*Respiratory Burst Oxidase Homologue D*), a gene involved in reactive oxygen species production, were upregulated under both long-term Al and low pH conditions. *NCED* (*Nine-Cis-Epoxycarotenoid Dioxygenase*), which encodes a key

enzyme in ABA biosynthesis; *PP2C* (*Protein Phosphatase 2c*), a negative regulator of ABA signaling; *ABI4* (*ABA-Insensitive 4*), a transcription factor involved in ABA signaling; *ABF1* (*Abscisic Acid Responsive Element-binding Factor*) and *AREB3* (*ABA-Responsive Element Binding Protein 3*), transcription factors that interact with ABA-responsive element sequences; *ABA4* (*Abscisic Acid-deficient 4*); *HB5* (*Homeobox Protein 5*), a homeobox transcription factor; *ERF7* (*Ethylene Response Factor 7*); *PLC1* (*Phospholipase C 1*), a phospholipase involved in ABA signaling showed increased expression only under long-term Al conditions. These results suggest that ABA signaling plays a role in the response of barley to Al stress.

The expression of suberin and ABA-related genes in barley roots subjected to different treatments was examined using RT-qPCR (refer to Figure 3.12 and 3.13). Barley roots of 6 days old were exposed to a nutrient solution that contained either 0 M $AlCl_3$ (control), 50 µM $AlCl_3$, or 50 µM $AlCl_3$ with 1 mM Si at pH 4.5 for 4 more days, and then RNA was extracted from three distinct root zones.

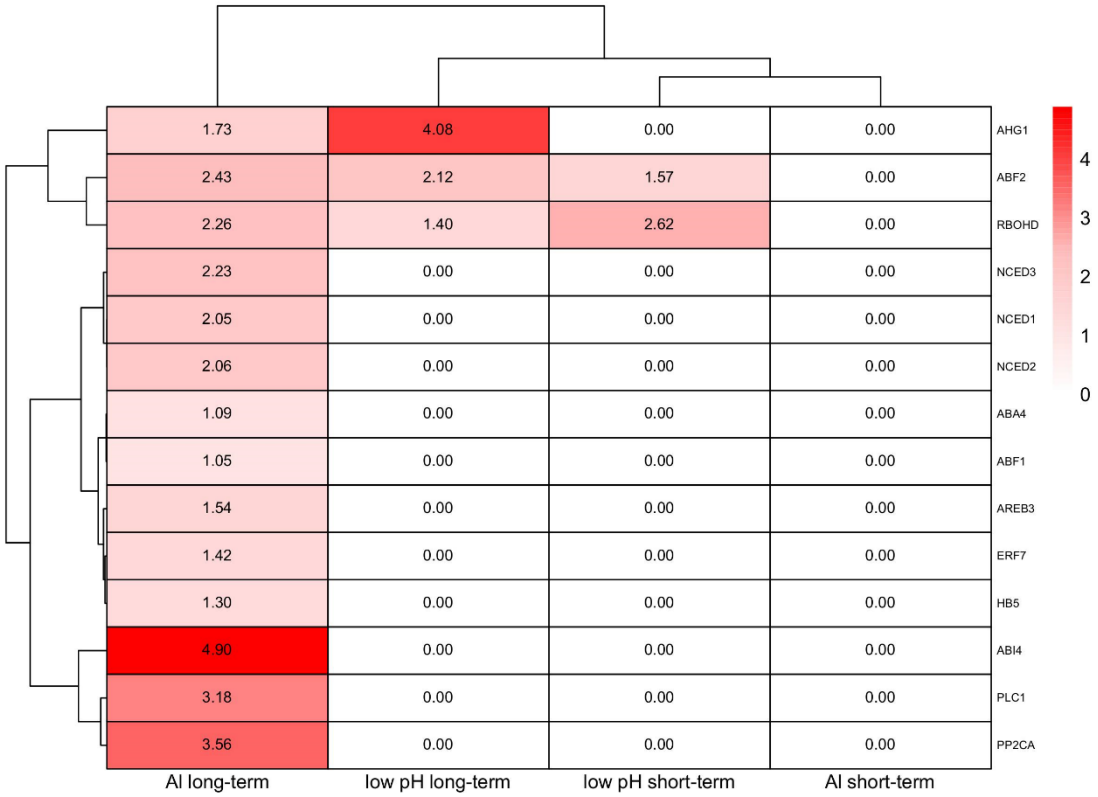

Figure 3.11 Expressions of ABA related genes of barley under different conditions. Expression data were obtained from (Szurman-Zubrzycka et al., 2021). The expression profile for each gene is shown as the log-ratio of signal intensity (log2 treat/control). Al long-term, 10 μM Al^{3+} for 7 days at pH 4.0; Al short-term, 10 μM Al^{3+} for 24 h at pH 4.0; low pH long-term, 7 days at pH 4.0; low pH short-term, 24 h at pH 4.0; control at pH 6.0. Gene annotation: *NCED*, *Nine-Cis-Epoxycarotenoid Dioxygenase*; *PP2C*, *Protein Phosphatase 2c*; *ABI4*, *ABA-Insensitive 4*; *ABF*, *Abscisic Acid Responsive Element-binding Factor*; *ABA4*, *Abscisic Acid-deficient 4*; *AREB3*, *ABA-Responsive Element Binding Protein 3*; *HB5, Homeobox Protein 5*; *ERF7, Ethylene Response Factor 7*; *PLC1*, *Phospholipase C 1*; *RBOHD*, *Respiratory Burst Oxidase Homologue D*.

Initially, two key genes, *CYP86A1* and *CYP86B1*, involved in suberin synthesis, were analyzed (Figure 3.12). These results show that under Al treatment, *CYP86A1* had upregulation only in zone A, while displaying no significant changes in other zones, consistent with previous transcriptomic sequencing findings. Interestingly, with Si addition under Al treatment, the expression of *CYP86A1* was significantly upregulated in all zones. On the other hand, the expression of *CYP86B1* was significantly upregulated in zones A and B under Al treatment, showing 3.2- and 4.1-fold increases, respectively. However, there was no significant difference in the expression of *CYP86B1* between the Si-supplemented Al treatment and control group.

Next ABA related genes were examined using the same RNA sample (Figure 3.13). The results demonstrated that the expression of ABA biosynthesis-related genes, *NCED1*, *NCED2*, and *Abscisic Aldehyde Oxidase* (*Ao5B*), which encodes the final enzyme in the ABA biosynthesis pathway, was significantly induced by Al treatment, especially in zone A and B. In contrast, the addition of Si decreased their expression levels. Similarly, the negative regulator of ABA, *PP2C4* showed a similar expression profile. Furthermore, *β-Glucosidase 8* (*BG8*), which encodes the enzyme responsible for the deconjugation of ABA, was significantly upregulated under Al stress, with the highest expression level

observed in zone A. *ABA-insensitive 5* (*ABI5*) gene expression was also significantly upregulated after Al treatment, more prominently in zones B and C, with no significant change in zone A. In contrast, the relative expression levels of ABA catabolism gene *ABA 8-Hydroxylase 1* (*ABA-OH-1*) and ABA signaling gene *PYR1-like protein 4* (*PYL4*) were significantly downregulated after Al treatment.

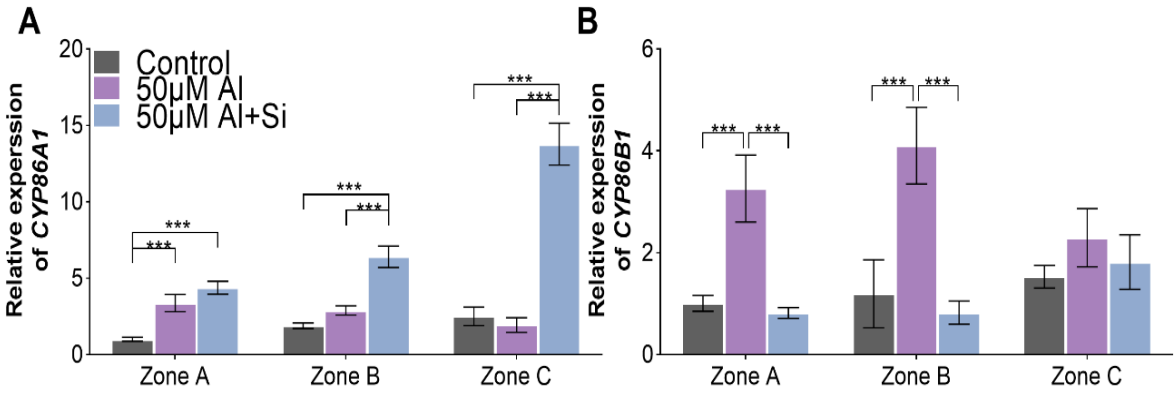

Figure 3.12 Expression analysis of *CYP86A1* and *CYP86B1* genes of barley using qPCR. Barley roots were exposed to a nutrient solution containing 0 M Al (control), 50 µM $AlCl_3$ or 50 µM $AlCl_3$ with 1mM Si additions for 4 days. Barley *ACTIN* expression was used as a control. The gene expressions in zone A under control were arbitrarily fixed at 1. Results are shown as mean expression ±SD of three independent experiments, ***P < 0.001.

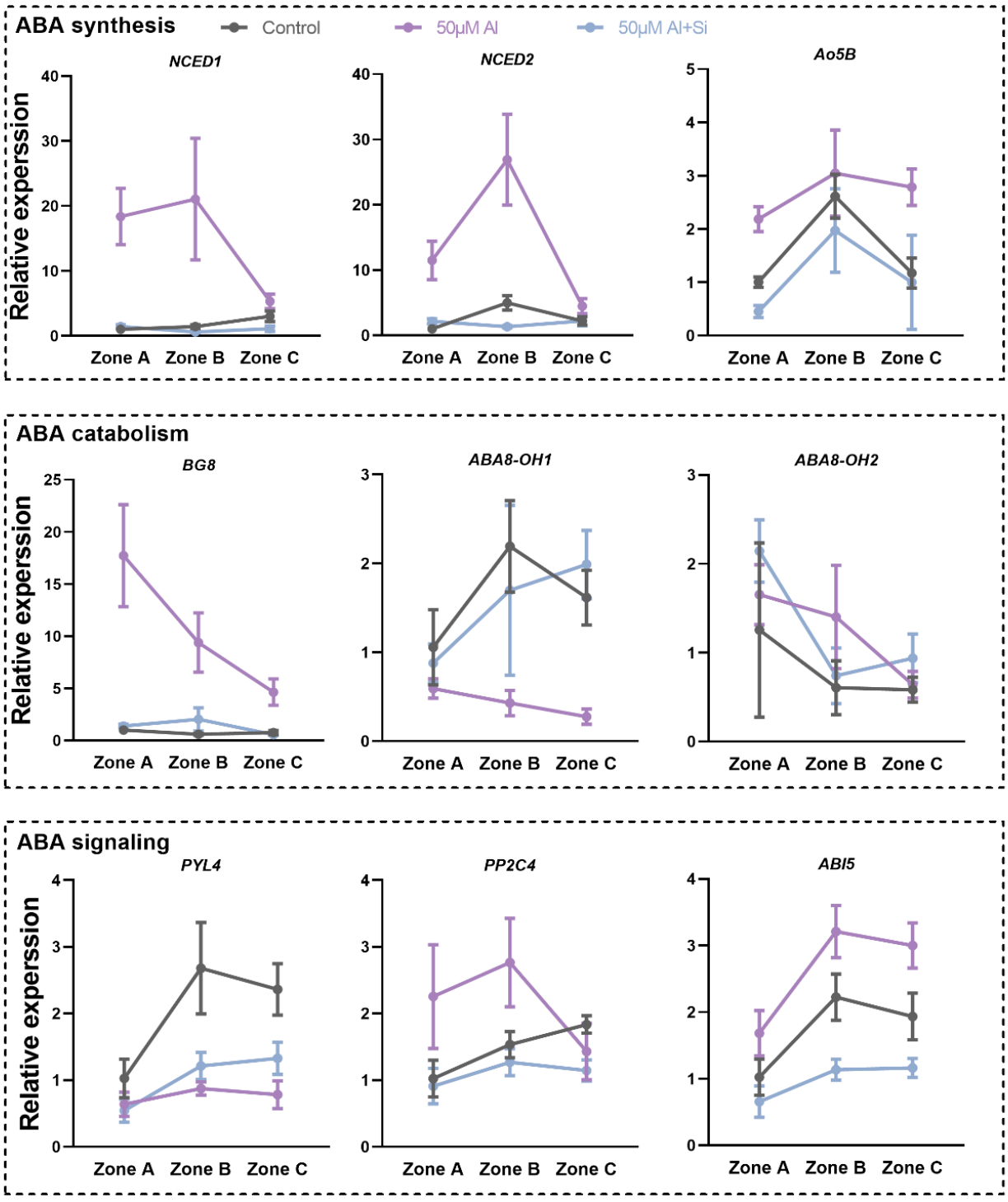

Figure 3.13 Expression analysis of ABA related genes of barley using qPCR. Barley roots were exposed to a nutrient solution containing 0 M Al (control), 50 µM $AlCl_3$ or 50 µM $AlCl_3$ with 1mM Si additions for 4 days. Barley *ACTIN* or *GPDH* expression was used as a control and gene-specifc primers were used for qRT-PCR. Results are shown as mean expression ±SD of three independent experiments. The gene expressions in zone A under control were arbitrarily fixed at 1.

3.3.2 Fluridone suppresses Al-related suberin formation

To investigate the role of ABA in Al-induced suberin formation, the impact of fluridone (Flu) was examined, a substance known to inhibit ABA biosynthesis in barley (Gamble and Mullet, 1986) and other gramineous plants (Hoffmann-Benning and Kende, 1992; Moore and Smith, 1984).

Six-day-old barley plants were cultivated in nutrient solution under various conditions for four additional days. The control group was grown at pH 4.5, while the Al treatment group was grown in the same solution with 50 µM $AlCl_3$. The Al+Flu treatment group was grown in a nutrient solution containing 50 µM $AlCl_3$ and 10 µM fluridone added at pH 4.5, while the Flu treatment group was grown in a nutrient solution containing 10 µM fluridone. The length of the seminal roots of barley seedlings was measured daily after treatment (Figure 3.14). Root elongation gradually increased over time under control conditions, from 2.79 cm on day 1 to 7.72 cm on day 5. In comparison to the control group, Flu treatment significantly inhibited root growth, and root growth was further reduced upon additional Al treatment. The length of the roots was significantly lower than that of the control at all time points, ranging from 0.46 cm on day 1 to 4.71 cm on day 5. Interestingly, there was no significant difference in root growth rate between the Al-treated group and the Al+Flu co-treated group.

To investigate the effect of Flu on suberin biosynthesis under Al treatment, we analyzed the amounts of aliphatic and aromatic suberin in barley roots subjected to different treatments (Figure 3.15). Barley plants were subjected to Flu alone or Flu combined with 50 µM Al treatment. The results showed that there was no significant difference in suberin content in barley roots between the Flu alone treatment and the Flu combined with 50 µM Al treatment, except for aliphatic suberin in Zone B.

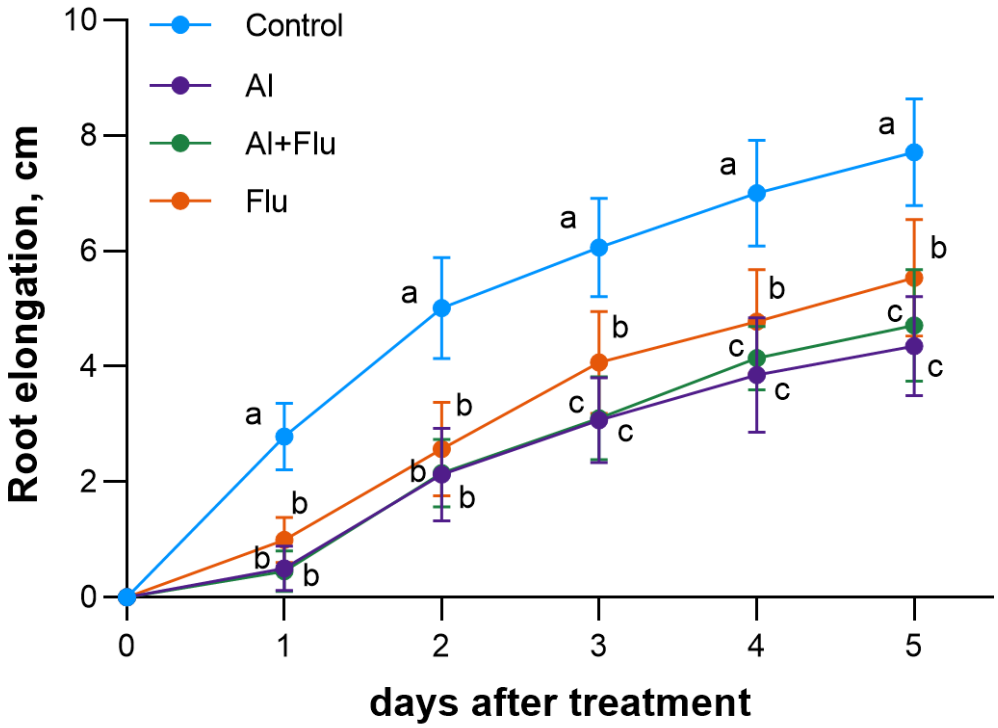

Figure 3.14 Root growth of barley plants grown under different treatment conditions. Control, barley plants grown in nutrient solution at pH 4.5; Al, barley plants grown in nutrient solution containing 50 µM $AlCl_3$ at pH 4.5; Al+Flu, barley plants grown in nutrient solution containing 50 µM $AlCl_3$ and 10 µM fluridone at pH 4.5; Flu, barley plants grown in nutrient solution containing 10 µM fluridone at pH 4.5. Results are shown as mean expression ±SD (n ≥ 50 seminal roots), different letters indicate significant differences ($p < 0.05$).

Specifically, the roots exposed to 50 µM Al with 10 µM Flu showed a total aliphatic suberin content of 1.32 ± 0.33 µg cm^{-2} in Zone A, 2.51 ± 0.64 µg cm^{-2} in Zone B, and 2.72 ± 0.35 µg cm^{-2} in Zone C, respectively. The aromatic suberin content was 5.89 ± 1.47 µg cm^{-2} in Zone A, 7.59 ± 1.11 µg cm^{-2} in Zone B, and 13.50 ± 0.25 µg cm^{-2} in Zone C, respectively. However, compared to the Al alone treatment (aliphatic suberin: Zone A, 3.47/ Zone B, 4.59/ Zone C, 10.22; aromatic suberin: Zone A, 7.13/ Zone B, 7.49/ Zone C, 20.77. As shown in Figure 3.7), the Al+Flu treatment led to a much lower suberin content in barley roots.

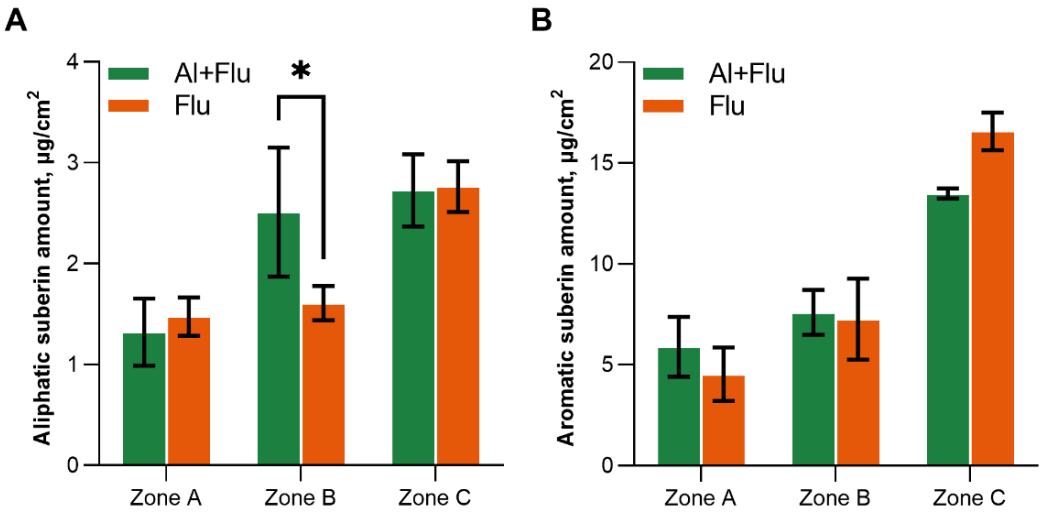

Figure 3.15 Total amounts of suberin in barley roots grown under different treatment conditions. Total amounts of (A) aliphatic and (B) aromatic suberin in barley seminal roots grown under 10 µM fluridone treatment with or without 50 µM $AlCl_3$ conditions. Results are shown as mean expression ±SD of three biological replicates, *P < 0.05.

An analysis of the composition of aliphatic suberin monomers in various zones of barley roots grown was conducted under distinct flu conditions (Figure 3.16). The aliphatic suberin monomers comprise diverse classes, including alcohols, diacids, fatty acids, and ω-hydroxy acids. These results indicate that there were no significant differences in the levels of primary alcohols, fatty acids, α-ω dicarboxylic acids, and ω-hydroxy acids in different zones of barley roots grown under Flu alone treatment and the Flu combined with 50 µM Al treatment. Similarly, the addition of Flu during Al treatment significantly decreased the levels of various aliphatic suberin monomers compared to the Al treatment alone (Figure 3.16 and 3.8).

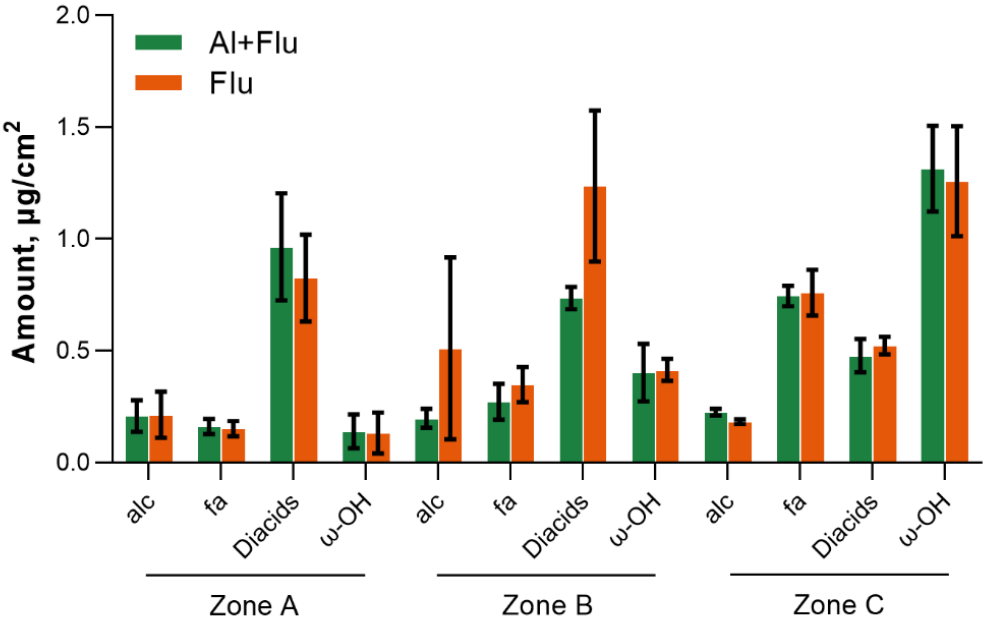

Figure 3.16 Amounts of substance classes of aliphatic suberin in barley seminal roots. Al+Flu, barley plants grown in nutrient solution containing 50 µM $AlCl_3$ and 10 µM fluridone at pH 4.5; Flu, barley plants grown in nutrient solution containing 10 µM fluridone at pH 4.5. Results are shown as mean expression ±SD of three biological replicates. No significant difference was detected. alc, primary alcohols; fa, fatty acids; diacids, α–ω dicarboxylic acids; ω-OH acids, ω-hydroxy acids.

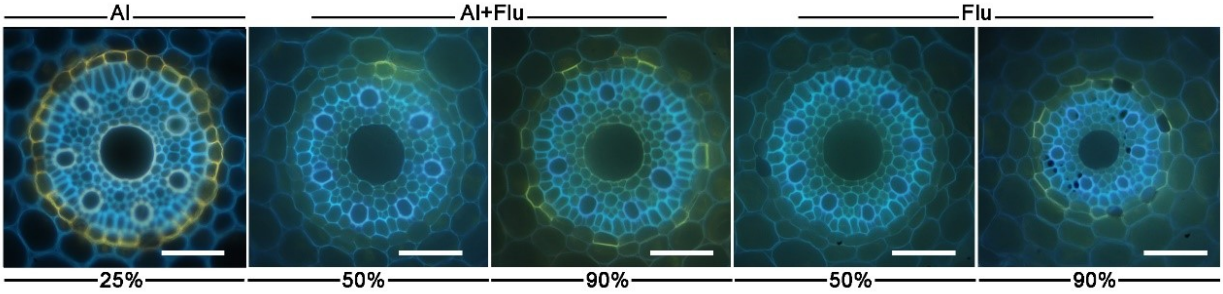

Figure 3.17 Development of suberin lamellae in the endodermis of barley seminal roots. Suberin lamellae in roots grown under different conditions were stained with FY088. The presence of suberin lamellae is indicated by a bright yellow fluorescence. Blue fluorescence indicates autofluorescence. Barley plants were grown under 50 µM $AlCl_3$ (Al), 50 µM $AlCl_3$ with 10 µM fluridone (Al+Flu), and 10 µM fluridone (Flu) treatment. Picture was taken at 25%, 50% or 90% of relative root length. The scale bar represents 50 µm.

Correspondingly, cross sections of barley seminal roots were investigated after FY staining (Figure 3.17). The staining results showed that Flu treatment significantly delayed the appearance of the suberization zone, with the first occurrence of single suberized cells observed only within the range of about 50-60% of root length. Even at the end of the root, complete suberization had not yet formed. Similarly, under the condition of adding flu during Al treatment, the pattern of suberization formation was similar to that of Flu treatment alone. Flu significantly inhibited the promoting effect of Al on suberization.

3.4 Suberin lamellae is a barrier to Al

To obtain evidence regarding the influence of suberin on aluminum transport, morin staining was utililized to localize the entry of aluminum into roots (Figure 3.18). The aluminum-dependent green fluorescence represents the presence of aluminum in both the cell cytosol and nucleus. Barley roots were exposed to either a standalone treatment of 50 μM $AlCl_3$ or a treatment of 50 μM $AlCl_3$ combined with 10 μM Flu. After four days of treatment, the root apices (zone A) were subjected to morin staining and cross sections were observed.

The results showed that, under the standalone Al treatment, green fluorescence was mainly distributed in the root cortex (Figure 3.18A). Conversely, in the case of Al treatment combined with Flu, the green fluorescence in the root cortex was significantly reduced. However, the central cylinder, especially the xylem, exhibited a significant increase in fluorescence compared to roots treated with Al alone. Additionally, interestingly, the epidermal cells of the roots treated with both Al and Flu showed a significant accumulation of Al (Figure 3.18B).

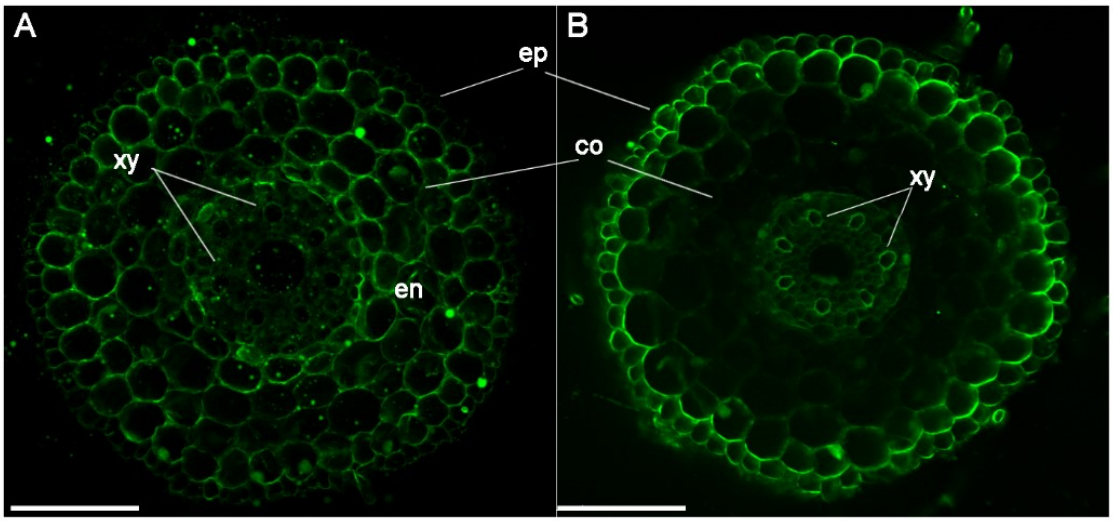

Figure 3.18 Subcellular distribution of aluminum. Al distribution in roots grown under different conditions was stained with morin (green fluorescence). Barley plants grown in nutrient solution containing 50 μM $AlCl_3$ (A) and 50 μM $AlCl_3$ with10 μM fluridone condition (B) for 4 d. Roots were sectioned at 20% of root length from the apex for morin staining and fluorescence observation. Bar = 100 μm. ep, epidermis; co, cortex; en, endodermis; xy, xylem.

3.5 Al tolerance of suberin-defective mutant is affected.

3.5.1 Suberin accumulation is affected in roots of the *cyp86b1* mutants

In this study, two loss-of-function mutants (*cyp86b1-1* and *cyp86b1-2*) were employed in the background of barley cv. Golden Promise. The *cyp86b1-1* alleles contained a 170 bp deletion, while the *cyp86b1-2* alleles contained a 168 bp inversion, resulting in the translation of a truncated protein (as depicted in Figure 3.19).

The difference in root growth between the mutant barley and wild-type barley was analyzed under both Al-treated and untreated conditions (Figure 3.20). The barley plants were first germinated for three days and then grown conventionally for three more days. Subsequently, 6-day-old barley plants were transferred to the treatment solution and allowed to grow for four more days. The control group was treated with a Magnavaca

nutrient solution at pH 4.5, while the Al group was treated with pH 4.5 supplemented with 50 µM $AlCl_3$. Afterward, the roots of 10-day-old barley plants were analyzed.

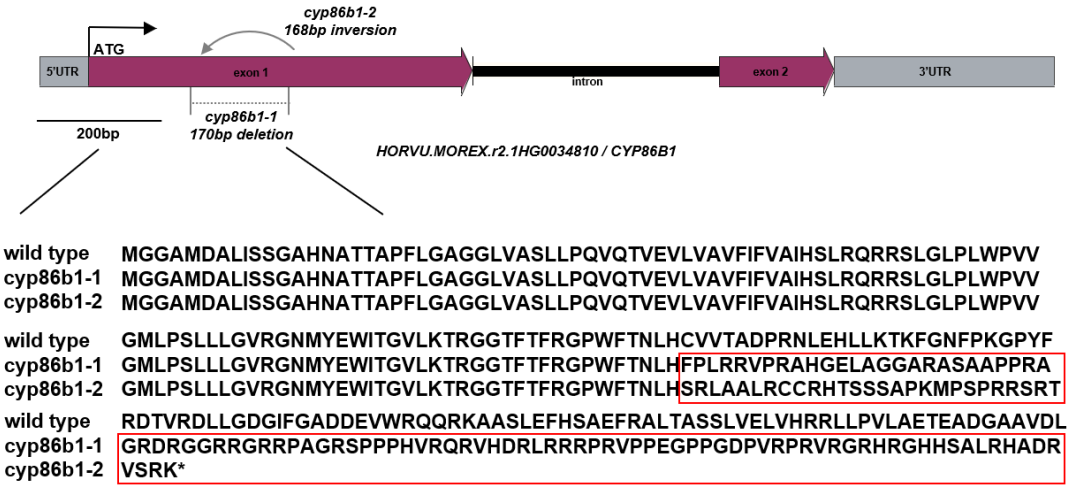

Figure 3.19 Gene structure of *CYP86B1* (*HORVU.MOREX.r2.1HG0034810*) with mutations in *cyp86b1* (*cyp86b1-1*: deletion and *cyp86b1-2*: inversion).

The results showed that, under control conditions, there was no significant difference in root length or dry weight between the *cyp86b1-1* and *cyp86b1-2* mutant barley plants and the wild-type barley plants (Figure 3.20). However, Al treatment significantly inhibited the root growth of both the wild-type and mutant barley plants. Furthermore, under Al treatment, the root length and dry weight of the *cyp86b1-1* and *cyp86b1-2* mutant barley plants were significantly lower than those of the wild-type barley plants.

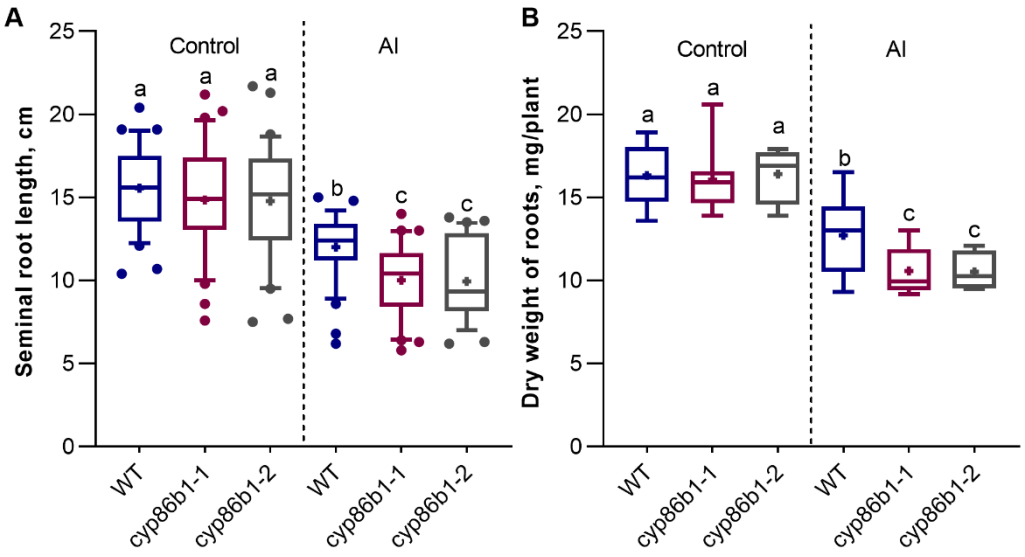

Figure 3.20 Effect of Al on root elongation and root dry weight of wild type and transgenic barley plants. Seminal root lengths (A) and roots dry weight (B) of barley plants grown in nutrient solution (control) or containing 50 µM $AlCl_3$ (Al) at pH 4.5 for 4 days. The boxes range from the 10 to 90 percentiles. The "+" in the box represents the mean value. The whiskers range to the outliers. Error bars represent SD, different letter indicate significant differences ($p < 0.05$).

Next, the aliphatic suberin content in the roots of barley plants treated with Al was analyzed in comparison to the control (Figure 3.21). In the control group without Al treatment, there was no significant difference in aliphatic suberin content between the *cyp86b1-1* and *cyp86b1-2* mutants and the wild-type barley. However, under Al treatment, the aliphatic suberin content in the mutant roots was lower than that in the wild-type barley. Notably, after Al treatment, the aliphatic suberin content in all three zones of *cyp86b1-2* mutant roots was significantly lower than that in the wild-type barley.

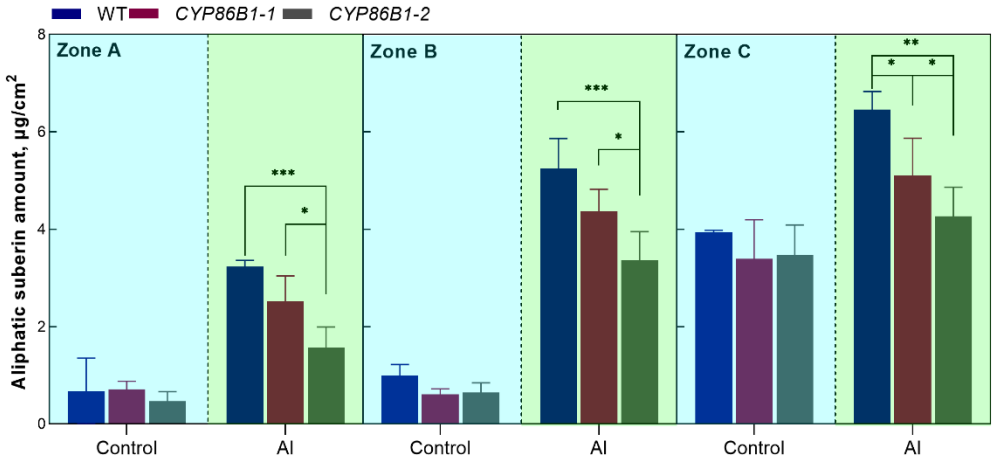

Figure 3.21 Total amounts of suberin aliphatic in wild type and transgenic barley roots. Barley plants were grown in nutrient solution (control) or containing 50 µM $AlCl_3$ (Al) at pH 4.5 for 4 days. Results are shown as mean expression ±SD of three biological replicates, *P < 0.05; **P < 0.01; ***P < 0.001.

The quantities of aliphatic suberin monomers in various regions of different barley roots grown under Al stress were analyzed (as presented in Figure 3.22-24). In Zone A, under control conditions, the C24 FA in the *cyp86b1-1* and *cyp86b1-2* mutants was significantly higher than that in the wild-type, while the other components showed no significant differences. None of the C20-C26 ω-OH was detected in all plants. Upon exposure to Al treatment, the C20-C24 ω-OH in the wild-type barley increased compared to the control group, but remained undetected in the mutants. Furthermore, under Al treatment, the mutants exhibited significantly lower levels of C16 and C18 ω-OH, as well as C18 diacid, compared to the wild-type (Figure 3.22).

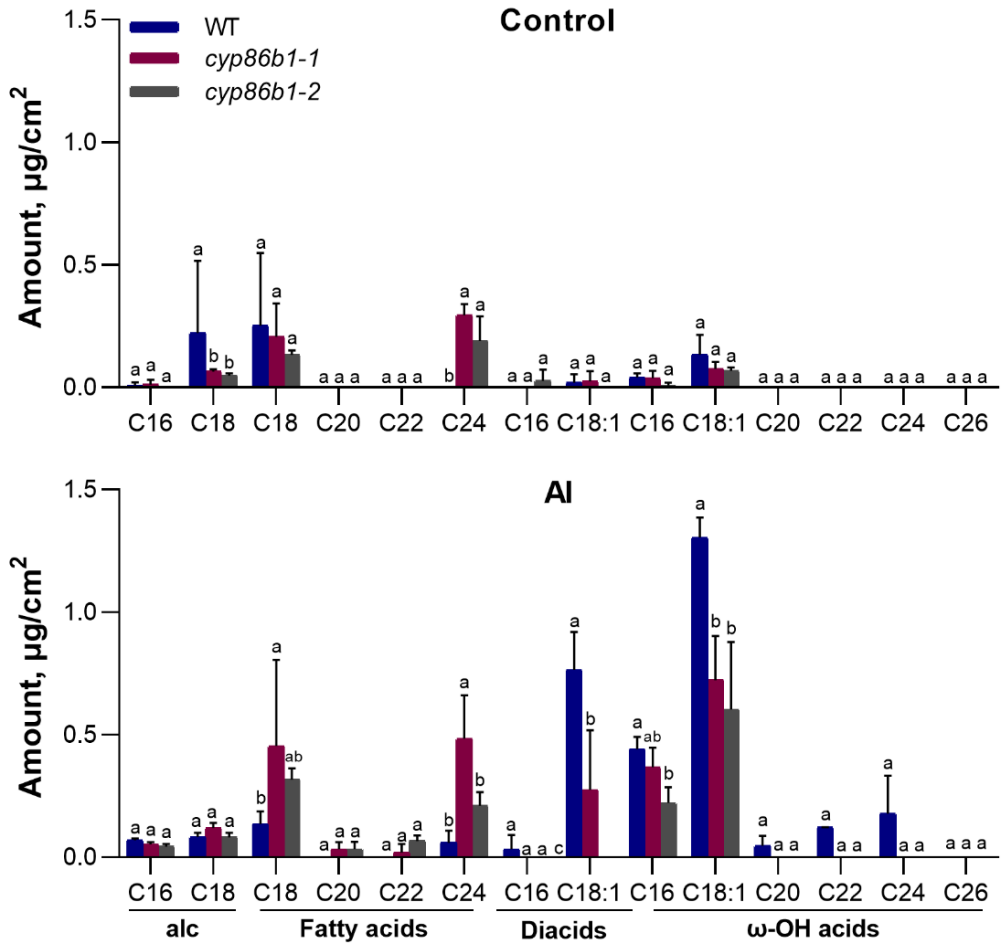

Figure 3.22 Amounts of monomers of aliphatic suberin in zone A of wild type and transgenic barley roots. Barley plants were grown in nutrient solution (control) or containing 50 µM $AlCl_3$ (Al) at pH 4.5 for 4 days. Results are shown as mean expression ±SD of three biological replicates, different letters indicate significant differences ($p < 0.05$). alc, primary alcohols; diacids, α–ω dicarboxylic acids; ω-OH acids, ω-hydroxy acids.

In Zone B, under control conditions, the levels of C16 and C18 ω-OH, as well as C18 diacid in the *cyp86b1-1* and *cyp86b1-2* mutants, were already significantly lower than in the wild-type. With the exception of trace amounts of C24 ω-OH detected in the wild-type, C20, 22, and 26 ω-OH were still undetected. Composition analysis of the Al-treated group revealed a similar trend in the changes of C20-C24 ω-OH as observed in Zone A.

In the wild-type barley, the levels of C20-C26 ω-OH increased compared to the control group, but remained undetected in the mutants, leading to significant differences in content between the wild-type and the *cyp86b1-1* and *cyp86b1-2* mutants. Moreover, the levels of C16 and C18 ω-OH, as well as C16 and C18 diacids, were lower in the *cyp86b1-1* and *cyp86b1-2* mutants than in the wild-type. Conversely, the levels of C20-C24 FA were higher in the mutant than in the wild-type (Figure 3.23).

The individual monomeric units with the entire aliphatic composition of zone C have been shown in Figure 3.24. In Zone C, under control conditions, there were no significant differences in the various components of aliphatic suberin between the mutant and the wild-type, except for C24 ω-OH. Compared to the control group, the various components of aliphatic suberin in the Al-treated group showed a certain degree of increase. Similarly, due to the loss of function in the *CYP86B1* gene in the mutant, the synthesis of C20-C26 ω-OH was hindered. Aluminum treatment did not increase the levels of C20-C26 ω-OH in the mutant, resulting in significant differences in content between the wild-type and the *cyp86b1-1* and *cyp86b1-2* mutants. Moreover, the levels of C16 and C18 ω-OH acids were lower in the *cyp86b1-1* and *cyp86b1-2* mutants than in the wild-type.

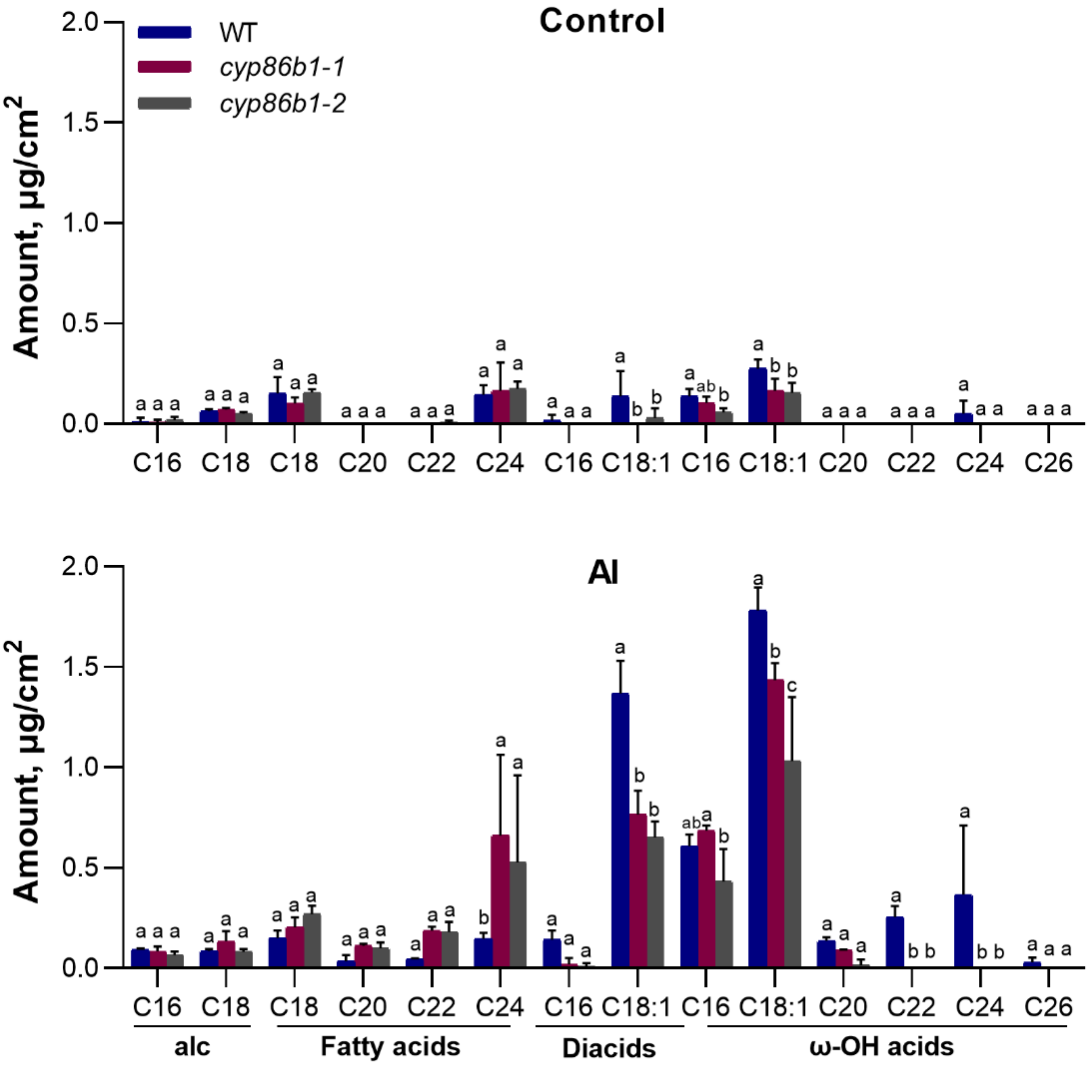

Figure 3.23 Amounts of monomers of aliphatic suberin in zone B of wild type and transgenic barley roots. Barley plants were grown in nutrient solution (control) or containing 50 µM $AlCl_3$ (Al) at pH 4.5 for 4 days. Results are shown as mean expression ±SD of three biological replicates, different letters indicate significant differences ($p < 0.05$). alc, primary alcohols; diacids, α–ω dicarboxylic acids; ω-OH acids, ω-hydroxy acids.

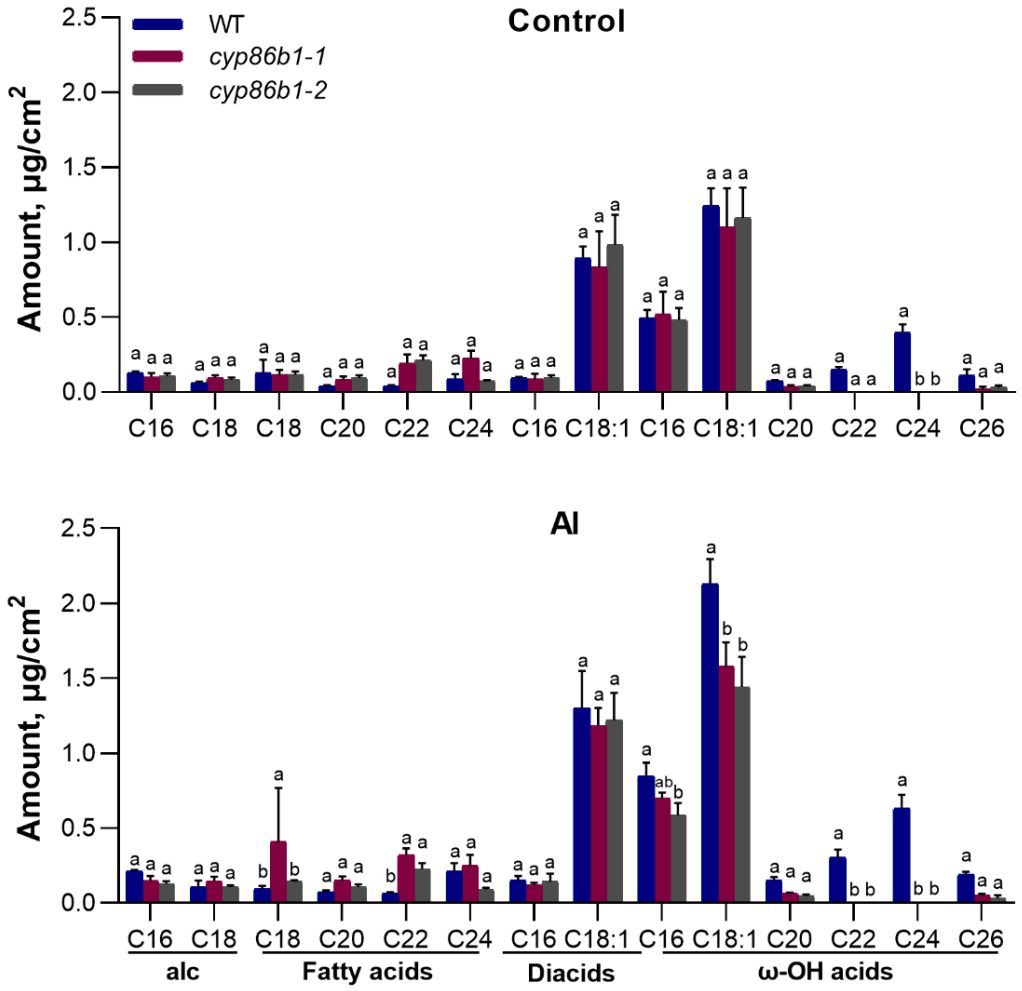

Figure 3.24 Amounts of monomers of aliphatic suberin in zone C of wild type and transgenic barley roots. Barley plants were grown in nutrient solution (control) or containing 50 µM $AlCl_3$ (Al) at pH 4.5 for 4 days. Results are shown as mean expression ±SD of three biological replicates, different letters indicate significant differences ($p < 0.05$). alc, primary alcohols; diacids, α–ω dicarboxylic acids; ω-OH acids, ω-hydroxy acids.

The contents of the four components of aliphatic suberin - primary alcohols, fatty acids, α–ω dicarboxylic acids, and ω-hydroxy acids in 10-day-old wild-type barley and *cyp86b1-1* and *cyp86b1-2* mutant barley are shown in Figure 3.25. For all four components, there was no significant difference in content between wild-type barley and

mutant barley in the control group, except for a slightly lower ω-hydroxy content in the mutant in zone c. In the case of primary alcohols, the content in wild-type barley and *cyp86b1-1* and *cyp86b1-2* mutants remained unchanged under Al treatment. Under Al treatment, for fatty acids, the content in zone a and zone b of wild-type barley was lower than that of the *cyp86b1-1* and *cyp86b1-2* mutants, while the content in zone c was also slightly lower than that in the mutants, but with no significant difference. Conversely, for α–ω dicarboxylic acids and ω-hydroxy acids, the contents in all three zones of the mutants were significantly lower than those in wild-type barley.

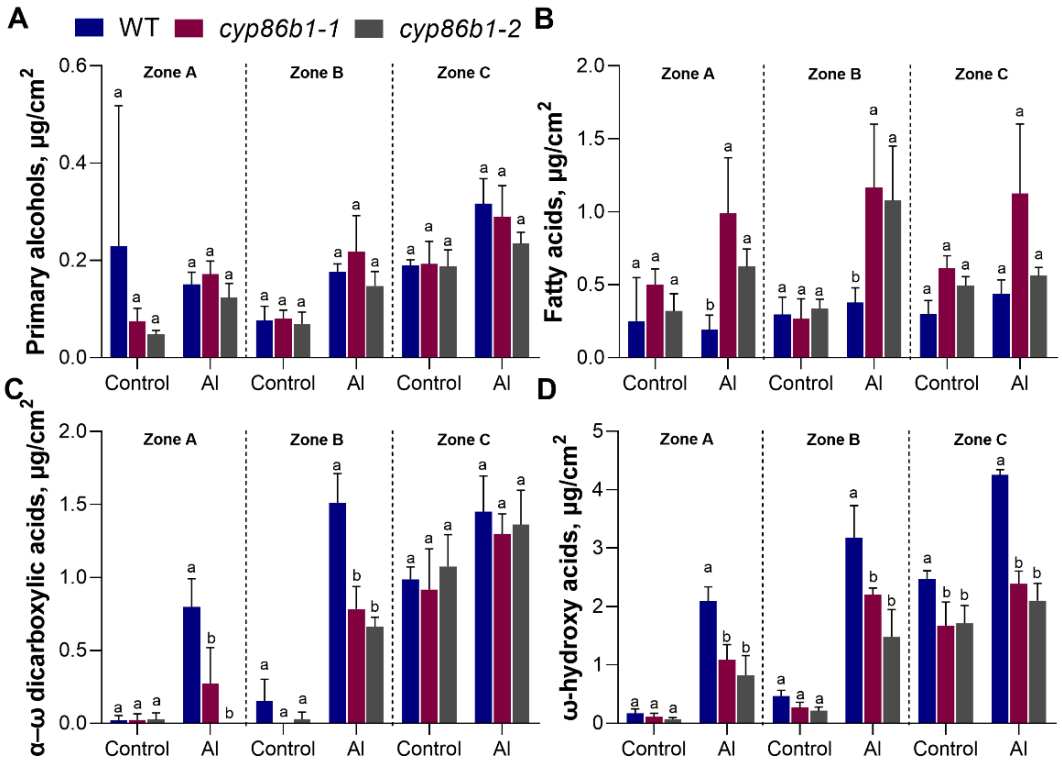

Figure 3.25 Amounts of substance classes of aliphatic suberin in wild type and transgenic barley seminal roots. Barley plants were grown in nutrient solution (control) or containing 50 µM $AlCl_3$ (Al) at pH 4.5 for 4 days. Results are shown as mean expression ±SD of three biological replicates, different letters indicate significant differences ($p < 0.05$).

3.5.2 Effect of Al stress on the barley *cyp86b1* mutants

Subsequently, after 4 days of treatment on wild-type barley and *cyp86b1-1* and *cyp86b1-2* mutant barley, the shoots of the barley plants were collected and analyzed. Shoot length and shoot dry weight of the barley was measured separately. The shoot section includes all parts above the seed.

The shoot length is shown in Figure 3.26A. There was no significant difference in shoot length between wild-type barley and *cyp86b1-1* and *cyp86b1-2* mutant barley in the control group. Moreover, Al treatment did not have a significant effect on shoot length for both wild-type barley and mutant barley. Conversely, the shoot dry weight of *cyp86b1-1* and *cyp86b1-2* mutant barley was significantly lower than that of wild-type barley, regardless of Al treatment. Similarly, Al treatment did not have a significant effect on the dry weight of barley shoots (Figure 3.26B).

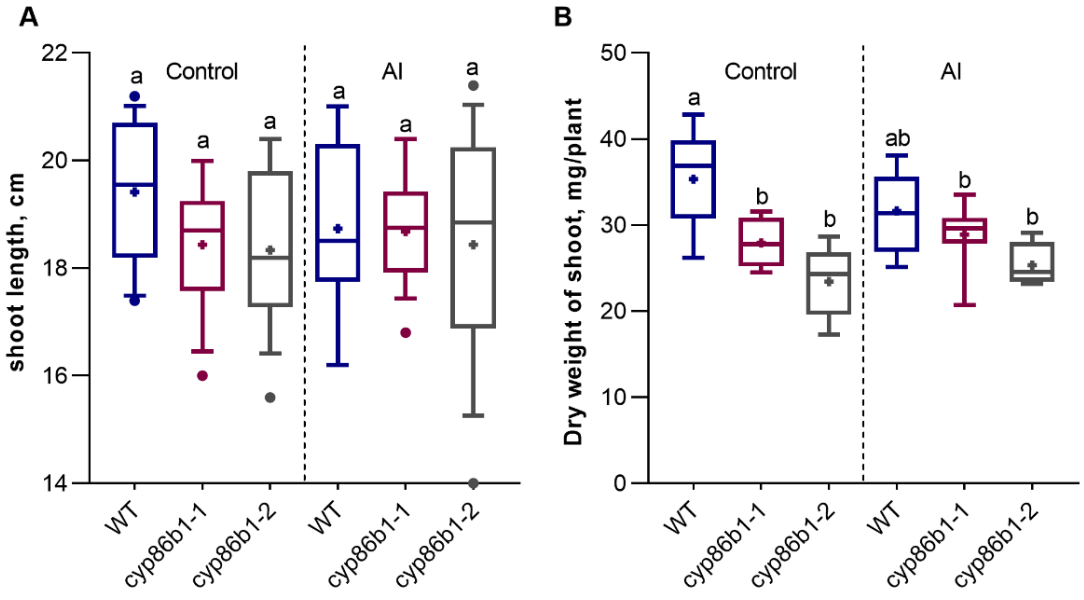

Figure 3.26 Effect of Al on shoot growth of wild type and transgenic barley plants. Shoot lengths (A) and shoots dry weight (B) of barley plants grown in nutrient solution (control) or containing 50 µM $AlCl_3$ (Al) at pH 4.5 for 4 days. The boxes range from the 10 to 90 percentiles. The "+" in the box represents the mean value. The whiskers range to the outliers. Error bars represent SD, different letter indicate significant differences ($p < 0.05$).

To further investigate the effects of Al and suberin on barley shoot development, the chlorophyll content and photosynthetic efficiency of wild-type barley and the *cyp86b1-1* and *cyp86b1-2* mutant barley under Al treatment was measured (Figure 3.27). Six-day-old barley plants were transferred to a culture solution containing 50 µM Al and their chlorophyll content and photosynthetic efficiency were measured daily for four consecutive days. Surprisingly, we found no significant differences in the chlorophyll content and photosynthetic efficiency between the Al treatment group and the control group in either wild-type barley or the suberin-deficient *cyp86b1-1* and *cyp86b1-2* mutant barley.

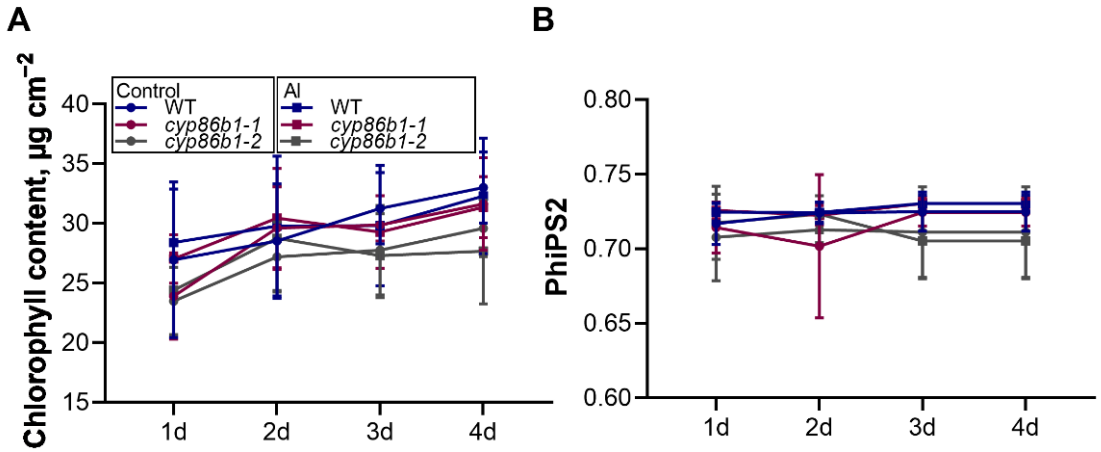

Figure 3.27 Effect of Al stress on chlorophyll content (A), and photosystem II efficiency (PhiPS2, B). Results are shown as mean expression ±SD. No significant difference was detected.

In addition, we also measured other pigments in the leaves (Figure 3.28). After four days of treatment, we found that there were no significant differences in the levels of flavonoids, anthocyanins, and nitrogen balance index between the Al treatment group and the control group in both wild-type barley and the suberin-deficient *cyp86b1-1* and *cyp86b1-2* mutant barley.

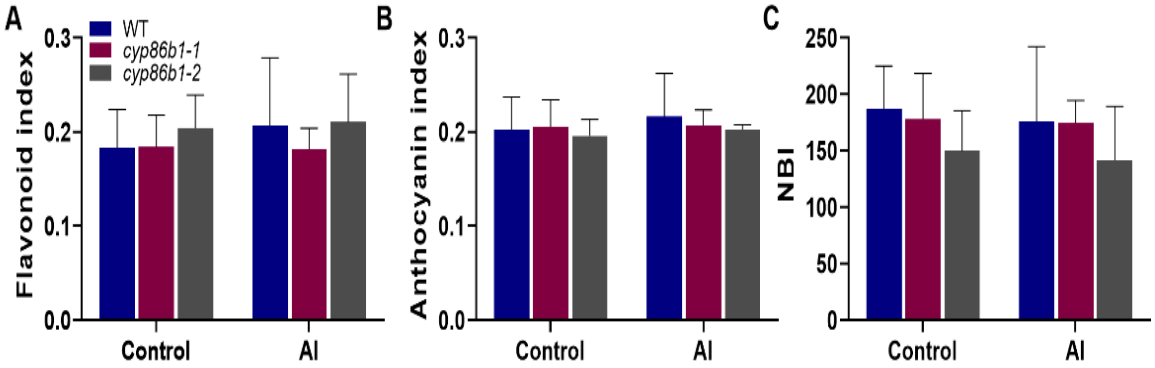

Figure 3.28 Flavonoid index, Anthocyanin index, Nitrogen Balance Index (NBI). Results are shown as mean expression ±SD. No significant difference was detected.

4. Discussion

Previous studies have reported significant genotypic variations in Al tolerance among different plant species (Darkó et al., 2004; Giannakoula et al., 2010; Meriga et al., 2010). These variations have been linked to differential regulation of antioxidant enzymes or different capacities for citrate secretion under short-term Al stress (Furukawa et al., 2007; Zhao et al., 2003). Barley is a cereal species known for its high sensitivity to aluminum, but variances in Al tolerance exist among barley cultivars. This study focused on cv. 'Scarlett' and 'Golden promise' which are relatively Al-sensitive compared to other barley cultivars, as even micromolar concentrations of Al significantly reduce root length (Vega et al., 2019). Nonetheless, the reduction of root growth is not solely attributed to Al but also to the combined effects of low pH and proton/H^+ toxicity. Previous reports indicate that barley is highly susceptible to H^+ toxicity (Guo et al., 2004; Zhao et al., 2003). The results of this study showed that barley seedlings were able to tolerate a moderate increase in pH from 4.5 to 5.8 without any significant effect on their root development. This suggests that barley has a high buffering capacity and can adapt to changes in soil acidity. However, when Al was added to the solution, a marked decrease in root length and dry weight was observed, indicating that Al toxicity was the main factor limiting root growth in barley under acidic conditions. The reduction in root length and dry weight could be attributed to the inhibition of cell division and elongation, as well as the disruption of nutrient uptake and transport by Al (Kochian et al., 2015). Therefore, the results of this study demonstrate that Al stress is more detrimental to barley root development than pH stress alone.

The relationship between suberin and pH is not well understood, but some studies have suggested that suberin may affect or be affected by pH in different ways (Feng et al., 2022). For instance, it has been suggested that low pH inhibits some crucial enzymes involved in suberin synthesis (van Doom and Perik, 1990). In this study, the effects of acidification on suberin synthesis in barley was examined. The findings indicate that the

suberin lamellae distribution and content of cv. 'Scarlett' did not significantly differ between pH 4.5 and pH 5.8 growth conditions after four days of treatment (Figure 3.2, 3.4-3.6). However, we speculate that more extended periods of acidification may further inhibit suberin synthesis genes.

Plants possess an impressive ability to adapt the level of suberization in their roots to various nutritional stresses. Not only does excess salt or drought cause changes in suberization, but deficiencies in essential elements such as K, Fe, or S can also lead to alterations in endodermal suberization (Barberon et al., 2016). In this study it was found that Al can strongly induce suberization (Figure 3.2-3.3 and 3.7-3.9), but the upregulation of genes associated with suberin synthesis only occurs after prolonged exposure to Al stress (Figure 3.10). The results of this study revealed that Al stress induced suberization in barley roots as a defense mechanism against Al toxicity. Suberin is a complex biopolymer that forms a protective barrier in the endodermis and limits the radial transport of water and solutes (Franke and Schreiber, 2007). The formation of suberin lamellae in barley roots was accelerated and intensified under Al stress conditions, especially at higher concentrations of Al. This suggests that suberization is an effective response to Al stress in barley, which may help to reduce the entry and accumulation of Al in the root tissues. However, suberization also has negative effects on root growth and function, such as reducing water uptake and nutrient availability (Ranathunge et al., 2011). Therefore, suberization may be a trade-off between protection and performance in barley roots under Al stress.

The aliphatic suberin monomers of barley are mainly composed of α–ω dicarboxylic acids, ω-hydroxy acids, primary alcohols, and fatty acids, which are derived from fatty acid metabolism (Kreszies et al., 2019). The α–ω dicarboxylic acids and ω-hydroxy acids are the main components of the polyester backbone of suberin, while the primary alcohols and fatty acids are attached to the backbone as side chains (Graça and Pereira, 2000). The

study indicate that Al stress induced a significant increase in α–ω dicarboxylic acids and ω-hydroxy acids in barley roots, especially in the oldest zone (Zone C), where suberization was most pronounced. This suggests that Al stress stimulated the biosynthesis of the polyester backbone of suberin in barley roots, which may enhance the barrier function of suberin against Al toxicity. The increase in α–ω dicarboxylic acids and ω-hydroxy acids under Al stress was mainly due to the upregulation of C18 and C16 chain lengths, which are the predominant chain lengths in suberin (Pollard et al., 2008). The C18 and C16 chain lengths may confer higher rigidity and stability to the suberin polymer (Graça and Pereira, 2000), which may improve its protective role against Al stress.

Silicon is, at 27.7%, the second most abundant element in the earth's crust, while Al is the third most abundant at 8.2% (Exley, 1998). They are primarily present in the soil in the form of insoluble aluminosilicates and their oxides. For most plants, Si is usually considered a beneficial plant nutrient rather than essential, but it has an important role in resisting pathogens and grazers, and in reducing various abiotic stresses including Al toxicity (Coskun et al., 2019; Wang et al., 2004). The study also showed that Si application alleviated the suberization induced by Al stress in barley roots. The mechanism of Si-mediated alleviation of Al stress is not fully understood, but it may involve the formation of Al-Si complexes in the root cell walls or apoplasts, which reduce the free Al concentration and prevent its uptake by root cells (Hodson and Evans, 2020; Wang et al., 2004). The reduced Al uptake may then decrease the need for suberization as a defense mechanism, resulting in lower suberin content in barley roots treated with Si. Alternatively, Si may also modulate the expression of genes involved in suberin biosynthesis or degradation (Fleck et al., 2011; Hinrichs et al., 2017; Vulavala et al., 2016; Wu et al., 2019), which could affect the suberin accumulation in barley roots under Al stress. Further studies are needed to elucidate the molecular mechanisms of Si-mediated alleviation of suberization in barley roots under Al stress.

The results showed that Flu treatment alone significantly inhibited root elongation in barley plants (Figure 3.14), consistent with previous studies that reported that Flu treatment reduced root growth in rice (Hoffmann-Benning and Kende, 1992) and maize (Moore and Smith, 1984). This suggests that ABA is required for normal root development in barley plants. However, Flu treatment did not alleviate the inhibitory effect of Al on root growth, indicating that ABA is not involved in Al-induced root growth inhibition.

A number of earlier studies had established a connection between ABA and enhanced suberization in various organisms. Here, we now demonstrate that lots of ABA related genes were regulated under Al stress (Figure 3.11 and 3.13). Meanwhile, Flu significantly reduced the suberin content and delayed the suberization process in barley roots under Al stress (Figure 3.15-3.17). Flu combined with Al treatment resulted in much lower levels of aliphatic and aromatic suberin in different zones of barley roots compared to Al treatment alone. This indicates that Flu inhibited the Al-induced suberin formation in barley roots. The results also showed that Flu treatment did not affect the composition of aliphatic suberin monomers in barley roots under Al stress. The levels of primary alcohols, fatty acids, α-ω dicarboxylic acids, and ω-hydroxy acids were similar between the Flu alone treatment and the Flu combined with Al treatment. This suggests that Flu did not alter the biosynthesis pathway of aliphatic suberin monomers in barley roots. These results also suggest that ABA is involved in the regulation of suberin formation and suberization process in barley roots under Al stress.

Morin staining showed that Flu significantly affected the distribution and transport of Al in barley roots under Al stress. Flu treatment combined with Al treatment resulted in a significant reduction of Al accumulation in the root cortex and a significant increase of Al accumulation in the central cylinder and the epidermis compared to Al treatment alone. Flu treatment inhibited the Al-induced suberin formation in barley roots, as shown by the lower suberin content and delayed suberization process. This indicates that suberin plays

an important role in limiting the entry and transport of Al in barley roots under Al stress. Suberin may act as a physical barrier to prevent Al from entering the root cells and reaching the sensitive tissues such as the central cylinder. Suberin lamellae are characterized by their alternating electron-lucent and -dense layers observed by transmission electron microscopy. These layers are hypothesized to consist of a suberin poly (aliphatic) domain and a suberin poly (phenolic) domain, respectively (Enstone et al., 2003). Previous studies have shown that suberin can bind metal irons such as cadmium, magnesium, and iron in plant roots (Enstone et al., 2003; Krishnamurthy et al., 2009; Liska et al., 2016; Machado et al., 2013). Suberin may also affect the expression and activity of transporters involved in Al uptake and efflux in plant roots. Further studies are needed to elucidate the molecular mechanisms of suberin-mediated Al resistance in barley roots under Al stress.

The results indicate that the *CYP86B1* gene is involved in the root growth response to Al stress in barley. The *CYP86B1* gene encodes a cytochrome P450 monooxygenase that catalyzes the hydroxylation of fatty acids in suberin biosynthesis, is required for very long chain ω-hydroxyacid and α,ω-dicarboxylic acid synthesis in root suberin polyester (Compagnon et al., 2009). In this study, we found that the loss-of-function mutations in the *CYP86B1* gene resulted in reduced root growth under Al stress, compared to the wild-type barley plants. This suggests that *CYP86B1* is required for maintaining normal root growth under Al stress. One possible explanation is that *cyp86b1* mutants have impaired suberin biosynthesis and deposition, leading to increased root damage and ion leakage under Al stress. To test this hypothesis, we measured the suberin content and composition in roots of the wild-type and mutant barley plants under both control and Al-treated conditions.

The results demonstrate that the *CYP86B1* gene affects the aliphatic suberin content and composition in roots of barley under Al stress. Among the aliphatic suberin components,

the ω-OH and diacids are considered to be the major products of CYP86B1-mediated hydroxylation (Compagnon et al., 2009). Therefore, the lower levels of ω-OH and diacids in the *cyp86b1* mutants indicate that the CYP86B1 enzyme is essential for their biosynthesis. Moreover, the absence of C20-C26 ω-OH in the *cyp86b1* mutants suggests that CYP86B1 is also responsible for the elongation of ω-OH beyond C18. As a result, the functional loss of the *cyp86b1* gene led to the inhibition of C20-26 ω-hydroxy acid synthesis and the consequent accumulation of a large amount of precursor substance, C20-24 FA. However, this mechanism was not sufficient to protect the roots from Al stress, as evidenced by the lower aliphatic suberin content in the cyp86b1 mutants under Al treatment.

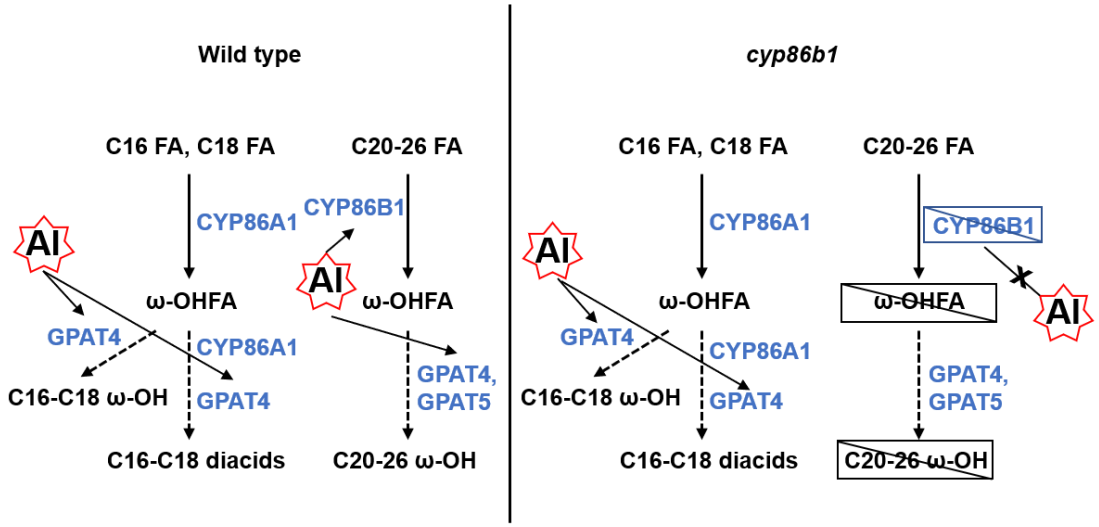

Figure 4.1 Hypothetical model for suberin synthesis in response to Al stress in roots of barley.

The differential distribution of aliphatic suberin components along the root axis also reflects the spatial regulation of suberin biosynthesis by Al stress. Furthermore, it was found that Al stress induced an increase in C20-C26 ω-OH in all three zones of the wild-type barley, but not in the *cyp86b1* mutants. This suggests that Al stress activates *CYP86B1* expression and activity in both zones, leading to enhanced suberin biosynthesis and elongation. However, the *cyp86b1* mutants are unable to respond to this signal due to the loss-of-function mutations in the *CYP86B1* gene.

The results reveal that the *CYP86B1* gene affects not only the aliphatic suberin content and composition in roots, but also the shoot growth and biomass of barley under Al stress. Among the aliphatic suberin components, the primary alcohols are derived from the reduction of fatty acids, while the α–ω dicarboxylic acids and ω-hydroxy acids are derived from the hydroxylation of fatty acids by *CYP86B1*. Therefore, the lower levels of α–ω dicarboxylic acids and ω-hydroxy acids in the *cyp86b1* mutants confirm that barley *CYP86B1* is essential for their biosynthesis. Interestingly, there was also a higher level of fatty acids in the *cyp86b1* mutants under Al treatment, which might be due to the accumulation of fatty acids that are not converted to other suberin components by CYP86B1. However, this accumulation did not confer any benefit to the roots under Al stress, as evidenced by the lower root growth and biomass of the cyp86b1 mutants.

In addition to the root phenotype, it was also found that the *cyp86b1* mutants had lower shoot biomass than the wild-type barley, regardless of Al treatment. This suggests that *CYP86B1* may has a role in shoot development and metabolism that is independent of Al stress. One possible explanation is that *CYP86B1* is involved in the biosynthesis of cutin, another complex biopolymer that is deposited in the cuticle layer of aerial plant organs (Beisson et al., 2012). Cutin plays a crucial role in protecting plants from water loss, pathogen infection, and environmental stresses (Schreiber, 2010). Previous studies have shown that CYP86B1 is expressed in various aerial tissues and contributes to cutin biosynthesis and deposition (Molina et al., 2009). Therefore, the loss-of-function mutations in the *CYP86B1* gene might impair cutin formation and function, leading to reduced shoot growth and biomass.

Al stress does not affect the photosynthesis and pigment metabolism of barley shoots in this study, regardless of the suberin content in roots. This is in contrast to previous studies that reported a decrease in chlorophyll content and photosynthetic efficiency in shoots of Al-stressed plants. One possible reason for this discrepancy is that the concentration of

Al treatment used in this study was relatively mild compared to those used in other studies (1mM $AlCl_3$, Panda et al., 2003). Another possible reason is that barley shoot has a high tolerance to Al stress and can maintain its function even under Al exposure. Furthermore, although more Al was able to penetrate into the vascular tissue through the endodermis, it remains to be further investigated whether more Al will be translocated to the shoots of barley. Moreover, the results suggest that suberin does not play a significant role in protecting barley shoots from Al stress, as the suberin-deficient mutants did not show any difference in shoot performance compared to the wild-type plants.

However, we cannot rule out the possibility that suberin might have a subtle effect on shoot physiology and metabolism that is not detected by these measurements. For instance, suberin might modulate the hormonal balance and signaling between roots and shoots under Al stress. Suberin might also influence the antioxidant defense system and oxidative stress response in shoots under Al stress.

5. Summary

Aluminum toxicity is the main factor inhibiting plant growth in acidic soils worldwide, and the root barrier formed by suberized cells is an important mechanism for plants to resist environmental stress. Therefore, the aim of this study was to investigate the effect of Al stress on the synthesis of suberin in barley roots and the role of suberin in resisting Al stress.

Through FY staining observation and GC chemical analysis, this study showed that 4 days of Al stress could significantly increase the distribution and content of suberin in barley roots. Analysis of RNA-seq data and qPCR analysis showed that Al stress could induce the expression of a series of genes related to suberin synthesis, among which the key gene for suberin synthesis, *CYP86B1*, was crucial in the Al stress response, while *CYP86A1* was relatively minor. Under Al stress, Al-induced suberization in the barley *cyp86b1* mutants was significantly lower than in wild-type barley. In parallel, a series of ABA-related genes involved in ABA biosynthesis, degradation, and signalling were upregulated under Al stress, indicating that Al treatment could induce ABA synthesis and possibly regulate Al-induced suberization by modulating the ABA pathway. Furthermore, in the presence of the ABA synthesis inhibitor fluridone, Al stress could no longer induce changes in suberin. Morin staining showed that the presence or absence of suberin lamellae had a significant effect on the transport of Al in roots. In the absence of suberin, more Al entered the xylem of the root. However, after 4 days of Al treatment, the presence or absence of suberin did not affect the growth status of the barley aboveground part. In summary, root suberin play an important role in resistance to Al stress of barley.

6. References

Andersen, T.G., Barberon, M., and Geldner, N. (2015). Suberization - the second life of an endodermal cell. Curr Opin Plant Biol *28*, 9-15.

Barberon, M., and Geldner, N. (2014). Radial transport of nutrients: the plant root as a polarized epithelium. Plant Physiol *166*, 528-537.

Barberon, M., Vermeer, J.E., De Bellis, D., Wang, P., Naseer, S., Andersen, T.G., Humbel, B.M., Nawrath, C., Takano, J., Salt, D.E., *et al.* (2016). Adaptation of Root Function by Nutrient-Induced Plasticity of Endodermal Differentiation. Cell *164*, 447-459.

Beisson, Fred, Li, Y., Bonaventure, Gustavo, Pollard, Mike, Ohlrogge, and John, B. (2007). The Acyltransferase GPAT5 Is Required for the Synthesis of Suberin in Seed Coat and Root of Arabidopsis. Plant Cell.

Beisson, F., Li-Beisson, Y., and Pollard, M. (2012). Solving the puzzles of cutin and suberin polymer biosynthesis. Curr Opin Plant Biol *15*, 329-337.

Bennet, R., and Breen, C. (1991). The aluminium signal: new dimensions to mechanisms of aluminium tolerance. Plant and soil *134*, 153-166.

Brundrett, M.C., Kendrick, B., and Peterson, C.A. (1991). Efficient lipid staining in plant material with Sudan Red 7B or Fluoral Yellow 088 in polyethylene glycol-glycerol. Biotechnic & Histochemistry *66*, 111-116.

Chang, Y.C., Yamamoto, Y., and Matsumoto, H. (1999). Accumulation of aluminium in the cell wall pectin in cultured tobacco (Nicotiana tabacum L.) cells treated with a combination of aluminium and iron. Plant, Cell & Environment *22*, 1009-1017.

Compagnon, V., Diehl, P., Benveniste, I., Meyer, D., Schaller, H., Schreiber, L., Franke, R., and Pinot, F. (2009). CYP86B1 is required for very long chain omega-hydroxyacid and alpha, omega -dicarboxylic acid synthesis in root and seed suberin polyester. Plant Physiol *150*, 1831-1843.

Cosgrove, D.J. (2005). Growth of the plant cell wall. Nat Rev Mol Cell Biol *6*, 850-861.

Coskun, D., Deshmukh, R., Sonah, H., Menzies, J.G., Reynolds, O., Ma, J.F., Kronzucker, H.J., and Belanger, R.R. (2019). The controversies of silicon's role in plant biology. New Phytol *221*, 67-85.

Cuenca, G., Herrera, R., and Merida, T. (1991). Distribution of aluminium in accumulator plants by X-ray microanalysis in Richeria grandis Vahl leaves from a cloud forest in Venezuela. Plant, Cell and Environment *14*, 437-441.

Darkó, É., Ambrus, H., Stefanovits-Bányai, É., Fodor, J., Bakos, F., and Barnabás, B. (2004). Aluminium toxicity, Al tolerance and oxidative stress in an Al-sensitive wheat genotype and in Al-tolerant lines developed by in vitro microspore selection. Plant Science *166*, 583-591.

Degenhardt, J.r., Larsen, P.B., Howell, S.H., and Kochian, L.V. (1998). Aluminum resistance in the Arabidopsis mutant alr-104 is caused by an aluminum-induced increase in rhizosphere pH. Plant Physiology *117*, 19-27.

Delhaize, E., and Ryan, P.R. (1995). Aluminum toxicity and tolerance in plants. Plant physiology *107*, 315.

Delhaize, E., Ryan, P.R., Hebb, D.M., Yamamoto, Y., Sasaki, T., and Matsumoto, H. (2004). Engineering high-level aluminum tolerance in barley with the ALMT1 gene. Proceedings of the National Academy of Sciences *101*, 15249-15254.

Enstone, D.E., Peterson, C.A., and Ma, F. (2003). Root Endodermis and Exodermis: Structure, Function, and Responses to the Environment. Journal of Plant Growth Regulation *21*, 335-351.

Exley, C. (1998). Silicon in life : A bioinorganic solution to bioorganic essentiality 1 JD Birchall memorial lecture. 1. Journal of Inorganic Biochemistry *69*, 139-144.

Famoso, A.N., Clark, R.T., Shaff, J.E., Craft, E., McCouch, S.R., and Kochian, L.V. (2010). Development of a novel aluminum tolerance phenotyping platform used for comparisons of cereal aluminum tolerance and investigations into rice aluminum tolerance mechanisms. Plant Physiol *153*, 1678-1691.

Feng, T., Wu, P., Gao, H., Kosma, D.K., Jenks, M.A., and Lu, S. (2022). Natural variation in root suberization is associated with local environment in Arabidopsis thaliana. New Phytol *236*, 385-398.

Fleck, A.T., Nye, T., Repenning, C., Stahl, F., Zahn, M., and Schenk, M.K. (2011). Silicon enhances suberization and lignification in roots of rice (Oryza sativa). J Exp Bot *62*, 2001-2011.

Franke, R., Briesen, I., Wojciechowski, T., Faust, A., Yephremov, A., Nawrath, C., and Schreiber, L. (2005). Apoplastic polyesters in Arabidopsis surface tissues--a typical suberin and a particular cutin. Phytochemistry *66*, 2643-2658.

Franke, R., and Schreiber, L. (2007). Suberin--a biopolyester forming apoplastic plant interfaces. Curr Opin Plant Biol *10*, 252-259.

Furukawa, J., Yamaji, N., Wang, H., Mitani, N., Murata, Y., Sato, K., Katsuhara, M., Takeda, K., and Ma, J.F. (2007). An aluminum-activated citrate transporter in barley. Plant Cell Physiol *48*, 1081-1091.

Gamble, P.E., and Mullet, J.E. (1986). Inhibition of carotenoid accumulation and abscisic acid biosynthesis in fluridone-treated dark-grown barley. Eur J Biochem *160*, 117-121.

Geldner, N. (2013). The endodermis. Annu Rev Plant Biol *64*, 531-558.

Giannakoula, A., Moustakas, M., Syros, T., and Yupsanis, T. (2010). Aluminum stress induces up-regulation of an efficient antioxidant system in the Al-tolerant maize line but not in the Al-sensitive line. Environmental and Experimental Botany *67*, 487-494.

Godon, C., Mercier, C., Wang, X., David, P., Richaud, P., Nussaume, L., Liu, D., and Desnos, T. (2019). Under phosphate starvation conditions, Fe and Al trigger accumulation of the transcription factor STOP1 in the nucleus of Arabidopsis root cells. Plant J *99*, 937-949.

Graça, J., and Pereira, H. (1997). Cork suberin: a glyceryl based polyester.

Graça, J., and Pereira, H. (2000). Suberin structure in potato periderm: glycerol, long-chain monomers, and glyceryl and feruloyl dimers. Journal of Agricultural and Food Chemistry *48*, 5476-5483.

Guo, T., Zhang, G., Zhou, M., Wu, F., and Chen, J. (2004). Effects of aluminum and cadmium toxicity on growth and antioxidant enzyme activities of two barley genotypes with different Al resistance. Plant & Soil *258*, 241-248.

Harman-Ware, A.E., Sparks, S., Addison, B., and Kalluri, U.C. (2021). Importance of suberin biopolymer in plant function, contributions to soil organic carbon and in the production of bio-derived energy and materials. Biotechnol Biofuels *14*, 75.

Hazen, S.P., Scott-Craig, J.S., and Walton, J.D. (2002). Cellulose synthase-like genes of rice. Plant Physiol *128*, 336-340.

Hinrichs, M., Fleck, A.T., Biedermann, E., Ngo, N.S., Schreiber, L., and Schenk, M.K. (2017). An ABC Transporter Is Involved in the Silicon-Induced Formation of Casparian Bands in the Exodermis of Rice. Front Plant Sci *8*, 671.

Hodson, M.J., and Evans, D.E. (2020). Aluminium-silicon interactions in higher plants: an update. J Exp Bot *71*, 6719-6729.

Hoekenga, O.A., Maron, L.G., Pineros, M.A., Cançado, G.M., Shaff, J., Kobayashi, Y., Ryan, P.R., Dong, B., Delhaize, E., and Sasaki, T. (2006). AtALMT1, which

encodes a malate transporter, is identified as one of several genes critical for aluminum tolerance in Arabidopsis. Proceedings of the National Academy of Sciences *103*, 9738-9743.

Hoffmann-Benning, S., and Kende, H. (1992). On the role of abscisic acid and gibberellin in the regulation of growth in rice. Plant physiology *99*, 1156-1161.

Horst, W.J., Wang, Y., and Eticha, D. (2010). The role of the root apoplast in aluminium-induced inhibition of root elongation and in aluminium resistance of plants: a review. Ann Bot *106*, 185-197.

Huang, C.F., Yamaji, N., Chen, Z., and Ma, J.F. (2012). A tonoplast-localized half-size ABC transporter is required for internal detoxification of aluminum in rice. Plant J *69*, 857-867.

Ishikawa, S., Wagatsuma, T., Sasaki, R., and Ofei-Manu, P. (2000). Comparison of the amount of citric and malic acids in Al media of seven plant species and two cultivars each in five plant species. Soil Science and Plant Nutrition *46*, 751-758.

Jessen, D., Olbrich, A., Knüfer, J., Krüger, A., and Fulda, M. (2011). Combined activity of LACS1 and LACS4 is required for proper pollen coat formation in Arabidopsis. Plant Journal for Cell & Molecular Biology *68*, 715-726.

Joubès, J., Raffaele, S., Bourdenx, B., Garcia, C., Laroche-Traineau, J., Moreau, P., Domergue, F., and Lessire, R. (2008). The VLCFA elongase gene family in Arabidopsis thaliana: phylogenetic analysis, 3D modelling and expression profiling. Plant Molecular Biology *67*, 547.

Kashino-Fujii, M., Yokosho, K., Yamaji, N., Yamane, M., Saisho, D., Sato, K., and Ma, J.F. (2018). Retrotransposon Insertion and DNA Methylation Regulate Aluminum Tolerance in European Barley Accessions. Plant Physiol *178*, 716-727.

Kidd, P., Llugany, M., Poschenrieder, C., Gunse, B., and Barcelo, J. (2001). The role of root exudates in aluminium resistance and silicon-induced amelioration of aluminium toxicity in three varieties of maize (Zea mays L.). Journal of Experimental Botany *52*, 1339-1352.

Kochian (1995). Cellular Mechanisms of Aluminum Toxicity and Resistance in Plants. Annual Review of Plant Physiology and Plant Molecular Biology.

Kochian, L.V., Pineros, M.A., Liu, J., and Magalhaes, J.V. (2015). Plant Adaptation to Acid Soils: The Molecular Basis for Crop Aluminum Resistance. Annu Rev Plant Biol *66*, 571-598.

Kolattukudy, P.E. (2001). Polyesters in higher plants. Biopolyesters, 1-49.

Kolattukudy, V.P.A.E. (1977). Biochemistry of Suberization. ω-Hydroxyacid Oxidation in Enzyme Preparations from Suberizing Potato Tuber Disks. Plant Physiology *59*, 667-672.

Kreszies, T., Shellakkutti, N., Osthoff, A., Yu, P., Baldauf, J.A., Zeisler-Diehl, V.V., Ranathunge, K., Hochholdinger, F., and Schreiber, L. (2019). Osmotic stress enhances suberization of apoplastic barriers in barley seminal roots: analysis of chemical, transcriptomic and physiological responses. New Phytol *221*, 180-194.

Krishnamurthy, P., Ranathunge, K., Franke, R., Prakash, H.S., Schreiber, L., and Mathew, M.K. (2009). The role of root apoplastic transport barriers in salt tolerance of rice (Oryza sativa L.). Planta *230*, 119-134.

Kumar, M., Campbell, L., and Turner, S. (2016). Secondary cell walls: biosynthesis and manipulation. J Exp Bot *67*, 515-531.

Larsen, P.B., Cancel, J., Rounds, M., and Ochoa, V. (2007). Arabidopsis ALS1 encodes a root tip and stele localized half type ABC transporter required for root growth in an aluminum toxic environment. Planta *225*, 1447-1458.

Larsen, P.B., Geisler, M.J., Jones, C.A., Williams, K.M., and Cancel, J.D. (2005). ALS3 encodes a phloem-localized ABC transporter-like protein that is required for aluminum tolerance in Arabidopsis. Plant J *41*, 353-363.

Layers, T.S.C. (2013). Structure and function of three suberized cell layers: epidermis, exodermis, and endodermis. Plant roots: the hidden half.

Lei, G.J., Yokosho, K., Yamaji, N., Fujii-Kashino, M., and Ma, J.F. (2017). Functional characterization of two half-size ABC transporter genes in aluminium-accumulating buckwheat. New Phytol *215*, 1080-1089.

Li, N., Meng, H., Xing, H., Liang, L., Zhao, X., and Luo, K. (2017). Genome-wide analysis of MATE transporters and molecular characterization of aluminum resistance in Populus. J Exp Bot *68*, 5669-5683.

Li, Y.Y., Yang, J.L., Zhang, Y.J., and Zheng, S.J. (2009). Disorganized distribution of homogalacturonan epitopes in cell walls as one possible mechanism for aluminium-induced root growth inhibition in maize. Ann Bot *104*, 235-241.

Ligaba, A., Katsuhara, M., Ryan, P.R., Shibasaka, M., and Matsumoto, H. (2006). The BnALMT1 and BnALMT2 genes from rape encode aluminum-activated malate transporters that enhance the aluminum resistance of plant cells. Plant Physiol *142*, 1294-1303.

Liska, D., Martinka, M., Kohanova, J., and Lux, A. (2016). Asymmetrical development of root endodermis and exodermis in reaction to abiotic stresses. Ann Bot *118*, 667-674.

Liu, J., Magalhaes, J.V., Shaff, J., and Kochian, L.V. (2009). Aluminum-activated citrate and malate transporters from the MATE and ALMT families function independently to confer Arabidopsis aluminum tolerance. Plant J *57*, 389-399.

Llugany, M., Poschenrieder, C., and Barcelo, J. (1995). Monitoring of aluminium-induced inhibition of root elongation in four maize cultivars differing in tolerance to aluminium and proton toxicity. Physiologia Plantarum *93*, 265-271.

Lu, S., Song, T., Kosma, D.K., Parsons, E.P., Rowland, O., and Jenks, M.A. (2009). Arabidopsis CER8 encodes LONG-CHAIN ACYL-COA SYNTHETASE 1 (LACS1) that has overlapping functions with LACS2 in plant wax and cutin synthesis. Plant J *59*, 553-564.

Ma, J.F. (2007). Syndrome of Aluminum Toxicity and Diversity of Aluminum Resistance in Higher Plants. In, pp. 225-252.

Ma, J.F., Hiradate, S., Nomoto, K., Iwashita, T., and Matsumoto, H. (1997a). Internal Detoxification Mechanism of Al in Hydrangea (Identification of Al Form in the Leaves). Plant Physiology *113*, 1033-1039.

Ma, J.F., Ryan, P.R., and Delhaize, E. (2001). Aluminium tolerance in plants and the complexing role of organic acids. Trends in plant science *6*, 273-278.

Ma, J.F., Zheng, S.J., and Matsumoto, H. (1997b). Specific secretion of citric acid induced by Al stress in Cassia tora L. Plant and cell Physiology *38*, 1019-1025.

Machado, A., Pereira, H., and Teixeira, R.T. (2013). Anatomy and development of the endodermis and phellem of Quercus suber L. roots. Microsc Microanal *19*, 525-534.

MacKinnon, N., Ridgway, J., Crowell, K.J., and Macdonald, P.M. (2006). Aluminum binding to phosphatidylcholine lipid bilayer membranes: aluminum exchange lifetimes from 31P NMR spectroscopy. Chemistry and physics of lipids *139*, 85-95.

Magalhaes, J.V., Liu, J., Guimaraes, C.T., Lana, U.G., Alves, V.M., Wang, Y.H., Schaffert, R.E., Hoekenga, O.A., Pineros, M.A., Shaff, J.E.*, et al.* (2007). A gene in the multidrug and toxic compound extrusion (MATE) family confers aluminum tolerance in sorghum. Nat Genet *39*, 1156-1161.

Marcus, S.E., Verhertbruggen, Y., Herve, C., Ordaz-Ortiz, J.J., Farkas, V., Pedersen, H.L., Willats, W.G., and Knox, J.P. (2008). Pectic homogalacturonan masks abundant sets of xyloglucan epitopes in plant cell walls. BMC Plant Biol *8*, 60.

Maron, L.G., Pineros, M.A., Guimaraes, C.T., Magalhaes, J.V., Pleiman, J.K., Mao, C., Shaff, J., Belicuas, S.N., and Kochian, L.V. (2010). Two functionally distinct members of the MATE (multi-drug and toxic compound extrusion) family of transporters potentially underlie two major aluminum tolerance QTLs in maize. Plant J *61*, 728-740.

Meriga, B., Attitalla, I., Ramgopal, M., Ediga, A., and Kavikishor, P. (2010). Differential tolerance to aluminum toxicity in rice cultivars: involvement of antioxidative enzymes and possible role of aluminum resistant locus. Acad J Plant Sci *3*, 53-63.

Metz, J.G. (2000). Purification of a Jojoba Embryo Fatty Acyl-Coenzyme A Reductase and Expression of Its cDNA in High Erucic Acid Rapeseed. Plant physiology *122*, 635-644.

Mohnen, D. (2008). Pectin structure and biosynthesis. Curr Opin Plant Biol *11*, 266-277.

Molina, I., Bonaventure, G., Ohlrogge, J., and Pollard, M. (2006). The lipid polyester composition of Arabidopsis thaliana and Brassica napus seeds. Phytochemistry *67*, 2597-2610.

Molina, I., Li-Beisson, Y., Beisson, F., Ohlrogge, J.B., and Pollard, M. (2009). Identification of an Arabidopsis feruloyl-coenzyme A transferase required for suberin synthesis. Plant Physiol *151*, 1317-1328.

Moore, R., and Smith, J.D. (1984). Growth, graviresponsiveness and abscisic-acid content of Zea mays seedlings treated with fluridone. Planta *162*, 342-344.

Nagata, T., Hayatsu, M., and Kosuge, N. (1992). Identification of aluminium forms in tea leaves by 27Al NMR. Phytochemistry *31*, 1215-1218.

Nezames, C.D., Ochoa, V., and Larsen, P.B. (2012). Mutational loss of Arabidopsis SLOW WALKER2 results in reduced endogenous spermine concomitant with increased aluminum sensitivity. Functional Plant Biology *40*, 67-78.

Nishiyama, Y. (2009). Structure and properties of the cellulose microfibril. Journal of Wood Science *55*, 241-249.

Pan, J.-w., Zhu, M.-y., and Chen, H. (2001). Aluminum-induced cell death in root-tip cells of barley. Environmental and experimental botany *46*, 71-79.

Panda, S., Singha, L., and Khan, M. (2003). Does aluminium phytotoxicity induce oxidative stress in greengram (Vigna radiata). Bulgarian Journal of Plant Physiology *29*, 77-86.

Pineros, M.A., Cancado, G.M., and Kochian, L.V. (2008). Novel properties of the wheat aluminum tolerance organic acid transporter (TaALMT1) revealed by

electrophysiological characterization in Xenopus Oocytes: functional and structural implications. Plant Physiol *147*, 2131-2146.

Pinot, F. (2011). Cytochrome P450 metabolizing fatty acids in living organisms. Febs Journal *278*, 181-181.

Polko, J.K., and Kieber, J.J. (2019). The Regulation of Cellulose Biosynthesis in Plants. Plant Cell *31*, 282-296.

Pollard, M., Beisson, F., Li, Y., and Ohlrogge, J.B. (2008). Building lipid barriers: biosynthesis of cutin and suberin. Trends Plant Sci *13*, 236-246.

Ranathunge, K., Schreiber, L., and Franke, R. (2011). Suberin research in the genomics era--new interest for an old polymer. Plant Sci *180*, 399-413.

Razem, F.A., and Bernards, M.A. (2003). Reactive oxygen species production in association with suberization: evidence for an NADPH-dependent oxidase. J Exp Bot *54*, 935-941.

Rengel, Z., Bose, J., Chen, Q., and Tripathi, B. (2015). Magnesium alleviates plant toxicity of aluminium and heavy metals. Crop and Pasture Science *66*, 1298-1307.

Rincón, M., and Gonzales, R.A. (1992). Aluminum partitioning in intact roots of aluminum-tolerant and aluminum-sensitive wheat (Triticum aestivum L.) cultivars. Plant Physiology *99*, 1021-1028.

Robbins, N.E., 2nd, Trontin, C., Duan, L., and Dinneny, J.R. (2014). Beyond the barrier: communication in the root through the endodermis. Plant Physiol *166*, 551-559.

Roland, J.C., Reis, D., Vian, B., and Roy, S. (1989). The helicoidal plant cell wall as a performing cellulose-based composite. Biology of the Cell *67*, 209-220.

Ryan, P.R., Ditomaso, J.M., and Kochian, L.V. (1993). Aluminium toxicity in roots: an investigation of spatial sensitivity and the role of the root cap. Journal of experimental botany *44*, 437-446.

Sasaki, M., Yamamoto, Y., and Matsumoto, H. (2012). Aluminum inhibits growth and stability of cortical microtubules in wheat (Triticum aestivum) roots. Soil Science and Plant Nutrition *43*, 469-472.

Sasaki, T., Yamamoto, Y., Ezaki, B., Katsuhara, M., Ahn, S.J., Ryan, P.R., Delhaize, E., and Matsumoto, H. (2004). A wheat gene encoding an aluminum-activated malate transporter. Plant J *37*, 645-653.

Schmohl, N., and Horst, W.J. (2000). Cell wall pectin content modulates aluminium sensitivity of Zea mays (L.) cells grown in suspension culture. Plant, Cell and Environment *23*, 735-742.

Schreiber, L. (2010). Transport barriers made of cutin, suberin and associated waxes. Trends Plant Sci *15*, 546-553.

Schreiber, L., Franke, R., and Lessire, R. (2005). Biochemical characterization of elongase activity in corn (Zea mays L.) roots. Phytochemistry *66*, 131-138.

Shen, R., Ma, J.F., Kyo, M., and Iwashita, T. (2002). Compartmentation of aluminium in leaves of an Al-accumulator, Fagopyrum esculentum Moench. Planta *215*, 394-398.

Sivaguru, M., and Horst, W.J. (1998). The distal part of the transition zone is the most aluminum-sensitive apical root zone of maize. Plant Physiology *116*, 155-163.

Somerville, C., Bauer, S., Brininstool, G., Facette, M., Hamann, T., Milne, J., Osborne, E., Paredez, A., Persson, S., Raab, T., *et al.* (2004). Toward a Systems Approach to Understanding Plant Cell Walls. Science *306*, 2206-2211.

Szurman-Zubrzycka, M., Chwialkowska, K., Niemira, M., Kwasniewski, M., Nawrot, M., Gajecka, M., Larsen, P.B., and Szarejko, I. (2021). Aluminum or Low pH - Which Is the Bigger Enemy of Barley? Transcriptome Analysis of Barley Root Meristem Under Al and Low pH Stress. Front Genet *12*, 675260.

Tahara, K., Hashida, K., Otsuka, Y., Ohara, S., Kojima, K., and Shinohara, K. (2014). Identification of a hydrolyzable tannin, oenothein B, as an aluminum-detoxifying ligand in a highly aluminum-resistant tree, Eucalyptus camaldulensis. Plant Physiol *164*, 683-693.

Thompson, J.E., and Fry, S.C. (2000). Evidence for covalent linkage between xyloglucan and acidic pectins in suspension-cultured rose cells. Planta *211*, 275-286.

van Doom, W.G., and Perik, R.R. (1990). Hydroxyquinoline citrate and low pH prevent vascular blockage in stems of cut rose flowers by reducing the number of bacteria. Journal of the American Society for Horticultural Science *115*, 979-981.

Vega, I., Nikolic, M., Pontigo, S., Godoy, K., Mora, M.d.L.L., and Cartes, P. (2019). Silicon Improves the Production of High Antioxidant or Structural Phenolic Compounds in Barley Cultivars under Aluminum Stress. Agronomy *9*.

Vioque, J., and Kolattukudy, P.E. (1997). Resolution and Purification of an Aldehyde-Generating and an Alcohol-Generating Fatty Acyl-CoA Reductase from Pea Leaves (Pisum sativum L.). Archives of Biochemistry and Biophysics *340*, 64-72.

Vishwanath, S.J., Delude, C., Domergue, F., and Rowland, O. (2015). Suberin: biosynthesis, regulation, and polymer assembly of a protective extracellular barrier. Plant Cell Rep *34*, 573-586.

Von Uexküll, H., and Mutert, E. (1995). Global extent, development and economic impact of acid soils. Plant and soil *171*, 1-15.

Vulavala, V.K., Elbaum, R., Yermiyahu, U., Fogelman, E., Kumar, A., and Ginzberg, I. (2016). Silicon fertilization of potato: expression of putative transporters and tuber skin quality. Planta *243*, 217-229.

Wang, J.P., Raman, H., Zhang, G.P., Mendham, N., and Zhou, M.X. (2006a). Aluminium tolerance in barley (Hordeum vulgare L.): physiological mechanisms, genetics and screening methods. J Zhejiang Univ Sci B *7*, 769-787.

Wang, P., Bi, S., Ma, L., and Han, W. (2006b). Aluminum tolerance of two wheat cultivars (Brevor and Atlas66) in relation to their rhizosphere pH and organic acids exuded from roots. Journal of agricultural and food chemistry *54*, 10033-10039.

Wang, X., Wang, Z., Zheng, Z., Dong, J., Song, L., Sui, L., Nussaume, L., Desnos, T., and Liu, D. (2019). Genetic Dissection of Fe-Dependent Signaling in Root Developmental Responses to Phosphate Deficiency. Plant Physiol *179*, 300-316.

Wang, Y., Li, R., Li, D., Jia, X., Zhou, D., Li, J., Lyi, S.M., Hou, S., Huang, Y., Kochian, L.V., *et al.* (2017). NIP1;2 is a plasma membrane-localized transporter mediating aluminum uptake, translocation, and tolerance in Arabidopsis. Proc Natl Acad Sci U S A *114*, 5047-5052.

Wang, Y., Stass, A., and Horst, W.J. (2004). Apoplastic binding of aluminum is involved in silicon-induced amelioration of aluminum toxicity in maize. Plant Physiol *136*, 3762-3770.

Weng, J.K., and Chapple, C. (2010). The origin and evolution of lignin biosynthesis. New Phytol *187*, 273-285.

Willats, W.G., McCartney, L., Mackie, W., and Knox, J.P. (2001). Pectin: cell biology and prospects for functional analysis. Plant molecular biology *47*, 9-27.

Wu, J., Mock, H.P., Giehl, R.F.H., Pitann, B., and Muhling, K.H. (2019). Silicon decreases cadmium concentrations by modulating root endodermal suberin development in wheat plants. J Hazard Mater *364*, 581-590.

Yamaguchi, M., Sasaki, T., Sivaguru, M., Yamamoto, Y., Osawa, H., Ahn, S.J., and Matsumoto, H. (2005). Evidence for the plasma membrane localization of Al-activated malate transporter (ALMT1). Plant Cell Physiol *46*, 812-816.

Yang, J.L., Zhu, X.F., Peng, Y.X., Zheng, C., Li, G.X., Liu, Y., Shi, Y.Z., and Zheng, S.J. (2011). Cell wall hemicellulose contributes significantly to aluminum adsorption and root growth in Arabidopsis. Plant Physiol *155*, 1885-1892.

Zeier, J., and Schreiber, L. (1997). Chemical composition of hypodermal and endodermal cell walls and xylem vessels isolated from Clivia miniata (identification of the biopolymers lignin and suberin). Plant Physiology *113*, 1223-1231.

Zhang, F., Yan, X., Han, X., Tang, R., Chu, M., Yang, Y., Yang, Y.H., Zhao, F., Fu, A., Luan, S.*, et al.* (2019). A Defective Vacuolar Proton Pump Enhances Aluminum Tolerance by Reducing Vacuole Sequestration of Organic Acids. Plant Physiol *181*, 743-761.

Zhang, Y., Guo, J., Chen, M., Li, L., Wang, L., and Huang, C.F. (2018). The Cell Cycle Checkpoint Regulator ATR Is Required for Internal Aluminum Toxicity-Mediated Root Growth Inhibition in Arabidopsis. Front Plant Sci *9*, 118.

Zhang, Z., Liu, D., Meng, H., Li, S., Wang, S., Xiao, Z., Sun, J., Chang, L., Luo, K., and Li, N. (2020). Magnesium alleviates aluminum toxicity by promoting polar auxin transport and distribution and root alkalization in the root apex in populus. Plant and Soil *448*, 565-585.

Zhao, Z., Ma, J.F., Sato, K., and Takeda, K. (2003). Differential Al resistance and citrate secretion in barley (Hordeum vulgare L.). Planta *217*, 794-800.

Zheng, S., and Yang, J. (2005). Target sites of aluminum phytotoxicity. Biologia Plantarum *49*, 321-331.

Zheng, S.J., Ma, J.F., and Matsumoto, H. (1998). High aluminum resistance in buckwheat: I. Al-induced specific secretion of oxalic acid from root tips. Plant Physiology *117*, 745-751.

Zhou, Y., Wang, Z., Gong, L., Chen, A., Liu, N., Li, S., Sun, H., Yang, Z., and You, J. (2019). Functional characterization of three MATE genes in relation to aluminum-induced citrate efflux from soybean root. Plant and Soil *443*, 121-138.

Zhou, Y., Xu, X.Y., Chen, L.Q., Yang, J.L., and Zheng, S.J. (2012). Nitric oxide exacerbates Al-induced inhibition of root elongation in rice bean by affecting cell wall and plasma membrane properties. Phytochemistry *76*, 46-51.

Zhu, X.F., Shi, Y.Z., Lei, G.J., Fry, S.C., Zhang, B.C., Zhou, Y.H., Braam, J., Jiang, T., Xu, X.Y., Mao, C.Z.*, et al.* (2012). XTH31, encoding an in vitro XEH/XET-active enzyme, regulates aluminum sensitivity by modulating in vivo XET action, cell wall xyloglucan content, and aluminum binding capacity in Arabidopsis. Plant Cell *24*, 4731-4747.

Zhu, X.F., Sun, Y., Zhang, B.C., Mansoori, N., Wan, J.X., Liu, Y., Wang, Z.W., Shi, Y.Z., Zhou, Y.H., and Zheng, S.J. (2014). TRICHOME BIREFRINGENCE-LIKE27

affects aluminum sensitivity by modulating the O-acetylation of xyloglucan and aluminum-binding capacity in Arabidopsis. Plant Physiol *166*, 181-189.

Zhu, X.F., Zheng, C., Hu, Y.T., Jiang, T., Liu, Y., Dong, N.Y., Yang, J.L., and Zheng, S.J. (2011). Cadmium-induced oxalate secretion from root apex is associated with cadmium exclusion and resistance in Lycopersicon esulentum. Plant Cell Environ *34*, 1055-1064.

Supplementary data

Table S1 Primers list.

Primer name	Sequence 5'-3'
Actin-Forward	GGCACACTGGTGTCATGGT
Actin -Reverse	GCGCCTCATCACCAACATA
CYP86A1-Forward	AGCTTCAGCTGTTGTTACTGG
CYP86A1-Reverse	TCCCTGGATGTTGCGTATGT
CYP86B1-Forward	TAGTGGTCTGATTCGCTGCC
CYP86B1-Reverse	CTATCCCTCACCAGACCCGA
GADPH-Forward	TGCTGCCAAGGCTGTTGGTAAG
GADPH-Reverse	AGTGGGAACCCGGAAAGACATAC
NCED1-Forward	CCAGCACTAATCGATTCC
NCED1-Reverse	GAGAGTGGTGATGAGTAA
NCED2-Forward	CATGGAAAGAGGAAGTTG
NCED2-Reverse	GAAGCAAGTGTGAGCTAAC
Ao5b-Forward	TTGGCGTTGTGATTGCTGAGAC
Ao5b-Reverse	AAAACGGGGGAGGATGGAAGTA
BG8-Forward	CCCCGGCCAGGCGTATTCC
BG8-Reverse	TCCCAGGCTTATTCGTCATCCA
ABA8-OH1-Forward	AGCACGGACCGTCAAAGTC
ABA8-OH1-Reverse	TGAGAATGCCTACGTAGTG
ABA8-OH2-Forward	GAGATGCTGGTGCTCATC
ABA8-OH2-Reverse	ACGTCGTCGCTCGATCCAAC
PYL4-Forward	CCCCCTCCGGTCAACTCTCG
PYL4-Reverse	CCACCACCACCACCACGGATTT
PP2C4-Forward	TGGCCTCTGGGATGTATTGTCG
PP2C4-Reverse	GAGCCGCTGGATCTGGGGAGTC
ABI5-Forward	CCGGTCCCTGTTGCCCCTAAAG
ABI5-Reverse	CGCCGCCCATACCGAG
CYP86B1 clone-Forward	ACGGCCATACGTTGCCATCA
CYP86B1 clone-Reverse	TCAGCTTTCTCCTGCAAAGTATCACT

Table S2 Gene ID used for RNA-seq and qPCR.

Gene name	Gene ID
CYP86A1	*HORVU.MOREX.r2.3HG0251350*
CYP86B1	*HORVU.MOREX.r2.1HG0034810*
KCS1	*HORVU.MOREX.r2.4HG0326360*
KCS2	*HORVU.MOREX.r2.7HG0592280*
KCS20	*HORVU.MOREX.r2.6HG0478730*
GPAT4	*HORVU.MOREX.r2.6HG0452720*
GPAT5	*HORVU.MOREX.r2.1HG0059530*
GPAT7	*HORVU.MOREX.r2.4HG0284030*
GDSL	*HORVU.MOREX.r2.4HG0317620*
FAR5	*HORVU.MOREX.r2.3HG0183570*
FAR4	*HORVU.MOREX.r2.3HG0183520*
FAR1	*HORVU.MOREX.r2.7HG0598950*
ABCG6	*HORVU.MOREX.r2.1HG0007740*
ABCG20	*HORVU.MOREX.r2.3HG0253120*
ABCG2	*HORVU.MOREX.r2.4HG0321420*
ABCG11	*HORVU.MOREX.r2.2HG0151890*
MYB9	*HORVU.MOREX.r2.6HG0512050*
MYB41	*HORVU.MOREX.r2.2HG0111800*
MYB107	*HORVU.MOREX.r2.7HG0551920*
ABA4	*HORVU.MOREX.r2.3HG0184690*
ABF1	*HORVU.MOREX.r2.6HG0513990*
ABF2	*HORVU.MOREX.r2.7HG0550580*
ABI4	*HORVU.MOREX.r2.7HG0533970*
AHG1	*HORVU.MOREX.r2.2HG0079050*
AREB3	*HORVU.MOREX.r2.1HG0056310*
ERF7	*HORVU.MOREX.r2.2HG0158950*
HB5	*HORVU.MOREX.r2.5HG0404470*
PLC1	*HORVU.MOREX.r2.1HG0011580*
NCED1	*HORVU.MOREX.r2.4HG0337890*
NCED2	*HORVU.MOREX.r2.5HG0392060*
NCED3	*HORVU.MOREX.r2.3HG0267820*
PP2CA	*HORVU.MOREX.r2.5HG0392330*
RBOHD	*HORVU.MOREX.r2.3HG0238280*

Acknowledgements

First, I would like to express my deep gratitude to my supervisor Prof. Dr. Lukas Schreiber for providing me this wonderful opportunity to work in his lab and for his invaluable guidance, support, and encouragement throughout my doctoral studies.

I am also grateful to the China scholarship council (CSC) for providing me with the fellowship that allowed me to pursue my studies.

I would like to extend my sincere appreciation to all lab mates for their help and suggestions and for the enjoyable and scientific atmosphere of the group. Thank to Dr. Viktoria V. Zeisler-Diehl for providing guidance in suberin analysis using GC/MS and for her patient assistance with every reagent order. Thank to Dr. Rochus B. Franke, Paul Grünhofer, Kiran Suresh, Dr. Priya Dharshini Thangamani, Dr. Nandhini Shellakkutti, and Dr. Johanna Baales for their valuable discussions and technical assistance with my experiments and other aspects of my work. Special thanks go to Dr. Tino Kreszies for his assistance with the element analysis experiments.

I am also grateful to my friend Li Guo and Qihui Zhang for their support in both work and life.

I cannot express enough gratitude to my parents for their unwavering love, care, and encouragement throughout my life.Last but not least, I would like to thank my beloved partner, Yangyang, for the understanding, patience, and support.